STRUCTURAL DEVELOPMENT OF THE DUN MOUNTAIN OPHIOLITE BELT IN THE PERMIAN, BRYNEIRA RANGE, WESTERN OTAGO, NEW ZEALAND.

A thesis submitted in partial fulfilment of the requirements for the

Degree of

Master of Science in Geological Science

at the

University of Canterbury

by

Thomas Keeley Adamson

2008

Abstract

The deformed Permian Dun Mountain Ophiolite Belt (DMOB) forms the basement of the Dun Mountain-Maitai terrane and is traceable through the entire length of New Zealand. The DMOB contains a variably serpentinised mantle portion and a crustal portion containing gabbros, dolerites, cross cutting dikes and extrusives, together they are similar to oceanic crust. The initial crustal portion, however, is atypical when compared to other ophiolites, being thin and lacking a sheeted dike complex, but has well spaced inclined intrusive sheets and sills. At least four post-Permian deformation periods affect the DMOB; collision and rotation during emplacement of the DMOB on the Gondwana margin, compression during Mesozoic orogenies, extensional deformation during the Gondwana break-up and transpressive deformation related to the modern plate boundary through New Zealand.

Structural work in the Northern Bryneira Range focused on well preserved outcrops to investigate crustal growth and contemporaneous deformation during the Permian. Structural evidence of Permian deformation was determined by examination of pseudostratigraphy, structures constrainable to the Permian, and the geometric relationships with the overlying Maitai sedimentary sequence. Crosscutting by intrusive phases was used to determine a chronological order of crustal growth and deformation episodes. It was concluded that all deformation was extensional and that two major phases of magmatism were separated by a period of deformation and were followed by ongoing syn-sedimentary deformation during the deposition of the Maitai Group. After removal of Mesozoic rotation, the resulting orientations of paleo-horizontal markers and diverse orientations of intrusive sheets were analysed. Two hypothesises were tested to assess the origin of inclined intrusive sheets: a) that the diverse orientations were the result of tectonic rotation coeval with the intrusion of dikes. b) that primary orientations of the sheets had been diverse. Results show that the sheets were intruded with diverse orientations, probably related to variation in the principle horizontal stress over time. Further rotation of the assemblage of sheets occurred during the last stages of magmatism and during the subsequent period of sedimentation. The last stage probably relates to large scale normal faulting during the development of the sedimentary basin.

Acknowledgements

There are a number of people I would like to thank for their contributions before and during my thesis study. A big thanks to my supervisors: John Bradshaw for insightful discussion and the hours spent reviewing my work; Uwe Ring for advise on structural issues.

I would like to thank a number of staff from the geology department: Rob Spears for thin section preparation; John Southwood and Anekant Wandres for help with computers; Vanessa Tappenden for logistical support; Jim Cole, Jarg Pettinga and Jamie Shulmeister for advise.

For help in the field, I would like to thank David Hood and Greer Gilmer for their tireless effort and questioning my logic.

Most importantly, I would like to thank mum and school teachers who never gave up on me when learning was difficult. It goes to show, when you teach someone how to learn and to try hard, anything is possible.

Table of Contents

List of Figures

Chapter 1: Introduction

1.1 Introduction

The Dun Mountain Ophiolite Belt (DMOB) forms a linear belt of rocks traceable through New Zealand for a length of ~1100 Km. This variably intact ophiolite forms the base of the Permian to Triassic Dun Mountain-Maitai terrane. The Alpine Fault in the South Island truncates the terrane for some ~460 Km. Intact portions of the DMOB have an atypical ophiolite sequence, with MORB to island arc geochemical affinity. At least five periods of deformation may have formed and later reactivated structures with in the DMOB:

1. extensional deformation during multiple phases of ocean crust formation;
2. compression during emplacement of the DMOB on to the Gondwana margin;
3. compression during Mesozoic orogenies, involving accretion of terranes to the Gondwana margin;
4. extensional deformation during the Gondwana break-up;
5. transpressive deformation related to the modern plate boundary through New Zealand.

The DMOB is well studied, although much of the existing literature focuses on geochemical, geochronological, gravity and magnetic aspects, with few authors looking purely at structure. This research has allowed the DMOB to be well constrained in space and time. The geodynamic setting of the DMOB formation, however, and evolution of the Permian Gondwana margin is less well known. Remote outcrop locations and poor preservation of structure has hampered structural studies.

This project focuses on structural problems relating particularly to the Permian development of the DMOB. Attention is given to variation within the pseudostratigraphy and cross cutting relationships, as a means to assess deformation during formation of the belt. It seeks to use structural techniques to evaluate the complex deformation associated with the multi-phase origin many past workers have alluded to. The primary tools employed to

aid this investigation being: a review of existing literature, detailed mapping on various scales, thin section petrology and analysis of structural data.

1.2 Geological problems presented by the DMOB

Although well studied, the role of the DMOB in evolutionary models of the south western Pacific Gondwana margin during and after the Permian is still not clear. The wealth of information gathered over the past decade regarding the petrology, geochemistry and age has produced well-understood igneous chronology and interpretations tectonic settings ranging from fore-arc to back-arc. But, even in the best-preserved sections, the DMOB is thinner and more complex than would be expected for a complete ophiolite. This structural study hopes to shed light on this aspect and test the following hypotheses:

a) That the complex and atypical ophiolite sequence is the result of the tectonic environment in which the ophiolite originated.

b) That cross cutting relationships between intrusive sheets and structures are the result of a multi-phase Permian evolution.

c) That thinning is the result of Permian extensional tectonics.

1.3 Aims of this project

The aims of this study are:

- to characterise the observed pseudostratigraphy in terms of structure, texture and composition;
- to characterise the observed structure in terms of form, orientation and cross-cutting relationships;
- to determine the chronology of deformation by combining magmatic and amagmatic structural information;
- to establish a dynamic model for structural development by comparing geometric information with other ophiolites and oceanic crust;

1.4 Methods

Fieldwork was conducted in the northern half of the Bryneira Range in Western Otago. Planar and linear orientation data, such as the attitude of bedding, faults, fractures and intrusive sheets were collected in the field. Photographic images were taken in digital form. Petrographic notes were made by thin section analysis, using a Zeiss microscope. All stereo-plots were produced with the computer program *Dips v. 5.103* from Rockscience Inc. and illustrated as equal area, lower hemisphere stereographic projections. This program was also used to rotate poles of planes. Mean planes were determined graphically on the corresponding plots. Geological maps of the field area were produced with *Corel Draw v. 12.* All images were processed with *Corel Draw v. 12.* Photographic images were processed (i.e. lines or text added) using *Corel Photo-Paint v. 12.*

1.5 Thesis Organisation

Chapter 2 reviews the geological make-up of the New Zealand sub-continent. Summarising New Zealand's tectonostratigraphic terrane framework and a synopsis of their tectonic evolution as a context to this study. This is followed by an account of the current state of knowledge about geographic extent, geochemistry, age and deformation history of the DMOB.

Chapter 3 gives an overview of the geology in the study area by examining the major geological features, and then describing the ophiolite pseudostratigraphy.

Chapter 4 is a detailed description and illustration of all the structures observed in the study area. It begins by describing the regional scale structures, then the faults and folds within the Dun Mountain-Maitai terrane. The second section deals with variation in structure at each level of pseudostratigraphy. The structures are characterised in terms of the pseudostratigraphic distribution, texture, form and cross-cutting relationships, and interpreted in terms of the rheological conditions under which they were thought to have formed. A third section describes the structure of the intrusive sheets that cut the crustal portion of the belt.

Chapter 5 investigates the orientation of intrusive sheets, and faults and fractures measured in the study area. Poles to planes of the major intrusive sheet varieties as well as faults and fractures are presented as stereo nets and re-orientated to their former positions using paleo-horizontal marker beds.

Chapter 6 begins with a summary of the structural components observed in the study area. A discussion then integrates information presented in Chapter 3, Chapter 4, Chapter 5 and the wider DMOB. Findings are compared to other ophiolite, oceanic crust and rocks that have undergone similar deformation. Finally, conclusions are presented followed by implications of this study to future work on the DMOB.

Chapter 2: Overview of New Zealand Geology and Dun Mountain Ophiolite Belt

2.1 Regional Geology of New Zealand

New Zealand is a large, mainly-submerged fragment of the Gondwana margin that was rifted away from the Antarctic-Australia sector in the Late Cretaceous. Pre-break-up rocks in New Zealand are divided into nine tectonostratigraphic terranes that can be traced offshore through islands and by dredging and appear to be typical of the whole sub-continent (Fig. 2.1). Ages range from early Paleozoic in the west to Cretaceous in the east.

Exact relationships between these elongate bodies of predominantly arc related sedimentary rock is still not clear. Relationships deduced via geochemistry, geochronology, provenance and structural studies show bulk terrane similarities with adjacent regions (i.e. Australia and Antarctica) and have led to a basic understanding of their geotectonic origin (Bradshaw, 2007; Bradshaw et al., 1997; Cooper and Tulloch, 1992; Wandres and Bradshaw, 2005).

2.1.1 New Zealand's Tectonostratigraphic framework

Tectonostratigraphic terranes of New Zealand are traditionally divided into two major provinces, the western province and the eastern province, separated in the middle by the **Median Tectonic Zone** (MTZ) (Bradshaw, 1993; Kimbrough et al., 1993) or Median Batholith (Mortimer et al., 1999). The following gives an outline of New Zealand's Tectonostratigraphic frame work, based on the summarised from Sutherland (1995), Mortimer et al (2004) and Wandres and Bradshaw (2005, and references therein).

The Western Province contains the **Buller terrane** and **Takaka terranes**, located to the west and east respectively, both trending north-south. The Buller terrane comprises of Late Cambrian to Early Ordovician, quartzose greywacke, deposited as part of a large

turbidite fan at a passive continental margin. The Takaka terrane, spanning the Cambrian to Early Devonian contains New Zealand's oldest rocks. There is great lithological diversity within the Takaka terrane. Volcanic, siliclasitic, and carbonates are found within fault bound packages which show variation in their internal stratigraphy. Similarities between the Buller and Takaka terranes suggest that they formed within the same major tectonic setting, in a basin with a waning sedimentary supply. Correlations between the Western province have been made with the Lachlan Fold Belt in Australia and various terranes in Antarctica (Bradshaw, 2007; Cooper and Tulloch, 1992). Magmatism has emplaced plutons within the Buller and Takaka terranes during the Middle Devonian, Carboniferous and Cretaceous times.

The MTZ contains suites of Carboniferous to Early Cretaceous subduction related plutons. Lesser amounts of volcanic and sedimentary rocks are also present. Magmatic activity started in the Carboniferous and culminated in the Early Cretaceous and formed within and adjacent to the edge of the Western Province as a magmatic arc complex (Mortimer, 2004; Mortimer et al., 1999). The MTZ has an important role in tectonic reconstructions as it records magmatism along the Gondwana margin, during the time in which the Eastern Province was formed.

The Eastern Province contains accreted allochthonous terranes ranging in age from the Permian to the late Cretaceous. On the basis of structural, geochemical and provenance, these terranes are best discussed in two groups separated by the **Livingstone Fault** (see Fig. 2.3 and 2.5). West and south of the Livingstone Fault the Brook Street, Murihiku and the Dun Mountain-Maitai terranes have simple structures, low temperature metamorphism and can be referred to as Central Arc terranes (Campbell, 2000). Terranes located to the north and east of the Livingstone Fault, the Caples, Torlesse and Waipapa terranes, have been subjected to polyphase deformations resulting in a more complex structure.

Brook Street terrane. The Permian Brook Street terrane is thought to represent a primitive, inter-oceanic arc assemblage. It is dominated by volcanoclastics of mainly basaltic-andesitic composition forming a thick (~14km) pile, now preserved as a homocline of east facing succession. A non-volcanic late Permian succession follows. The terrane is cut by mafic bodies (Trodhjemite, gabbro and granite). Permian rocks are

unconformably overlain by Early Jurassic sandstones and conglomerate (Landis et al., 1999).

Murihiku terrane. The Late Permian to Late Jurassic Murihiku terrane is dominated by volcanoclastic marine sandstone succession, which includes minor conglomerates, mudstones and tuffs. This ~15 km pile has a simple internal structure, forming a ~450 km long Southland-Kauhia Synclinal structure (Fig 2.3) with low grade metamorphism. Deposition of these rocks likely occurred in a long-lived back-arc or fore-arc basin (Ballance and Campbell, 1993; Coombs et al., 1996).

***Dun Mountain-Maitai terrane*.** The Early Permian to Early to Middle Triassic Dun Mountain-Maitai terrane contains the subject of this study. In summary, the basal DMOB is semi-continuous, exposed as a near complete ophiolite and/or a tectonic mélange. In areas where these rocks are not exposed a continuous magnetic lineament can be followed. The overlying **Maitai Group** is composed of well stratified, moderately metamorphosed, volcanoclastic, sedimentary succession.

Livingstone Fault. The Livingstone Fault System is of importance to this study, being eastern terrane boundary of the Dun Mountain-Maitai terrane. In the context of this chapter it marks a boundary between the Mesozoic accretionary wedge system to the east and “within-arc” terranes to the west.

Caples terrane. The Caples terrane is a mainly marine volcanoclastic succession, deposited in submarine-fans, adjacent to an active arc. Sediment was derived from a source intermediate between oceanic and continental arcs. These rocks are now tectonically imbricated and weakly metamorphosed. The boundary between it and the juxtaposed Torlesse terrane is a cryptic suture overprinted by the **Otago Schist**.

Torlesse terranes. The Torlesse sedimentary rocks of the South Island are divided into two sub-terranes on the basis of age. To the west, the Permian to Late Triassic **Rakaia terrane** and in the east the more extensive Late Jurassic to Early Cretaceous **Pahau terrane**. Between these two terranes is the **Esk Head Mélange**, a zone of intense deformation of weak sediments. Both the Rakaia and Pahau terrane contain repetitive

quartzofeldspathic sandstone-mudstone turbidites. Minor chert, limestone and basalt are thought to be oceanic relics. The Rakaia terrane formed as part of an east facing accretionary wedge, resulting in multiple phases of deformation and tectonic overprinting, with metamorphic grade increasing to the west into the **Haast Schist** (Mortimer, 2004)**.**

In the north island the Torlesse terrane continues, with further subdivision into the Triassic to late Jurassic **Bay of Islands terrane** (after Kear and Mortimer, 2003) and the Late Jurassic to Early Cretaceous **Waipa Supergroup.**

2.2 Tectonic evolution of New Zealand

The western province terranes were amalgamated sometime in the Early to Mid Devonian (Rattenbury et al., 1998) and accreted to the Gondwana margin by the Late Devonian (Weaver et al., 1991). Initiation of the long-lived convergent margin system began some time in the Permian along the south-western margin of Gondwana. The long-lived MTZ, associated with subduction along Gondwana's margin, can also be traced into neighbouring regions. Its known extent within the New Zealand region is north west from Nelson along the Lord Howe Rise to as far north as the New Caledonia basin (Sutherland, 1999). To the southeast of New Zealand, MTZ rocks can be traced in to the Campbell Plateau, and in the Amundsen Province of Western Antarctica (Bradshaw et al., 1997). Discrete pulses in magmatism are observed between ~310 and ~135 Ma in both MTZ rocks and there Antarctic equivalents (Kimbrough et al., 1994).

The origin of Permian to late Cretaceous terranes to the east of the MTZ is still not well understood. All are considered allochthonous, becoming juxtaposed by discontinuous oblique convergence over 200 Ma (Sutherland, 1999). The outboard regions of the Gondwana margin probably looked similar to the Southeast Asian basins of today, containing back-arc, fore-arc and trench slope basins accompanied by inter-arc and arc volcanism.

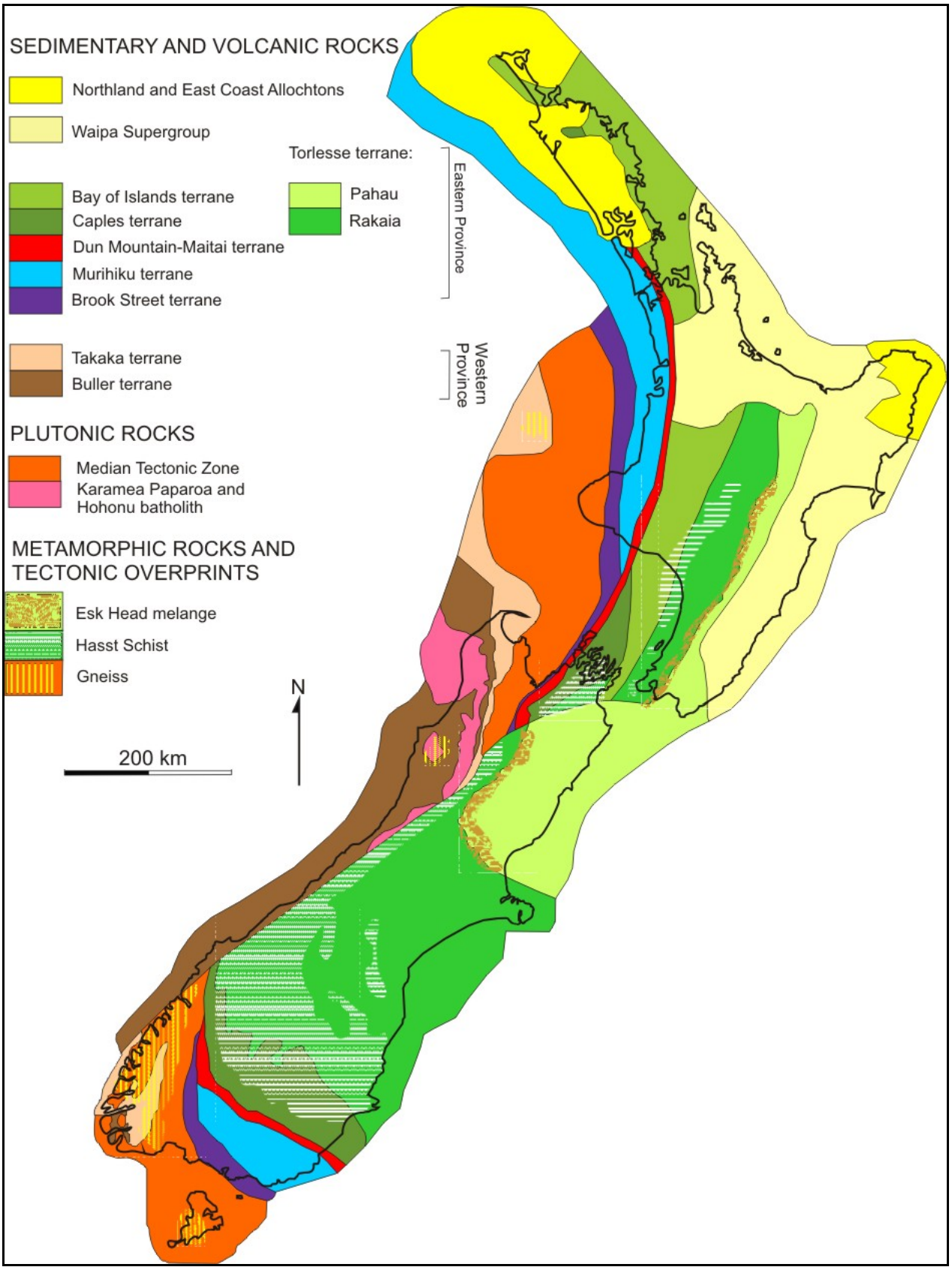

Fig. 2.1: Map of New Zealand showing the positions of terrane on land and projected offshore. Modified from Mortimer et al (2004).

Convergence during the Mesozoic ended in mid Cretaceous times, quickly being replaced by rift tectonics, leading to the separation of New Zealand from Antarctica and Australia around 83-85 Ma (Laird and Bradshaw, 2004). This period of extension was accompanied by widespread passive margin sedimentation, plume volcanism and subsidence. At 45 Ma a new plate boundary developed southwest of New Zealand (Sutherland, 1995). Asymmetric spreading southwest of New Zealand led to the development of the Alpine fault system by 24 Ma (Lamarche et al., 1997).

The present day plate configuration (Fig. 2.2) is dominated by the oblique continent–continent collision between the Australia and Pacific plates. Subduction under the North Island from the east is linked with subduction of the opposite polarity in the Puygsegur Trench by the transpressive Alpine fault. Ongoing oblique reverse movement along the Alpine Fault and interrelated faults has resulted in widespread deformation and active orogenesis of the Southern Alps.

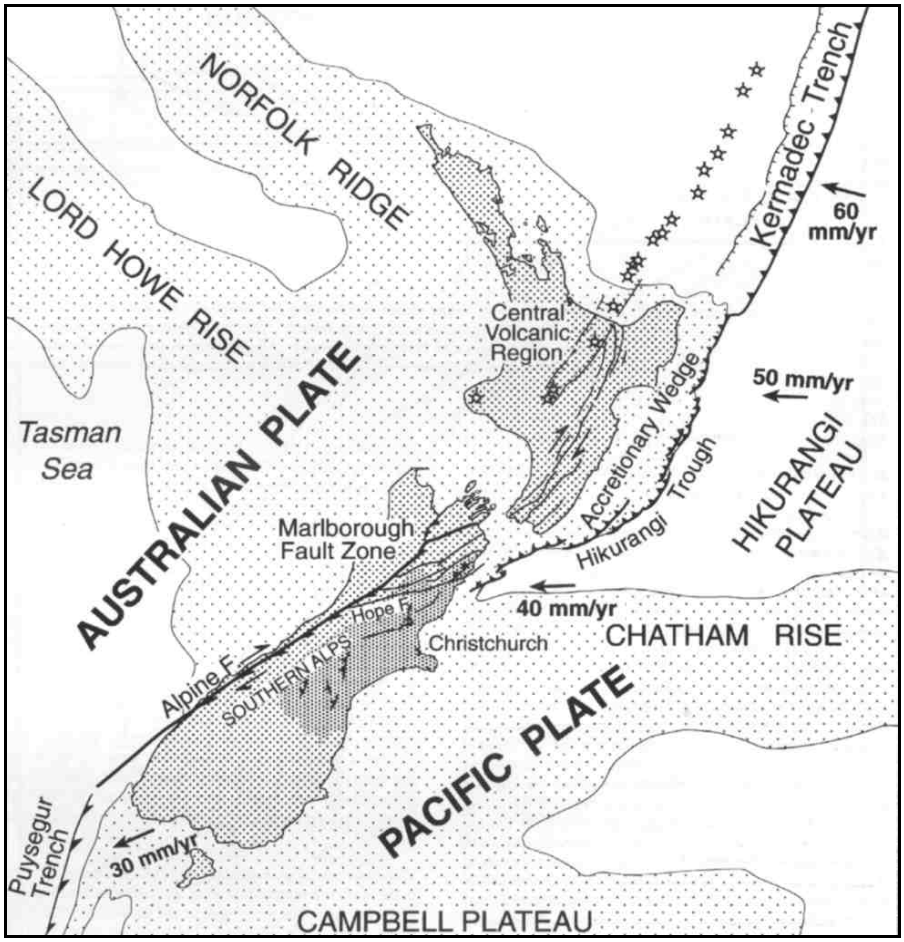

Fig. 2.2: Present day Australian-Pacific plate setting, showing the main structural features associated with oblique convergence through the New Zealand continental crust. From Pettinga (2001).

2.3 Dun Mountain Ophiolite Belt

In the wake of active mineral exploration along the DMOB from the early sixties and the Penrose Field Conference on ophiolites in 1972 (Anonymous, 1972), a period of intense investigation commenced. This formed the foundation for future investigations and the application of recently defined ophiolite and plate tectonic models. First to apply the plate tectonic model was Landis and Bishop (1972) who regarded the DMOB as crust and upper mantle. The DMOB was defined as an ophiolite suite or the remnants of one preserved as a tectonic mélange by Blake and Landis (1973) and Coombs et al (1973). A comprehensive review was published by Coombs et al (1976), in which new data is collated to review the nature, tectonic setting and origin of the DMOB during the Permian and Mesozoic. Coombs et al (1976) found that the belt could be divided in to segments south of the Alpine Fault based on geochemistry and structure (see later). Segments directly to the south of the Alpine Fault (e.g. Red Mountain-Mossburn) contain primary ophiolitic rocks typical of an ocean spreading ridge. Whereas the segment southeast of Mossburn (Fig. 2.3) has arc-like geochemical characteristics. These fundamental ideas still stand today.

2.3.2 Geographic extent

In the late sixties and seventies magnetic and gravitational surveys traced the extent of the DMOB. Before this time the large outcrops of ultramafics and associated crustal rocks were well documented, clearly extending 150 km north of the Alpine fault in Nelson and 185 km to the south in Otago and Southland. Hatherton, (1967; 1969) was the first to note the continuous, positive magnetic lineament which he named the Junction Magnetic Anomaly. Further work (Hatherton and Sibson, 1970) showed that the Junction Magnetic Anomaly could be linked with other small outcrops of ophiolitic rocks in the North and South Islands. In the South Island there is no exposure of ultramafic material from Mossburn to the Pacific coast (Fig.2.3), but the magnetic anomaly is traceable throughout this distance (Woodward and Hatherton, 1975). Apart from the ~460 km offset on the Alpine fault and numerous small offsets and breaks, the magnetic anomaly appears to be present throughout the New Zealand continent (Hunt, 1978). In a recent study by Eccles

et al (2005) used aeromagnetic imaging to acquire detailed structural information along the Dun Mountain-Maitai terrane in north of the North Island.

2.3.3 Large scale structure of the DMOB

A clear understanding of the DMOB structure is critical for the understanding of its tectonic origin. The nature of DMOB structure spans a spectrum of forms from near complete ophiolite sequence through fragmented ophiolite mélange, to complete absence. The following sections are a synthesis of the most recent work on the DMOB, reported south to north, using the segments defined in Coombs et al (1976) south of the Alpine Fault.

2.3.3.1 Lintley-Otanomomo Segment

From the Pacific Ocean the belt trends to the south east toward the Mossburn area (Fig. 2.3). Only three poorly exposed igneous complexes are found. This segment is defined by its silicic composition and, in the absence of an ultramafic portion, does not constitute an ophiolite (Coombs et al., 1976).

In the east of Waipahi (Fig. 2.3), there are a series of elongate fault bound slivers that outcrop discontinuously for approximately 13 km. Here, the Dun Mountain-Maitai terrane is ~10 km wide, containing mainly Maitai Group sediments overlying attenuated and dismembered DMOB fragments. The sequence of altered basalts and intrusive sheets (dolerites) dip moderately to steeply northeast and are therefore overturned, striking with the regional trend to the northwest-southeast (Cawood, 1987; Coombs et al., 1976) Repetitions of DMOB blocks are seen in the overlaying Maitai sequences. This repetition is the product of asymmetric folding that was disrupted by faulting, possibly during the juxtaposition of the Caples terrane (Mesozoic) (Cawood, 1987).

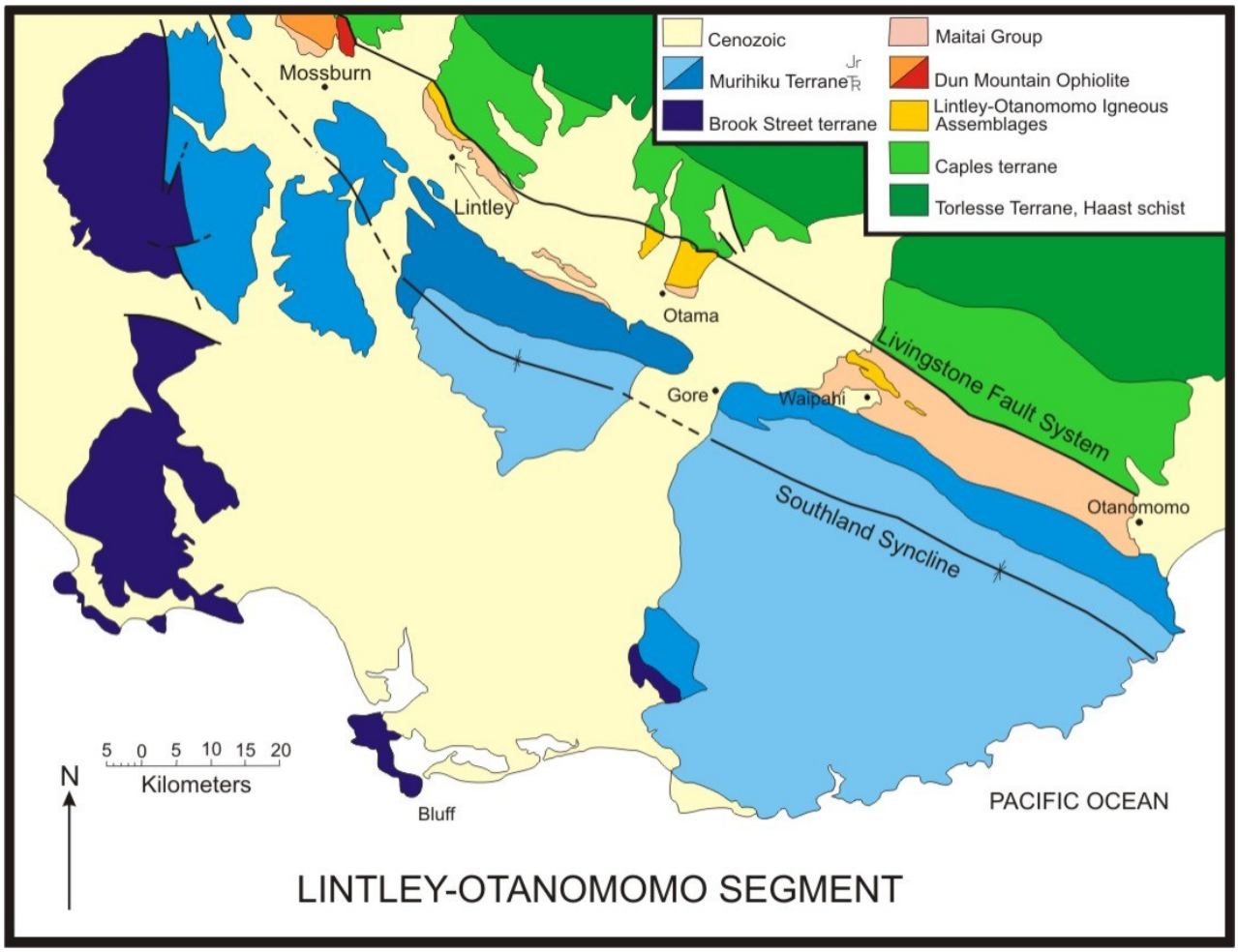

Fig. 2.3: Geological map of the Lintley-Otanomomo segment of the DMOB and surrounding terranes. Modified from Kimbrough et al (1992).

A small outcrop is found at Otama, northwest of Gore (Fig. 2.3). The igneous rocks found here are not well exposed, most rocks being deeply weathered and contact zones are lacking ((Wood, 1956)). The sequence has the same structural trends as the other DMOB occurrences in the Lintley-Otanomomo segment, being overturned and facing south (Coombs et al., 1976).

Further west at Lintley region (Fig. 2.3) the DMOB has a simple, non-repeating structure, trending northwest-southeast and dipping moderately to steeply to the northeast. Here the belt is less than 1 km wide and composed of discontinuous bodies of quartz rich intrusive sheets and plagiogranite, for ~8 km along strike. Igneous rocks are surrounded by Maitai Group sediments, their relationship is unknown and stratigraphic position nonconforming (Cawood, 1986). To the northeast, the Livingstone Fault System forms a broad zone up to 600m wide, containing fragments of both the Caples and Dun Mountain-Maitai terranes.

2.3.3.2 Red Mountain-Mossburn Segment

The Red Mountain-Mossburn Segment (Fig. 2.4) of the DMOB begins north of Mossburn, continuing northeast until truncated north of Red Mountain by the Alpine Fault. This segment has a diverse structure, containing relatively intact to dismembered ophiolite sequences and ophiolitic mélange units. Northwest of the Mossburn, the DMOB rocks have a normal mafic igneous association.

The Bald Hill area is the first portion of the Red Mountain-Mossburn segment (Fig. 2.4). On the west side of this ~10 km a typical **Livingstone Volcanic Group** sequence (basalts, intrusive sheets and gabbros) in depositional contact with the overlying Maitai Group, both are overturned, dipping steeply to the northeast (Stratford et al., 2004). To the east, a large fault bound section of sheared serpentinite mélange contains inclusions of limestones, siltstones and quartzofeldspathic sandstones (Coombs et al., 1976; Turnbull, 2000). Repetitions of fault bound Livingstone Volcanic Group occur partially within the Caples terrane further east. Blocks of Maitai Group rocks appear to the southeast partially against the Livingstone Fault (Turnbull, 2000). Cawood (1986) attributes this repetition to deformation by sinistral-verging steeply plunging folds.

Further north in the Windon Burn-Lake Mavora area (Fig. 2.4), the DMOB has been tectonically disrupted. Two Mélange units replace coherent ophiolite sequence; the **Windon Mélange** lies to the east, and the **Upukerora Mélange** to the west. The Windon Mélange contains sheared volcanics that include large (up to 5 km long) tectonic inclusions of gabbro, dolerite, siltstones and quartzofeldspathic sandstones (Craw, 1979). The fault bound Upukerora Mélange contains gabbros, peridotite and diorite inclusions in a serpentinite matrix, correlating with the Patuki mélange in the Nelson segment (Turnbull, 2000). From the Windon burn headwaters, a belt of disrupted ophiolite, containing Upukerora Mélange and semi-intact Livingstone Volcanic Group (Kelsey, 1981), continues north for ~20km to be faulted out south of Lake McKellar.

The DMOB is only represented by thin smears of serpentinite and volcanics north of Lake Mckellar to the Hollyford area (Coombs et al., 1976; Turnbull, 2000). Semi-coherent

crustal sequences are seen again at Serpentine Saddle (Fig. 2.4) (Hyslop, 1978). From here, the belt progressively thickens towards the Northern Bryneira Range, the subject of this study, where the crustal sequence is at its thickest. Beyond a relatively intact sequence continues to Red Mountain.

The ophiolite sequence found a Red Mountain (Fig. 2.4) is the most complete section south of the Alpine Fault. From east to west, the DMOB is comprised of the **Dun Mountain Ultramafics Group**, separated from the less mafic plutonic and volcanic rocks of the Livingstone Volcanic Group by the Peanut Fault (Sinton, 1975; Sinton, 1980). The general sequence consists of a basal zone of 1-3 km of residual harzbergite and lesser dunite (Dun Mountain Ultramafics Group; mantle sequence) tectonically overlain with a ~1250m zone of interlayered dunite, clinopyroxenite and mafic gabbros (Livingstone Peridotite**;** first of the crustal sequence units). Both zones are variably altered to serpentinite. This upper ultramafic unit grades into isotropic gabbros (200-1000m thick). These contain an increasing abundance of crosscutting mafic to intermediate dikes that locally reach 100% concentration. Above the dikes, metavolcanic greenschists with relict pillow structure are cut by some mafic dikes (0-1200m thick), which continue to the upper boundary of the Livingstone Subgroup (Coombs et al., 1976; Sinton, 1975; Sinton, 1980).

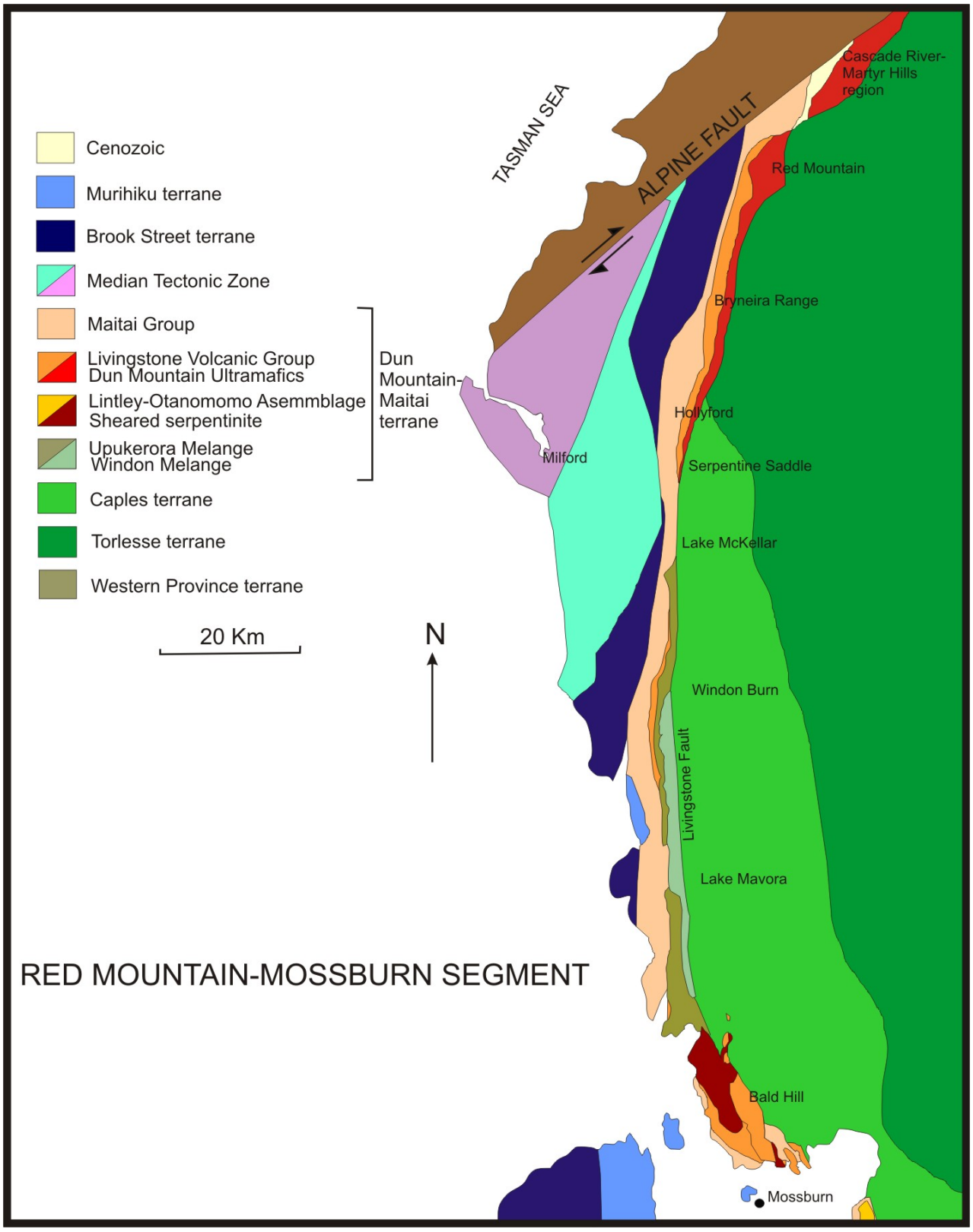

Fig. 2.4: Geological map of the Red Mountain-Mossburn segment of the DMOB and surrounding terranes. Modified from Kimbrough et al (1992) and Turnbull (2000).

The structure of the Red Mountain region is relatively simple, the ophiolite sequence strikes north-south, dipping steeply to the east and is regarded as overturned (Coombs et

al., 1976). Numerous faults cut the crustal sequence at Red Mountain, all show post-Mesozoic reactivations or origins (Sinton, 1975).

North of the Red Mountain area, in the Cascade River-Martyr Hills region, the belt continues with a semi-complete sequence abutting with the Alpine Fault (Coombs et al., 1976).

2.3.3.4 Nelson Segment

North of the Alpine Fault, the DMOB continues as a semi-continuous strip to D'Urville Island (Fig. 2.5). The Dun Mountain Ultramafic Group and the Livingstone Volcanic Group are found immediately north of the Alpine Fault and run for ~80 km to the Duppa Fault (Rattenbury et al., 1998), reappearing on D'Urville Island further north. The crustal and mantle sequences of the Nelson segment DMOB are very similar to the Red Mountain area, described in the last section (section 2.3.3.3). A well preserved Maitai Group sequence is found west of the DMOB, as part of the Roding Syncline (equivalent to the Key Summit Syncline south of the Alpine Fault (Rattenbury et al., 1998).

The structure of the Nelson segment DMOB is discontinuous and highly fragmented. Immediately north of the Alpine Fault is the Red Hills massif (Fig. 2.5) it contains a 9km wide body of variably serpentinised Dun Mountain Ultramafics Group and an attenuated Livingstone Volcanics Group sequence (Rattenbury et al., 1998). The Red Hill massif trends north-south and dips steeply to the west. The contact between the Dun Mountain Ultramafics Group and Livingstone Volcanic Group is faulted and numerous northwest-southeast and northeast-southwest faults cut the belt (Walcott, 1969). North of the Red Hills fault (Fig. 2.5), the belt has a northeast trend, thinning until the Duppa Fault, where it is completely faulted out. Over this length the DMOB dips steeply and is younging to the west; all contacts between groups are faults. The last major outcrop of the DMOB occurs on the eastern edge of D'Urville Island. An isolated block of plutonic and ultramafics are found in the south and are overturned dipping steeply to the east (Johnston, 1996).

Two serpentinite bearing Mélange units, the Patuki and Croisilles Mélange, are found to the east of the DMOB. The Patuki Mélange runs the length of the Nelson segment, and is found east of the DMOB when present. North of the Duppa Fault, the Patuki Mélange

forms north-northeast trending belt at the base of the overlying Maitai Group. Further east the discontinuous Croisilles Mélange lies in the Caples terrane (Rattenbury et al., 1998). Mélange rocks contain sedimentary, volcanic and plutonic fragments in a serpentinite matrix (Dickins et al., 1986; Johnston, 1996). On D'Urville Island, the Putaki Melange is found on the east and as fault bound bodies within the Livingstone Volcanic Group (Johnston, 1996).

2.3.3.5 North Island DMOB occurrences

There is only one known out crop of Dun Mountain Ophiolite in the North Island near Piopio (~70km south of Hamilton). The Wairere Serpentinite is exposed as a 50m by 650m strip along the Waipa Fault trace, conceding with the underlying magmatic anomaly (O'Brien and Rodgers, 1973). This lensodal body is interpreted to be diaperic, intruding contemporaneously to Oligocene limestone deposition (O'Brien and Rodgers, 1973).

2.3.3.6 Summary of DMOB large scale structure

The DMOB has large variation in structure, composition and preservation along the strike of the belt. There is apparent mirror symmetry either side of the Alpine Fault, in the preserved thicknesses and distribution of rock groups. Immediately northwest and southeast of the Alpine Fault, large lenses of serpentinised ultramafic rock underlie incomplete crustal sequences (for example, Red Hill in the Nelson segment and Red Mountain in the south). North and south of these areas (Nelson and Red Mountain segments respectively), the belt thins and has better preservation of crustal sequences overlying altered ultramafic rocks and serpentinite (for example, the Bryneira Range). These rocks are often in sedimentary contact with the overlying Maitai group sediments. In the same directions, mantle sequence is replaced by, and crustal sequence becomes enclosed in, serpentinite bearing mélange units. The relationship of the mélange and the overlying DMOB is unresolved. South of Five River Planes the abrupt change from mafic igneous association to silicic igneous association reflects a change in the tectonic origin of magmas.

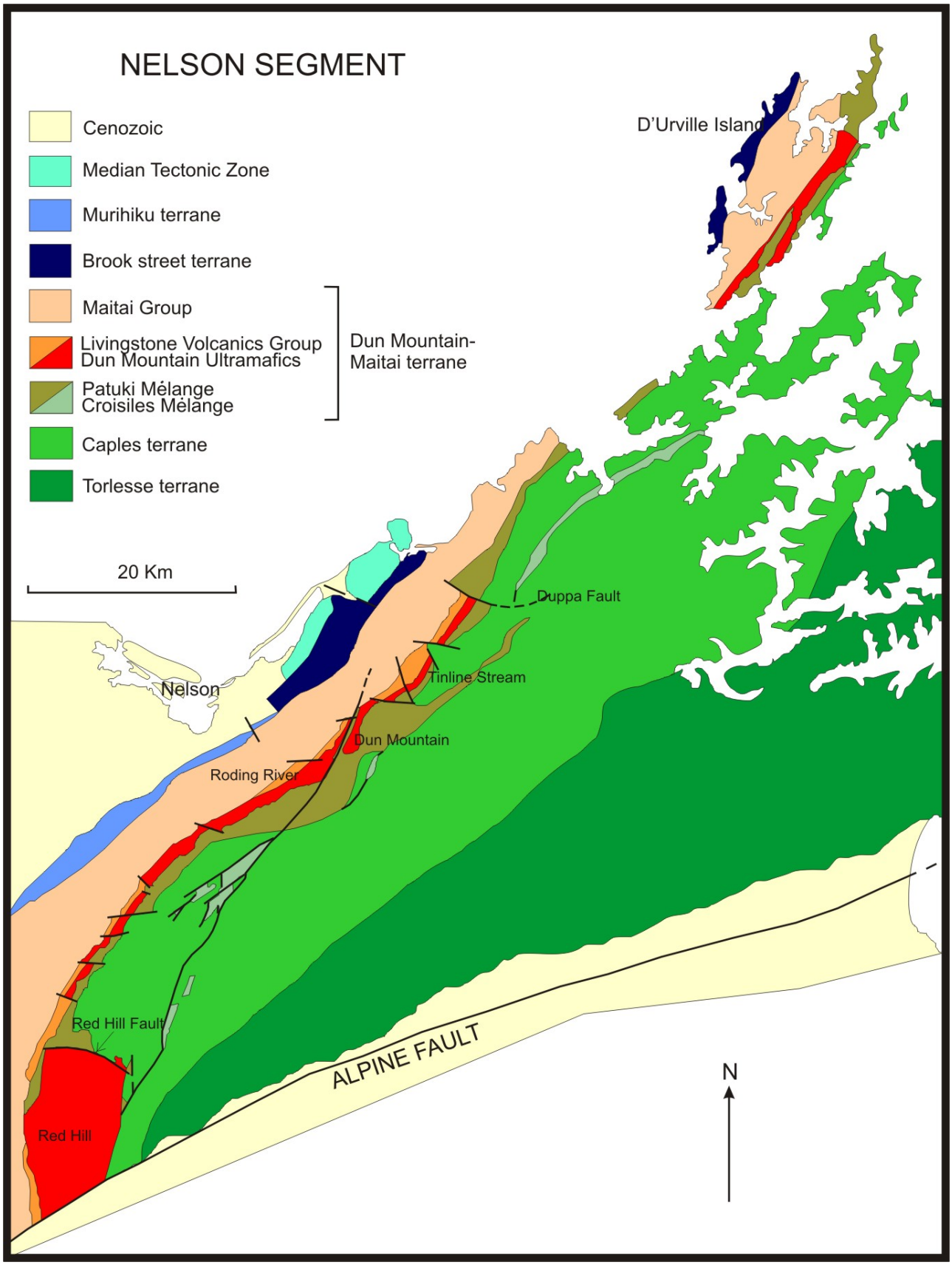

Fig. 2.5: Geological map of the Nelson segment of the DMOB and surrounding terranes. Modified from Kimbrough et al (1992).

Consistently steep to overturned DMOB and the Key Summit-Roding Synform, are probably the result of folding during terrane accretion to the Gondwana margin during the Mesozoic (Cawood, 1987). Deformation during the oroclinal bending and numerous orogens has further deformed the belt.

2.4 Metamorphism

The metamorphic history of the DMOB is complex. Early metamorphic events are characterised by low-pressure sea-floor amphibolitisation, affecting lower crustal and mantle during the formation oceanic crust. Later, regional events caused high-pressure metamorphism to greenschist, pumpellyite-actinolite and locally, lawsonite-albite-chlorite or prehnite-pumpellyite facies. This later overprint affected rocks of the Livingstone Volcanics Group and overlying Maitai Group sediments (Coombs et al., 1976).

2.5 Age

A number of geochronological studies have been conducted in recent times along the length of the South Islands DMOB. Kimbrough et al (1992) used zircon U/Pb method on zircon found within plagiogranite and determined ages of 275-285 Ma at a number of locations along the belt. Sivell and McCulloch (2000) report a reliable isochron age of 278 +/- 4 Ma from the analysis of Sm-Nd isotropic data for younger volcanics in the Nelson area. They also give less precise Nd-isotope ages of 308+/- 12 Ma and 295+/- 24 Ma, for older volcanics. Most recently, Jugum (pers. comm..,2008) obtained zircon U/Pb ages of 269 +/- 2 Ma for Plagiogranites near Otama (Lintley-Otanomomo segment), 275 +/- 2 Ma for Early Plagiogranite in the Livingstone Mountains and 276 +/- 2 Ma for Plagiogranite Breccia Pipe near Lake Never (both within the Mossburn-Red Mountain segment). Most ages lie in a narrow band between 270-280 Ma, apart from Sivell and McCulloch (2000) older 295-308 Ma dates.

2.6 Geochemistry

Geochemistry was used for the first time as a discriminator for tectonic setting by Sinton (1975) who worked in the extensive Red Mountain area. He noted that there were apparently two suites of geochemically distinct rocks found within the ophiolites body. These results were achieved by analysis of field relations and chemical composition variations. Three evolutionary stages were deduced. Stage I involved the development of lower crustal and mantle rocks. Stage II, being closely associated, involved intrusion of dikes and eruption of lavas, with compositions similar to modern MORB spreading centers. Stage III magmatism is dominated by differentiated volcanism, typical of an island arc setting. A later paper by Coombs et al (1976) reconfirmed this.

Sivell (and others) (Sivell, 1988; Sivell, 2002; Sivell and McCulloch, 2000; Sivell and Rankin, 1982) have published extensively on the geochemistry in the DMOB. Sivell has worked exclusively on the DMOB in the Nelson region, particularly D'Urville Island. Sivell and McCulloch (2000) used discrimination techniques involving isotropic and geochemical components in combination with field studies to develop an evolutionary model for the DMOB. Three magma stages are defined from the upper crustal lavas and intrusives: Stage 1 primary pillow basalts have geochemical characteristics similar to MORB. Overlying stage 2 sheeted flow basalts resemble depleted BABB. Stage 3 mafic to silicic magmas intrude these, and have a distinct subduction related geochemical signature, similar to island arc tholeiites found in immature arcs. Sivell and McCulloch (2000) conclude that contrasting compositions of the three stages of magmatic suites suggests that pre-existing crust, probably of back-arc basin origin (stage 1 and 2 magmas), was intruded by stage 3 magmas of the onset of subduction at c.278 Ma.

Sano et al (1997) worked on the geochemistry of dike rocks in the Nelson segment of the DMOB. Samples were taken from the Livingstone Volcanic Group at Roding River and the Dun Mountain Ultramafics Group. Differences were found in the major and trace element compositions. Dike from the Livingstone Subgroup were found to have MORB or back-arc basin affinities, the Red Hills basalts having an island arc affinity.

Chapter 3: Introduction to the Geology of the Bryneira Range

3.1 Location of the study area

The area chosen for this study was the northern half of the Bryneira Range in Western Otago, South Island, New Zealand (Fig.3.1). It forms an elongate mountainous ridge, running northeast-southwest, parallel to the main axial ranges of the Southern Alps. The Bryneria Range is bounded by rivers, the Pyke River to the west and the Olivine River and Hidden Falls Creek, both to the east. The latter two rivers are anticedent, and truncate the range at each end. To the north the Olivine River swings to the west to join the Pyke Valley, in the south Hidden Falls Creek cuts west to join the Hollyford valley.

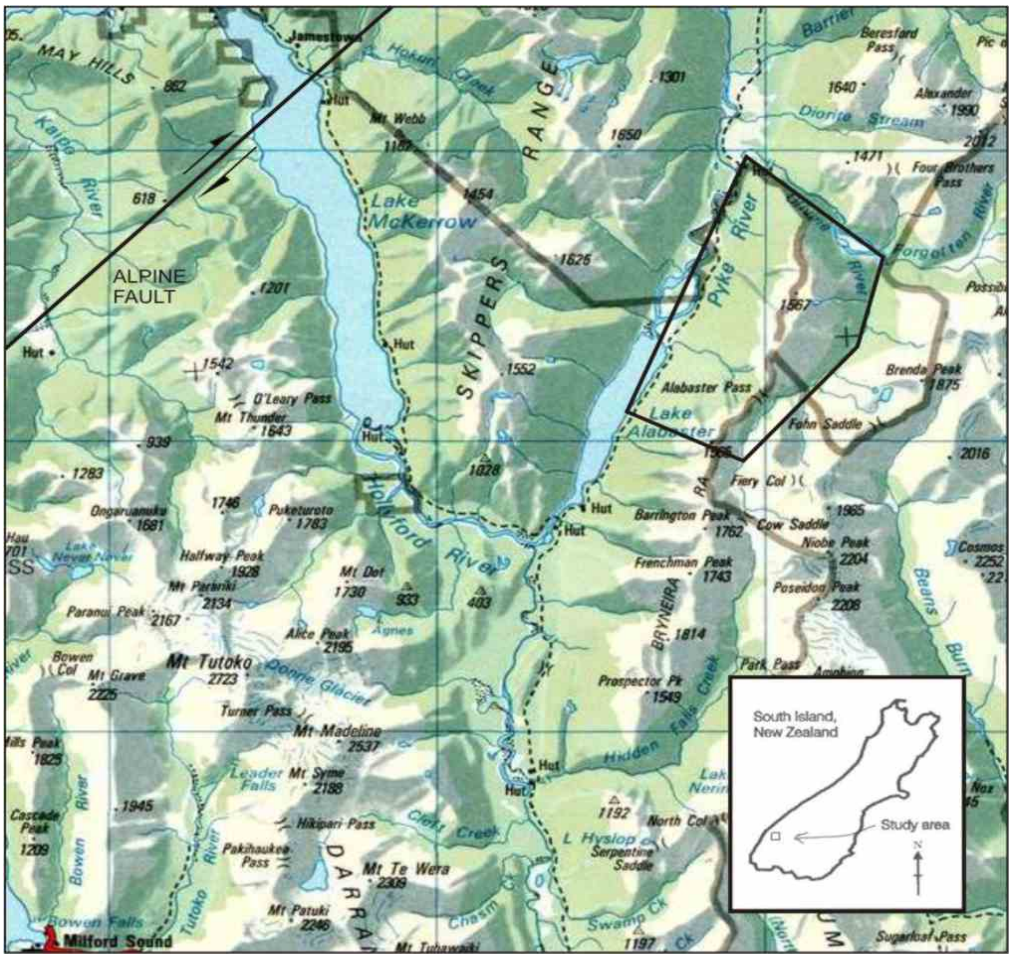

Fig. 3.1: Location of the study area. Grid spacing is 10km. Source: MapToaster ((2001))

In the northern half of the Bryneira Range (Fig 3.2 A and 3.2B), the DMOB (Dun Mountain Ophiolite Belt) is exposed above the bush line. Clear exposure was key for this study, as thick bush found on the mountain flanks makes detailed observation unattainable. Major lithological contacts are evident by remote observation of topographic and vegetation changes, both above and below the bush line. Geologically, this section of the DMOB is the last intact crustal section before the belt is tectonically thinned towards the south. Further south, the Maitai Group sedimentary units dominate the geology of the Southern Bryneria Range as the DMOB thins to a narrow band ~1km wide (Hyslop, 1978; Turnbull, 2000).

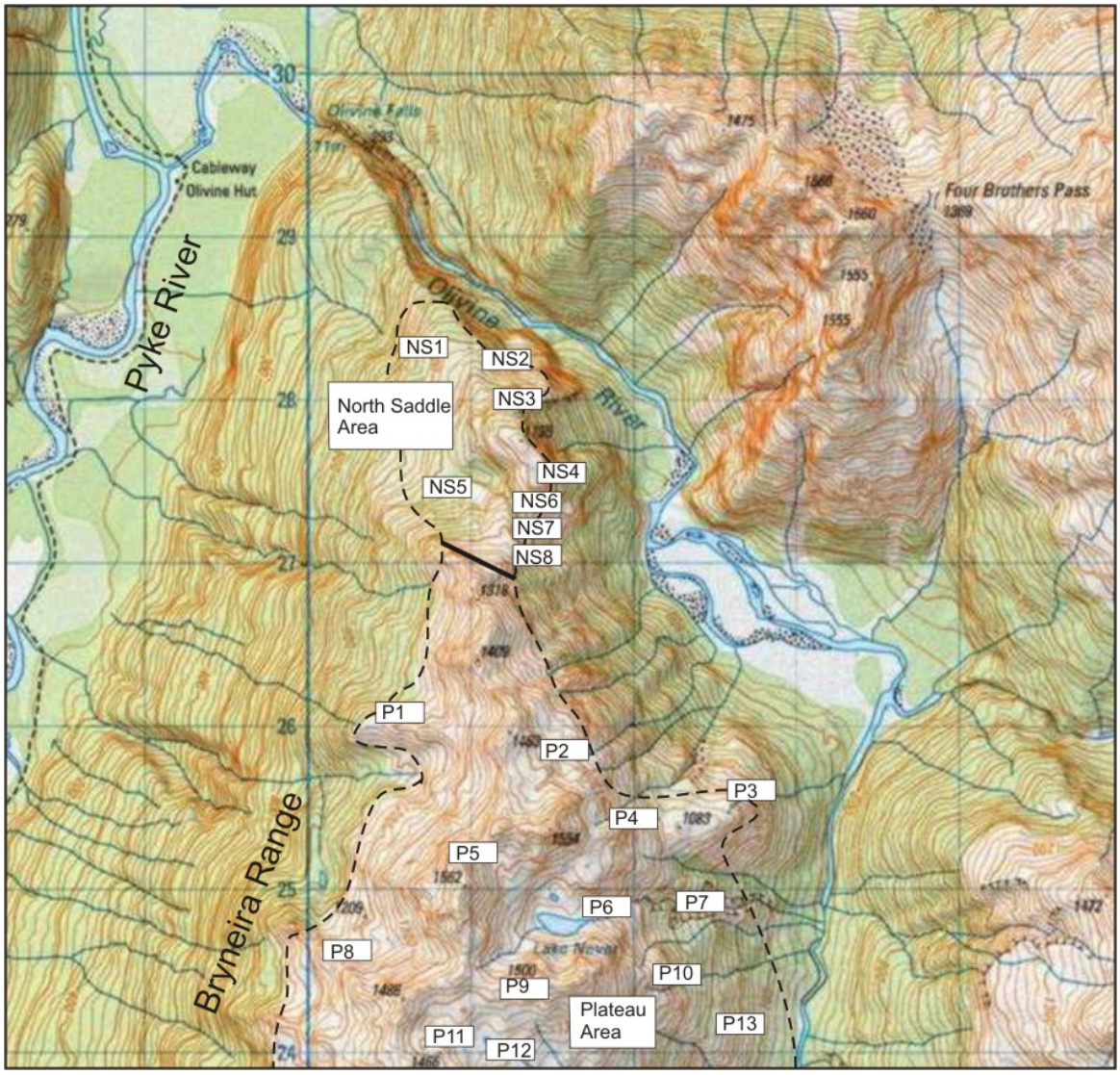

Fig. 3.2A: Map of the northern half of study area. White rectangles mark the approximate position of outcrops referred to in the text. Dashed line shows the approximate boundary of workable outcrop. The solid line shows the boundary between outcrop areas. Grid spacing 1 km. Source MapToaster (2001).

The quality of the exposed rocks in the Northern Bryneira Range is variable, with much of the area covered in broken rock and scree. Investergations focused on small glacially smoothed sections where the relationshps between lithologies were clear. Information was collected in detail on various scales and compiled to give a full record through the DMOB cross-section (see figures 3.3 and 3.7).

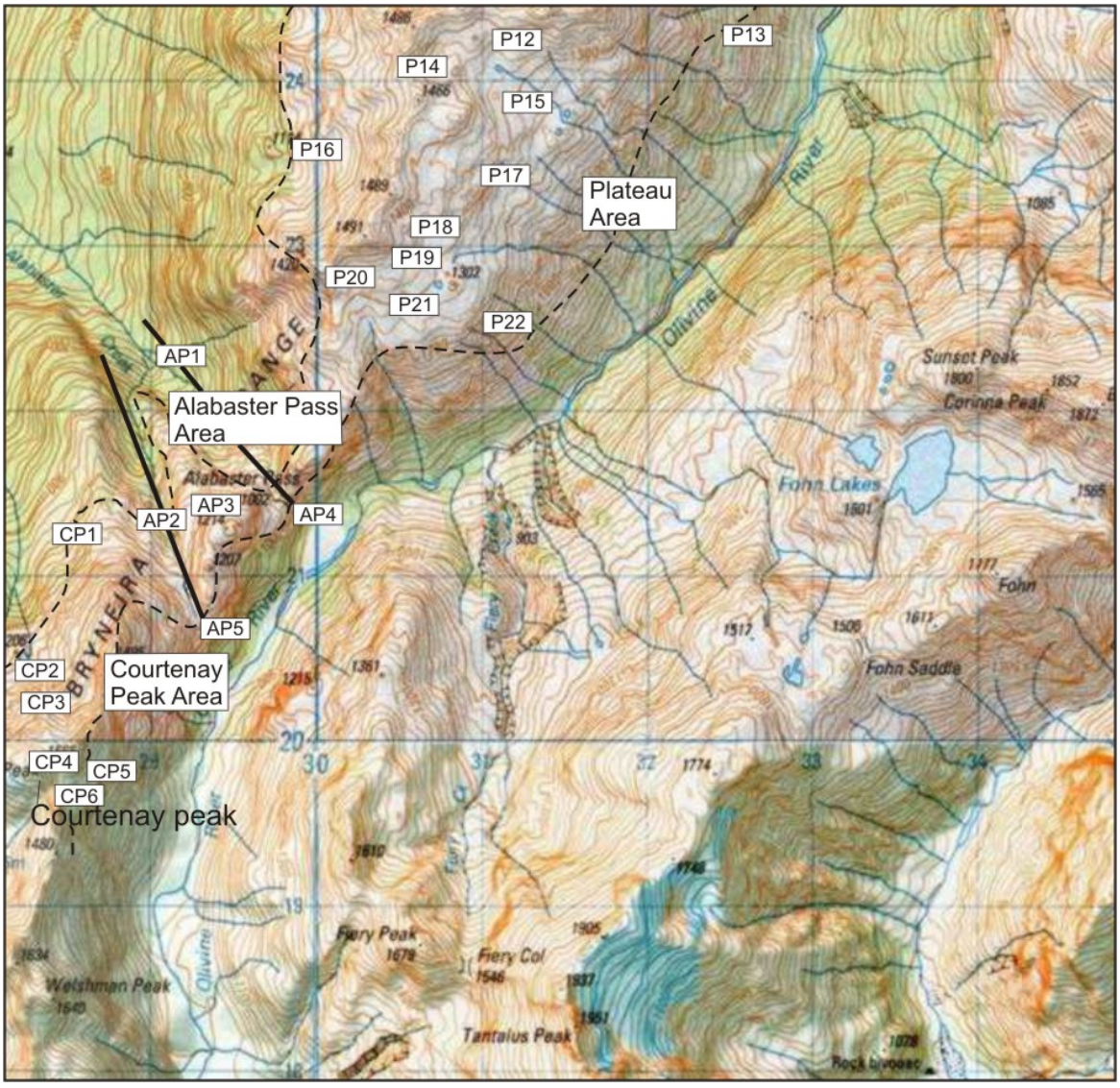

Fig. 3.2B: Map of the southern half of study area. White rectangles mark the approximate position of outcrops referred to in the text. Dashed line shows the approximate boundary of workable outcrop. Solid line shows the boundary between blocks. Grid spacing 1 km Source MapToaster (2001).

The length of the study area was divided into four blocks, each of characteristic morphology and structure. Each block is coded with a prefix (NS for North Saddle Area, P for Plateau Area, AB for Alabaster Pass Area and CP for Courtenay Peak Area), followed by a number relating to an outcrop where observations were recorded (for example, NS 5

in Fig.3.2a). This outcrop coding system is employed in the text as a means to quickly identify a geographic location.

3.2 Geological overview of the study area

The Bryneira Range area essentially represents a cross-section through the Dun Mountain-Maitai terrane, having been rotated into a sub-vertical orientation. In the west, the younger Maitai Group sediments overlie the Dun Mountain Ophiolite, the basement of the Dun Mountain-Maitai terrane. A generalised lithological column for the Dun Mountain-Maitai terrane is shown in figure 3.3. The Hollyford Fault truncates the top of the Maitai Group and the base of the Dun Mountain Ophiolite abuts the Livingstone Fault. Both are discussed in the structure chapter (Chapter 4).

As the Bryneira Range is in close proximity to the Red Mountain Block to the north, the same nomenclature used by Turnbull (2000) and Sinton (1975) is applied to the structures and lithologies observed in the study area.

The **Dun Mountain Ultramafics Group** (DMUG) is predominantly made up of sheared serpentinite, and runs the entire length of the study area, immediately west of the Livingstone Fault. The characteristic red-brown weathering of these ultramafic rocks is reflected in the names of many local topographic features (for example, Firey Col). From Firey Col in the south, Dun Mountain Ultramafic Group can be traced along the Olivine Bench, across the Olivine River, towards Four Brothers Pass north of the study area (Fig 3.4), reaching maximum ~1.5 km thickness on the Olivine Bench. The Dun Mountain Ultramafics Group represents the incomplete mantle portion of the DMOB.

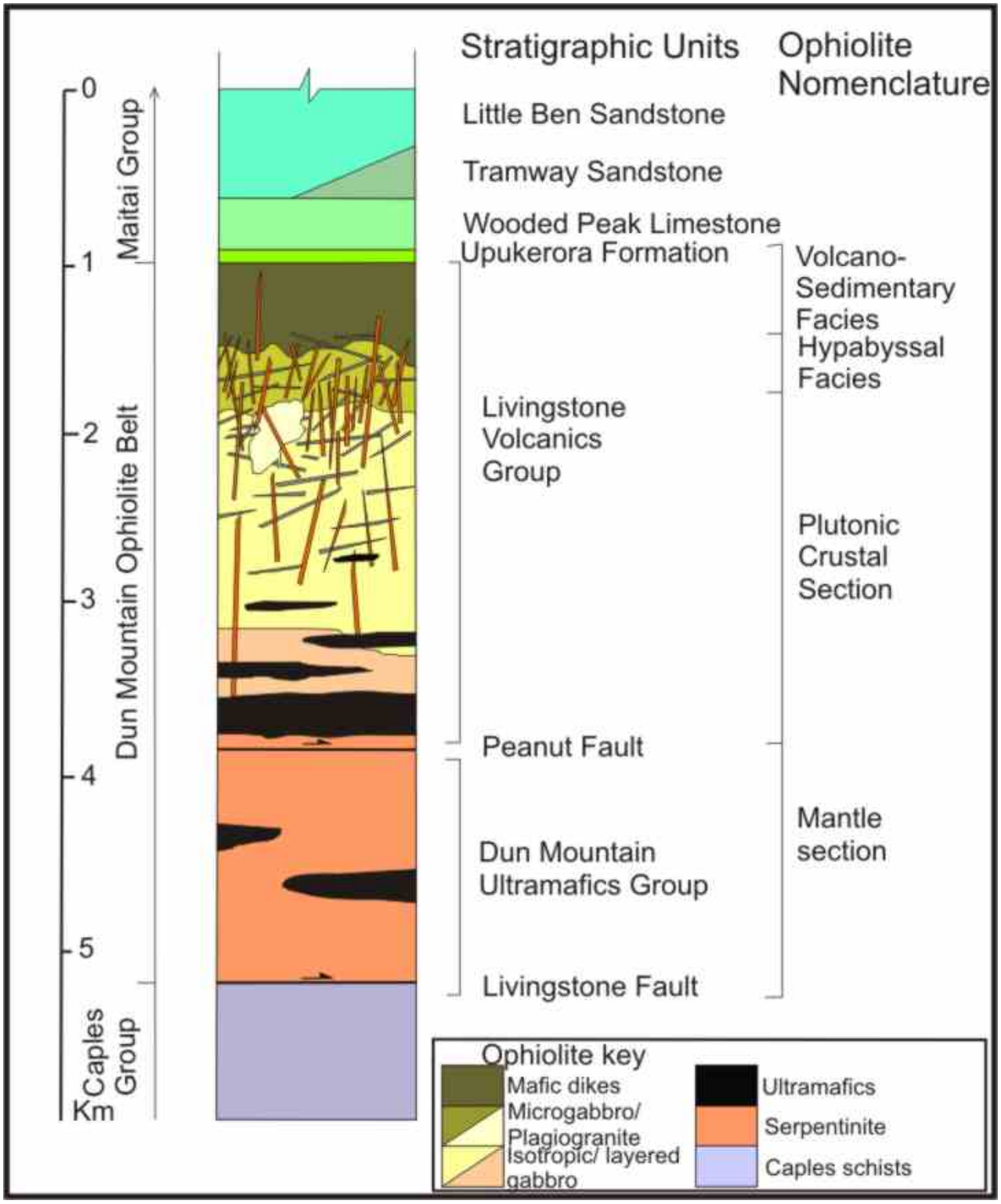

Fig. 3.3: Generalised lithological column of the Dun Mountain Maitai terrane though the Bryneira range study area.

Fig. 3.4: Photo of DMUG general landscape, looking from the Bryneira Range towards Cow Saddle. Livingstone Subgroup in the foreground, distinct orange DMUG rocks in the middle-ground and Caples terrane form the sky-line ridge.

The **Livingstone Volcanics Group** is the crustal portion of the ophiolite, comprising of ultramafics, gabbros, intrusive sheets and volcanics. This group forms the bulk of the DMOB in the study area, being ~2.5-3.5 km thick, with the gabbroic portion roughly following the ridge crest of the Bryneira Range (Fig. 3.5). The Northern Bryneira Range has some of the best and thickest exposures of Livingstone Volcanics Group in the entire DMOB.

Fig. 3.5: Photo of Livingstone Volcanics Group general landscape. Looking north across the Plateau Area, parallel to the range.

Above the DMOB are the **Maitai Group** rocks. Few exposures are seen in the study area because of the dense and steep vegetation that conceals it (Fig. 3.6). The Maitai Group consists of well-bedded metamorphosed sedimentary rocks (Turnbull, 2000). The sedimentary contact between Dun Mountain Ophiolite and Maitai Group was observed in one location (CP4), where the upper most weathered pillow lavas contact the **Upukerora Breccia**, a distinctive polymictic igneous breccia and the first member of the Maitai Group. In sharp sedimentary contact with the breccia is the **Wooded Peak Limestone**, a turbiditic limestone containing atomodesmatinid prisms (Kimbrough et al., 1992). Underlying limestone was could be made out in bush-clad hill slopes by karst surfaces and benching of the mountain flanks (fig. 3.6). The Wooded Peak Limestone is estimated to be ~500 m thick for the length of the study area. No higher units in the Maitai group were recorded, but what was probably the **Tramway Formation** was noted at point 344m

above the Pyke River and Alabaster Creek (GR. D39 280235). The Maitai Group sediments are truncated by the Hollyford Fault in the Pyke Valley (Turnbull, 2000).

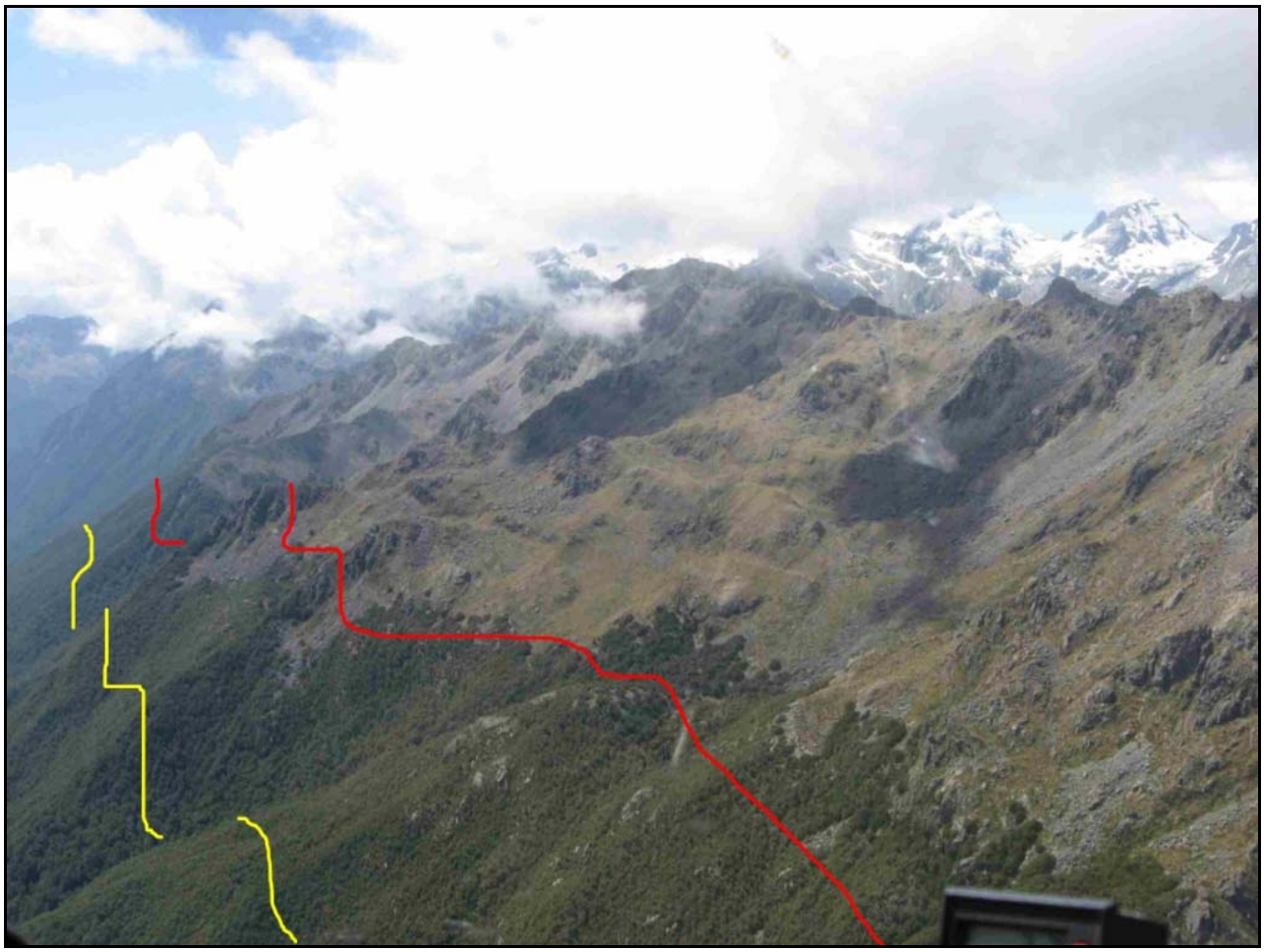

Fig. 3.6: Photo of the upper Livingstone Volcanics Group and Maitai Group general landscape, looking northeast across the western flanks of the study area. The yellow line indicates the approximate position of the Maitai Group-Livingstone Volcanics Group contact. The red line shows the approximate position of the contact between the volcanic and hypabyssal facies in the Livingstone Volcanics Group.

The Maitai Group rocks are folded to form the regionally extensive Key Summit Syncline (Turnbull, 2000). In the study area, this structure is preserved with the western limb partially truncated by the Hollyford Fault and has a slight plunge to the south.

3.3 Ophiolite Pseudostratigraph

The DMOB pseudostratigraph is shown in the five columns of Figure 3.7., from the four previously defined areas (NS, P, AP, CP). Each column represents a portion of the total ophiolite thickness; the entire sequence was never exposed with out interruption by bush, topography or faulting. The approximate position of each column is marked on the accompanying map.

Below, the typical lithologies found in the mantle section and crustal section (containing; plutonic crustal section, hypabyssal and volcano-sedimentary facies (division after: Schroetter et al (2003)) are described. There was no definitive division between these facies. All rocks in the crustal portion are affected by pervasive intra-oceanic hydrothermal metamorphism, the prefix meta- is applicable to all rock names but will be emitted from the following discussion.

3.3.1 Mantle section

The term ‘mantle section’ is used here to describe the Dun Mountain Ultramafics Group. In the Northern Bryneira Range the Dun Mountain Ultramafics Group is on average ~1200m thick, compared with 4800m at Red Mountain in the north, 1100m at Cow Saddle and 400m at Serpentine Saddle, both to the south (Hyslop, 1978). Sheared serpentinite encloses small tectonic inclusions (1-50 m^2) of serpentinised peridotite and dunite. Highly disrupted mafic dikes were rarely observed.

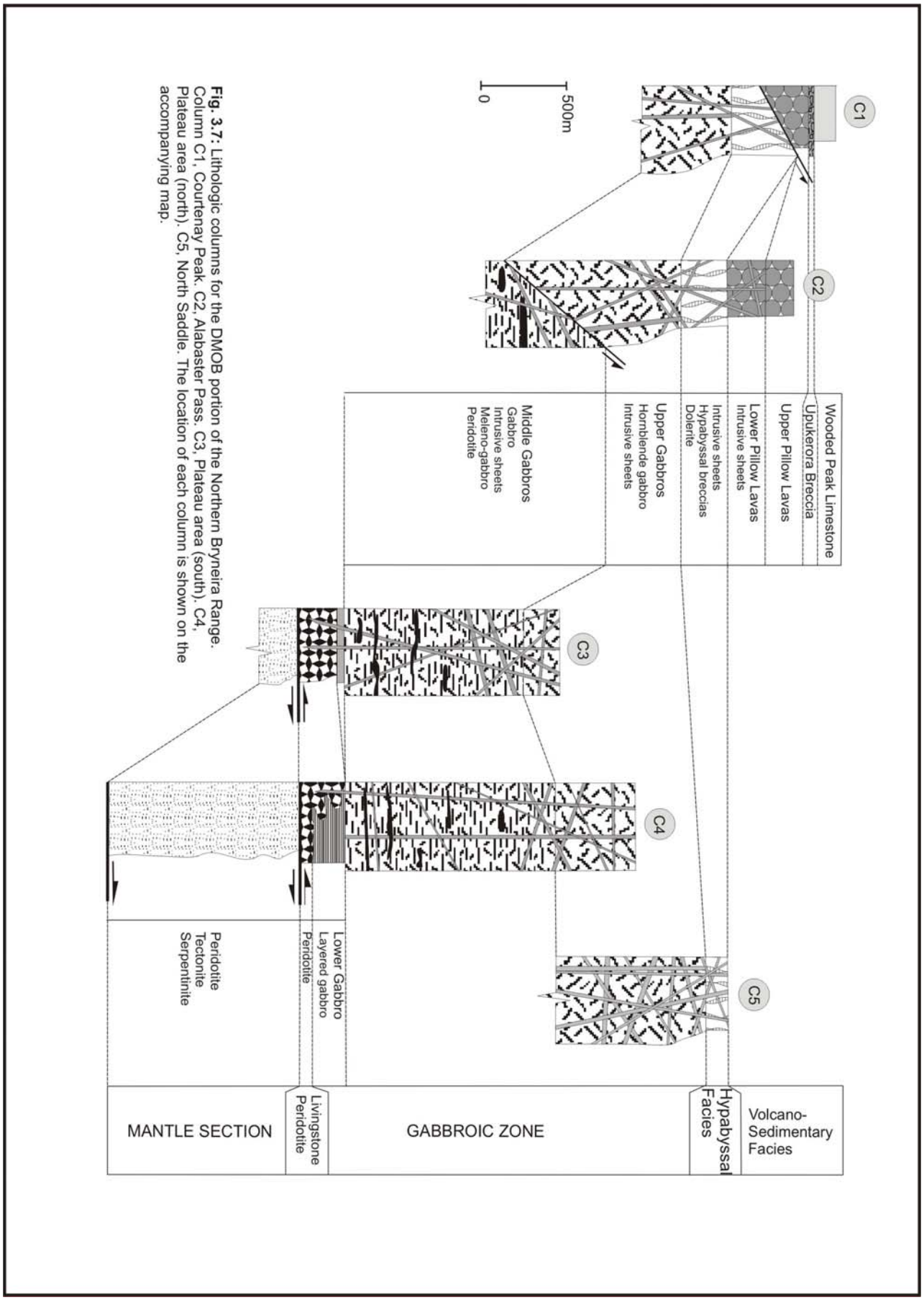

Fig. 3.7: Lithologic columns for the DMOB portion of the Northern Bryneira Range. Column C1, Courtenay Peak. C2, Alabaster Pass. C3, Plateau area (south). C4, Plateau area (north). C5, North Saddle. The location of each column is shown on the accompanying map.

Most of the serpentinite is a highly sheared, dark green variety. Lesser amounts of a more coherent dark grey serpentine forms discontinuous bodies lower in the mantle section. Serpentinite is highly fractured by chaotic joint sets, which yield no common orientation. A large zone of shearing is similar to Sinton (1975; 1980) description of the Peanut Fault at Red Mountain (see section 4.1.5.2). The brittle nature and lack of cohesion between the blocks suggest that these sheared zones are recently re-activated features (Fig.3.8).

Mafic dikes observed in lower Red Mountain Ultramafics are metasomatised to rodingite (Hyslop, 1978; Sinton, 1975) and highly disrupted. Few examples of these dikes were encounted in the study area, the largest being 3m wide and traceable for 15m.

Small areas of serpentinised ultramafics show relic crystalline texture. Pyroxene often remains unaltered and olivine is completely replaced by serpentinite. Chromitite was seen in high concentration in a few locations within the serpentinised peridotites. Chromitite concentrations are enclosed in serpentinised dunite (Fig 3.9), outcrops were generally $<5m^2$.

The poor preservation of the mantle section provided little conclusive information with regard to the thinning of the DMOB. It is probable that Mesozoic to recent deformations have taken advantage of more malleable serpentinite. Consequently, little time was spent within the mantle section.

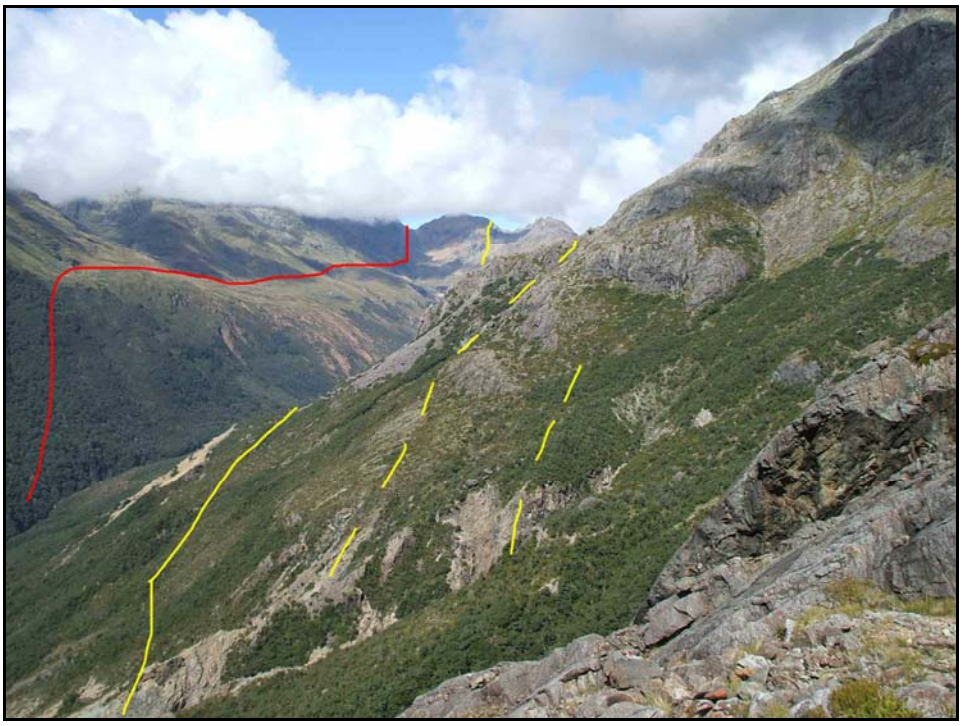

Fig. 3.8: Photo looking south from P7, showing the Livingstone Fault (red line), cutting across the Olivine Bench to Fiery Col in the background. The Peanut Fault (yellow solid line) is seen here cutting a bench in the eastern flank of the Northern Bryneira Range, passing out of view to reappear in a col west of Fiery Col. Dashed yellow lines are approximate positions of shear zones associated with the Peanut Fault.

Fig. 3.9: Chromite concentrations within serpentinised dunite. This example is a scree block found close to the Peanut Fault.

3.3.2 Plutonic crustal section

The Plutonic crustal section is divided into two zones based on textural and compositional changes. The boundaries of these zones are hard to define due to the structural history of the belt. The two zones being: 1) Livingstone Peridotite zone. 2) Gabbroic zone.

3.3.2.1 Livingstone Peridotite zone

Above the Peanut Fault, away from the intense deformation and serpentinisation, is the Livingstone Peridotite, containing ultramafics and meleno-gabbros for a preserved thickness of 400-500m. Variability in thickness and serpentinisation of the lower portion of this zone made discrimination from the underlying Dun Mountain Ultramafics Group rocks difficult. Sinton (1975) described this group of rocks as the Livingstone Peridotite, as they form a close association with the gabbros, yet have a very high mafic component. In the Bryneira Range these rocks are Pyroxenitic to Dunitic in mineral composition.

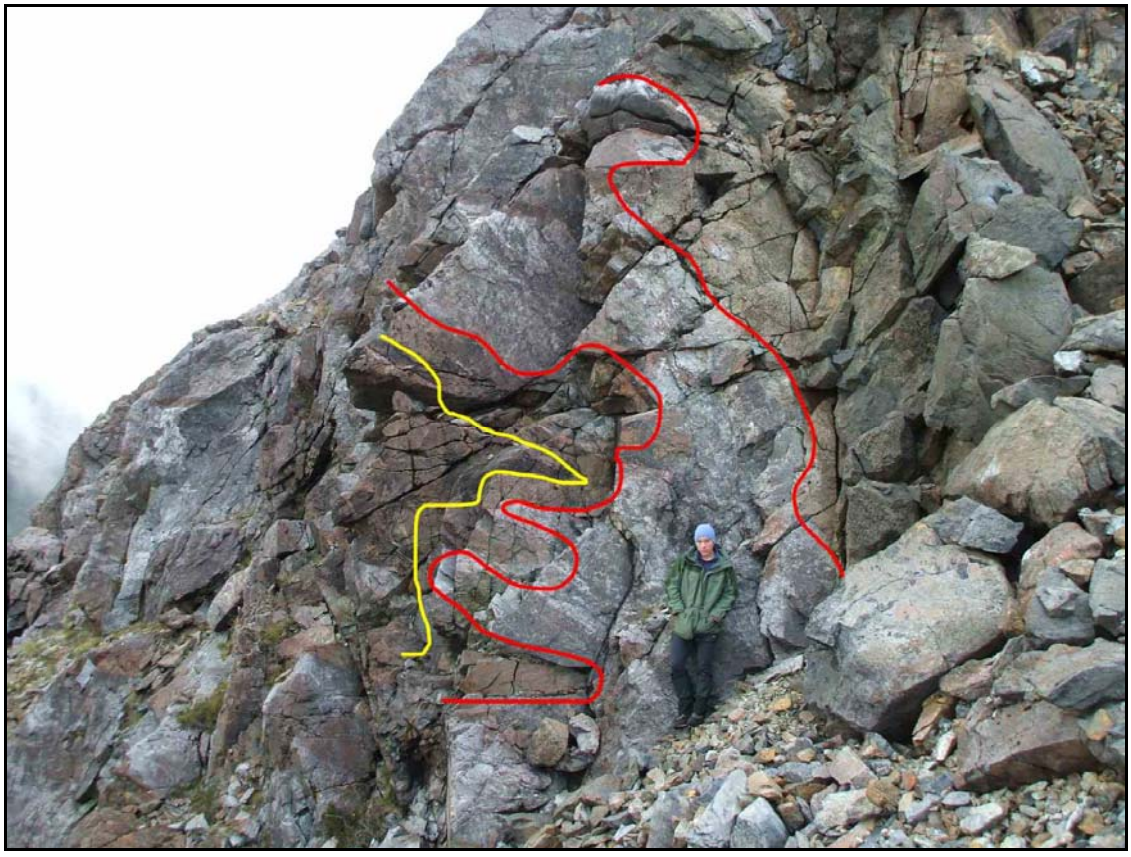

Fig. 3.10: Sharp boundaries between Livingstone Peridotite and layered gabbros. The yellow indicates the gradational boundary between clinopyroxene peridotites and clinopyroxinites. The red lines mark the boundary between clinopyroxinites and layered gabbros. Photo taken at P22.

At the base of the Gabbroic zone, the Livingstone Peridotites have a sharp contact cutting layered gabbros (Fig. 3.10). A clinopyroxenite layer, from 5cm to 5m thick, often rims contacts with gabbroic rocks (Fig. 3.10). Wehrlites containing feldspar usually occur close to the gabbroic zone. Variably sized inclusions of felsic material are often seen within the peridotites up to 50m below the contact with the gabbroic zone (Fig. 3.11).

Fig. 3.11: Peridotite containing blocks of gabbro that were melted from nearby layered gabbro.

Above the contact with the layered gabbros, a sequence of ultramafic (Livingstone Peridotite) pods or layers is found within the gabbros. Initially these bodies are up to 50m thick and are semi-continuous along strike, but decline in thickness and continuity up section to appear as elliptical pods (Fig. 3.12). Often tarns and depressions would indicate the whereabouts of these rocks, due to the ease in which the ultramafics weather. These layers repeat up section approximately 3-4 times. Sinton (1975) gives a

detailed account of these cyclic, clinopyroxene peridotites and the changing petrology up section.

Fig. 3.12: An ultramafic 'pod' about 25 m across. The majority of this 'pod' is clinopyroxene peridotite, near the sharp contacts with surrounding cumulus gabbros there is 20cm of feldspar baring clinopyroxene peridotite, probably assimilated during injection.

Ultramafic rocks of the Peridotite zone range from cumulate dunites to cumulate clinopyroxenite, with most being wehrlites or feldspathic wehrlites. In general, the higher concentrations of olivine are found towards the lower portion of the zone. Clinopyroxene peridotites are fine grain crystalline and weather to a distinctive dark brown (Fig. 3.12). Anhedral clinopyroxene crystals show alteration of serpentinite with magnetite concentrated along cleavage planes. Olivine is often completely pseudomorphed by serpentine and chlorite, leaving a mesh like pattern. Any feldspar (occasionally present) is completely replaced by very fine grain alteration products (clay minerals).

3.3.2.2 Gabbroic zone

The gabbroic zone is the most complete of the plutonic crustal section, having a preserved thickness of ~2000-2500 m thick in the study area. The gabbroic zone is here divided in to three portions; lower, middle and upper gabbros. Each portion corresponds to textual change, these being layered, cumulate and isotropic zones respectively. The gabbroic zone is cut by the all intrusive sheet phases (see section 3.4.3).

Lower/Layered gabbros:

The layered gabbros showed variation in thickness along the belts strike. The largest area being seen at P3, where a ~400m by 200m block is surrounded by variably serpentinised ultramafics. All other occurrences were seen above the Peanut Fault in isolated or semi-continuous bands, running a few hundred meters along strike and no thicker than 100m. A contact between the layered and isotropic gabbros was not observed but Sinton (1980) suggests it is gradational in nature. Layering orientation was recorded at all outcrops to be used as potential paleo-horizontal indicators (see section 5.1).

Layered gabbros were observed in two textural forms; modal (gradational segregation of felsic and mafic bands, figure 3.13) and isomodal (discrete bands of felsic and mafic minerals, figure 3.14) grading of mafic minerals (after Nicolas, 1989).

Modally graded layering in the layered gabbros is predominant (>90%, Fig. 3.13), and commonly found close to the contact with the underlying Livingstone Peridotite. Layering is varied from millimetre to meter scale ‘beds’, but typically forms 1-5cm layers over which the mafic component increased downwards to a variable maximum, in a cyclic manner. Modally layered gabbro contains relic feldspar and clinopyroxene, with small amounts of magnetite and brown hornblende. Brown hornblende is commonly seen around grains and along cleavage plains of clinopyroxenes. It also forms a close association with magnetite, which it often envelopes. Relic feldspars are recrystallsed with metamorphic clay minerals, appearing as grey, translucent masses in thin section.

Isomodal layering is encountered within the lower isotropic gabbros (Fig. 3.14) and is typically found in small isolated outcrops. Isomodal layering forms semi-continuous bands

where mafic and felsic rich layers are completely separated. Mafic layers are 0.5-3cm thick, and felsic layers being 3-20cm thick. There was considerable grain size variation between layers, spanning the medium to fine grain crystalline range. Isomodal layering was found within the lower and middle gabbros, it is not thought too be related to modal layering and was rarely observed.

Fig. 3.13: Modally graded layered gabbro seen here at P3. This example shows large variation in layer thickness.

Fig. 3.14: Isomodal layering of gabbro within cumulate gabbros. Note the variation in layer thickness of the mafic rich layers.

Middle/cumulate gabbros:

The cumulate gabbros are complex and have rapid vertical and lateral changes in texture and composition (Fig. 3.15). Detailed mapping of gabbros was not feasible due to poor exposure, continuous disruption by intrusive sheets and faulting. The middle isotropic gabbros form a ~600-800m thick zone. Relationships between gabbros of different composition are often ductile or brittle in nature. Gabbros generally become more felsic and uniform up section. Large blocks of lithologies belonging to layered gabbros and ultramafics are found within the middle isotopic gabbros. It is hard to tell if these blocks were rafted up from below or are part of non-planer boundaries at the base and sides of partially crystallised, periodically replenished magma chambers. Organization is on a gross scale, with inter-layered units of; gabbros, clinopyroxene-brown hornblende gabbro, rare norites and anorthosites. Sinton (1975) gives a detailed account of the cyclic nature of the lower layered gabbros and middle isotropic gabbros. He associates the repetition of

units to crystallisation rate and/or temperature gradients within the magma chamber. Similar repetitive cycles were noted in the Bryneira Range.

Textural variation within the middle gabbroic portion common, but generally most have a medium crystal grain size and cumulus crystal relationships. Occasionally linear fabrics indicate magmatic flow, by alignment of crystals. Weathering and metamorphism has affected the original mineralogy of these gabbros. In most cases, original mafic minerals have been completely replaced or psudomorphed by brown hornblende and occasionally chlorite. Feldspars are now cloudy, commonly albitised or replace by secondary assemblages, particularly actinolite, prehnite and possibly pumpellyite (Hyslop, 1978; Sinton, 1975). All olivine is serpentinised.

Fig. 3.15: Typical isotropic gabbros from low in the gabbroic zone, pictured here at Lake Never (P6). The red gabbro on which the hammer lies is highly altered olivine-clinopyroxene gabbro, relic oikocryrsts are visible as black spots. The white gabbro is clinopyroxene-brown hornblende gabbro.

Upper/isotropic gabbro:

Cumulate gabbros gradationally give way to less mafic upper/isotopic gabbros (Fig. 3.16). The upper gabbros contain predominately hornblende gabbro with minor compositional variation, plagiogranite and schistose amphibolites occur rarely and structural complexities rapidly lessen. Hornblende gabbros are usually medium grained hypidiomorphic (subhedral) texture, coarse grain varieties occur locally, as well as isolated pegmatite. Brown hornblende found in the middle isotropic gabbros are replaced by green hornblende in the upper isotopic gabbros.

Fig. 3.16: Typical isotropic gabbro seen in the upper portion of the gabboic zone. Close to the hammer is coarse grain, further to the left is a more typical medium grain size. An orange intrusive sheet is seen to the right of the hammer.

Schiotose amphibolite was seen in one location (P19), structurally above the plagiogranite described below. It is are grey-green in colour, fine grained and distinctively banded in fresh exposure. These rocks appeared gradational to adjacent gabbros, but a

full interpretation was obscured by scree. Dikes with chilled margins (orange intrusive sheets, see later) crosscut the schistose amphiobolite and the area adjacent to it. Schistosity is controlled by concentrations of amphibole and felsic minerals. A consistent orientation for the schistosity was not determined. Boudinage of planes within the rock (Fig. 3.17) and anastomosing lensodal packets indicate deformation by extension in an unconsolidated state.

Fig. 3.17: Schistose amphibolite seen here in a boulder below an escarpment. Note the boudinage orange layer below the adze of the hammer.

Only one large plagiogranite body was seen study area and formed a massive but generally lobate mass (Fig. 3.18). Contacts with the surrounding gabbro and dike rock are both intrusive and faulted, small dikes of plagiogranite intruding upwards from the main body for ~100m. At least one phase of dikes cut the plagiogranite. Plagiogranites contained quartz, albite, actinolite and minor chlorite.

Fig. 3.18: A large outcrop of plagiogranite seen at P18. Plagiogranite is the white rock in the middle distance, the skyline length of the field of view being approximately 600m**.**

3.3.3 Hypabyssal facies

The Hypabyssal facies are the rock found between the extrusives and the gabbros. In the Bryneira Range this is a poorly defined zone atypical of most ophiolites, where usually a sheeted dike complex develops. Two hypabyssal facies occur above the plutonic crustal section, the major being the intrusive sheets and minor one being dolerite. The term ‘intrusive sheet’ is used here to describe a sill or dike, as ‘sill’ and ‘dike’ imply some knowledge about their original orientation.

At the top of the upper gabbros there is a change to dolerites of the hypabyssal facies. Dolerites are fine grain hornblende gabbros, making distinction between what is dolerite or intrusive sheet difficult, as both have similar field appearance. It is possible that some of these rocks are recrystallsed intrusive sheets, which no longer display their original morphology.

Fig. 3.19: Intrusive sheets cutting middle isotropic gabbros at P4.

Intrusive sheets are found in the mantle and crustal portions of the DMOB. In the Dun Mountain Ultramafic and lower gabbros, few intrusive sheets were seen. Concentrations of 20-30% were seen in the middle gabbros (Fig. 3.19), with abundance increasing up through the upper gabbros (Fig. 3.20). In the hypabyssal facies, intrusive sheets locally occupy a maximum of 80-90% of the outcrop, but more commonly 30-50%. The transition from intrusive sheets to extrusive volcanics varies. At some locations dolerites were followed by a zone of blocky dikes with 5 cm thick chilled glassy margins until the first pillows were seen ~50m up section (e.g. CP4). In other places intrusive sheets cut through pillow lavas, occasionally including them as breccia packets. Above the hypabyssal facies, intrusives decrease until 100% pillow lavas (e.g. NS1) are seen.

Intrusive sheet thickness varies between 5cm to c. 15m, but they are most commonly 0.5-1.5m thick. Cross cutting between dikes of the same or different composition is widespread. Crystallinity of intrusive sheets varies from very fine to fine grained, ranging

from doleritic to aphyric textures. Most have 1-3cm chilled aphyric margins, often jointed by a chill fracture pattern. The width of a chilled margin is dependent on the width of the sheet and/or relative temperature of the surrounding country rock. Generally, there is a tendency for the younger sheets in any crosscutting relationship to be finer grained (also noted by Sinton, 1980).

Fig. 3.20: Intrusive sheets cutting upper gabbros at NS8. This example illustrates “pseudo-sheeting” where clusters of intrusive sheets are stacked in groups of 3-6. Red lines highlight younger intrusives and yellow lines highlight older intrusives, the letter ‘a’ highlights septa of gabbro.

Two locations were found where small areas (1-2 m^2) of hydrothermal sulphide deposits rotted and stained wall rock (Fig. 3.21a). Both locations (NS1 and AP3) were found near the hypabyssal-volcanic facies transition, where the first of the pillow lavas were recorded. At NS1, metallic deposits of pyrite were clearly visible (Fig.3.21b).

Fig. 3.21: A) Rusty stained pillow lava around a fissure containing sulphide rich precipitates. **B)** A close-up of hydrothermally deposited sulphides, note the metallic luster in places.

3.3.3.1 Intrusive Sheet Chronology

A number of consistently crosscutting intrusive sheet phases have been recognised in the study area, comprising of two major intrusive sheet types and four minor or rare types. Intrusive sheet phases are used in this study to define relative timing of events using a known crosscutting order. A clear understanding of their characteristics and order is crucial in the following chapters. Here, each of the intrusive sheet types are described and summarised as a final table (Table 1).

Major intrusive sheet phases;

Grey Intrusive sheets (GIS) are the first major phase of intrusion. They are typically grey-to-grey-orange in weathered appearance and consistently light grey in fresh samples (Fig. 3.22). GIS are found within the lower isotropic gabbros through to the lower pillow lavas. Nowhere are they seen cutting layered gabbros. Widths ranged from ~10cm to 4m, a general increase in size is seen up section, at maximum they occupy up to 30% of an outcrop. Each GIS is well separated by a septa of ‘country rock’; no sheeting (consecutive stacking of intrusive sheets) was observed. Chilled margins on GIS increase in thickness up section from the middle gabbros where there is slight fining of grain-size towards the margins, to 2 cm to 4 cm of chilling in the extrusives. Cross-cutting and chilled margins suggest injection occurred during and after a main magmatic phase responsible for growth the host gabbros.

Textures of the GIS range form fine to medium grain holocrystalline. Feldspar phyric GIS with euhedral feldspar lath shapes up to 7mm long, were commonly seen in middle gabbro (also noted by Sinton, 1980). Generally GIS consist of fine grain brown hornblende, highly altered anhedral gains and relics laths of feldspar, with no orientation, are completely recrystallisation to secondary metamorphic assemblages (albite-clinozoisite or albite-pumpellyite Sinton, 1975).

Fig. 3.22: OIS (orange intrusive sheet, see below) and GIS are seen here cutting pillow lavas at AP3. A much wider GIS is crosscut by the OIS and lies under the blue handle of the hammer.

Orange Intrusive Sheets (OIS) are the most prevalent intrusive sheet type. Much variation in colour, distribution, thickness, continuity and orientation is found within the OIS group. Colour ranges from brown-green to bright orange, and is commonly grey-orange (dun) colour (Fig. 3.16, 3.22, 3.23). Thickness ranges from 10cm to 15m, usually ~1.5m. Unlike the GIS, individual OIS can be traced up to ~250m, often sidestepping and

suddenly stopping. OIS are found throughout the crustal portion and probably the mantle portion of the study area. Sheets are spaced, again having septa of country rock separating them. Clustering of three to six thin sheets are commonly seen in the upper gabbros and pillow lava. Small areas are found where OIS dominated the outcrop area (up to 80%), particularly directly under the first pillow lavas (AP3 and CP5) and also within the upper gabbros (NS2). Chilled margins ranging from 2-7cm are present on all OIS contacting country rock, but occasionally absent where OIS of a similar age crosscut. Large variation in colour, orientation, chilling and crustal distribution suggests that OIS magma injection occurred over some time.

The texture of the OIS varies from very fine to fine grain crystalline, most being fine grain. In thin section OIS are equigranular, containing dusty feldspars, quartz, a remnant mafic mineral and limonite. Feldspars are given their dusty appearance by secondary growth of clay minerals. Remnant mafic minerals were probably once amphiboles are now pseudomorphed by chlorite and epidote (Hyslop, 1978; Sinton, 1975). Some samples contained small amounts of a secondary blue-green amphibole.

Fig. 3.23: A very orange OIS cuts older dikes in middle gabbros.

Minor intrusive sheet phases;

Primary dikelets are found exclusively lower in the isotopic gabbros. Concentrations decreased form a maximum of ~5% of the outcrop area in the lower part of the middle isotropic gabbros. They typically have dark brown to dark red-brown weathered surfaces (Fig. 3.24). Thicknesses were in the range of 2-25cm. Chilled margins are lacking and sheets often curved, indicating their formation occurred when the surrounding gabbros were still hot. Textures vary from fine to very fine grain crystalline. Compositions were different in the two samples taken; one is dominated by brown hornblende and chlorite (P4) and the other by clinopyroxene (P6). All feldspars are completely recrystallsed to very fine grain dusty secondary assemblages. Primary dikelets are thought to be related to magma chamber processes.

Fig. 3.24: A primary dike cutting lower level gabbros.

Amphibole Rich Intrusive sheets (ARIS) (after Sinton, 1975) are found in the middle gabbros. They cut all intrusive sheets including, and younger than, the GIS. Concentrations are varied, occurring in most outcrops, but never more than ~3% of the area. None were seen in the upper gabbros and hypabyssal zones, although they may relate to the black dikes described below. When weathered they often developed a rusty brown crust. Fresh or un-weathered samples are typically black with white or orange streaks. Thickness was consistently close to an average of ~40cm, but thicker examples were encountered. No chilled margins with country rock or other intrusive sheets were observed. The streaking in these sheets is the result of melted wall rock being mixed in with the mafic intrusive material. Often enclaves of wall rock are incorporated into and transported within a swirly intrusive sheet fabric. Boundaries are often curved and branched. No common orientation was measured. Textures vary from fine to very fine grain crystalline apart from included blocks that maintained their original textures. Flow banding and irregular shapes are common. ARIS are dominated by brown hornblende and contain small amounts of highly altered feldspar.

Fig. 3.25: An Amphibole rich intrusive sheet cutting lower isotropic gabbros. This example appears light in colour due to its weather surface. Note the blocks of gabbro within the sheet and ductile folding of enclave material.

Black dikes are found rarely in the upper gabbro and hypabyssal zones. Only two were seen in outcrop at NS5 and NS8 (see: Fig 3.25 and Fig 4.33), and another from a distance near Alabaster Pass. All examples were ~1.5m wide and traceable for ~30m before obscured by bush. Weathered surfaces are dark grey, and fresh surfaces being dark green grey. Texture was typically fine grain holocrystalline. In hand sample, black dikes melenocratic appearance is the result of approximately 70% amphibole, with minor felsic component most likely being feldspar. No thin section was taken of black dike. Sinton (1975) possibly recognised these black dikes as hornblende-phyric dikes.

Fig. 3.26: A black dike (under hammer) is seen here intruded by an OIS. See figure 4.33 for a full view of the out crop.

White dikes are seen in the hypabyssal and volcanic zones. Again these dikes are rare, with only two examples observed at AP3 (see Fig.3.28) and CP6. White dikes are the youngest dikes observed in the study area and possibly injected contemporaneous to the Upukerora Breccia sedimentation. White dikes are light grey in fresh and weathered

surface and 0.7 to 1.2m in width. Both examples were traceable for ~50m before being obscured by scree or bush. Large 5cm chilled margins, in places harbouring amygdaleised vesicles, form against country rock. Parallel banding within these dikes indicates multiple injection of new magma along its center, leaving new chilled margins. Gashes possibly formed by tension, occur perpendicular to the margins and are now amygdaleised. White dikes are hypocrystalline to aphyric, rare phenocrysts were mafic but not identifiable in hand sample. No thin sections were taken of white dikes. Sinton (1975) also noted white dikes cutting all other intrusive sheets, and identified their composition as picritic.

Relative Age	Major type	Minor type	Crustal Level of abundance	Within type Crosscutting	Notes
Oldest		Primary dikelets	Middle gabbros	Yes	
	Grey Intrusive Sheets		All levels, except lower gabbros and upper pillows	Yes	
Break?		Amphibole rich Intrusive sheets	Middle gabbros	No?	
		Plagio-granite	Upper gabbros	No	Dated near Lake Never at 276+/-2 Ma
			Upper gabbro and hypabyssal	No	
	Orange Intrusive Sheets	Black Dikes	All Levels	Yes	Crosscutting, abundant chilled margins and orentations indicate long period of intrusion.
Youngest		White Dikes	Pillow lavas	No	

Table 1: Table showing the order of intrusive sheet injection and the relative ages.

3.3.4 Volcano-sedimentary facies

Dense vegetation covers most of the area underlain by the volcano-sedimentary facies. Pillow lavas (Livingstone Volcanics Subgroup), Upukerora Breccia and Wooded Peak Limestone (both of the Maitai Group) are discussed here. Younger Maitai Group sediments have no direct relationship to the underlying DMOB and will not be discussed.

3.3.4.1 Pillow Lavas

Pillow lavas of the Livingstone Volcanics Group form a ~300-600m wide band (Fig. 3.27) and can be divide in two portion, one associated with GIS (lower pillow lavas) the other with OIS (upper pillow lavas). Variation in thickness is possibly the result of erosion form scarps created by ocean floor faulting, proximity to volcanic edifices and younger faulting. Where well exposed, variably preserved pillow lava flows extend laterally until truncated by faulting. Much of the volcanic sequence is tectonised, obscuring the original features.

Pillow lavas contain a variety of intrusive sheet types. At Alabaster Pass (AP3), pillows are cut by both GIS and OIS just above the hypabyssal facies. At an outcrop ~400m west of AP3, pillow lavas were seen without intrusive sheets. Pillows seen east of Courtney Peak (CP6), directly below the contact with the Upukerora Breccia, contained few intrusive sheets (Fig. 3.28). Intrusive sheets cut through the entire volcanic sequence and possibly entered the above Upukerora Breccia. No sediment layers occur within the pillow lavas in the Northern Bryneira Range, but they have been noted elsewhere (Sinton, 1975).

The pillows conform to the classic morphology for under sea eruptions and are generally well preserved. Pillow lavas are feldspar-augite phyritic, the feldspar and groundmass being completely replaced by secondary mineral assemblages (probably actinolite, albite and chlorite). Ilimenite is responsible for the red-brown colour (Fig. 3.27). In highly weathered hand-samples, pillows appear grey-blue with a light green holoclastic quench rim.

Fig. 3.27: Pillow lavas east of Courtney Peak. The vague 'layering' can be seen dipping toward the left hand side of the picture and may represent individual pillow lava packets or flows. Later faulting has caused movement along these plains.

3.3.4.2 Upukerora Breccia

On the western side of Courtney Peak (CP4 to CP2) a ~40m thick sequence of Upukerora Breccia outcrops (Fig. 3.29). A depositional contact with the underlying volcanic rock is followed by repetitive cycles of coarse, poorly sorted, polymict igneous breccias that grades into poorly sorted sandy horizons.

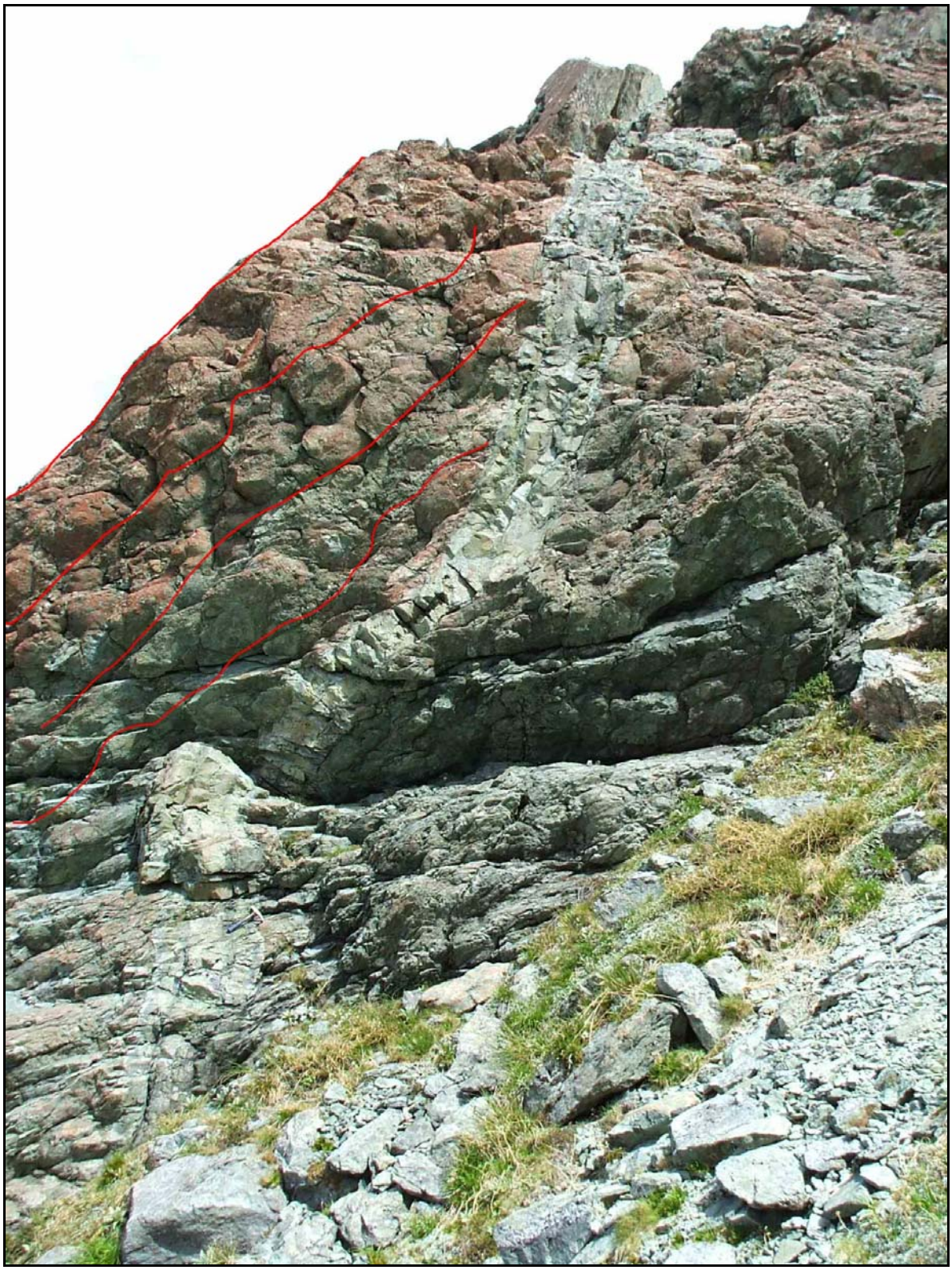

Fig. 3.28: Youngest dike (white dike) found high in the upper pillow lavas, approximately 100m from the Livingstone Volcanics Subgroup-Upukerora Breccia contact. Red lines highlight layers of pillow lavas.

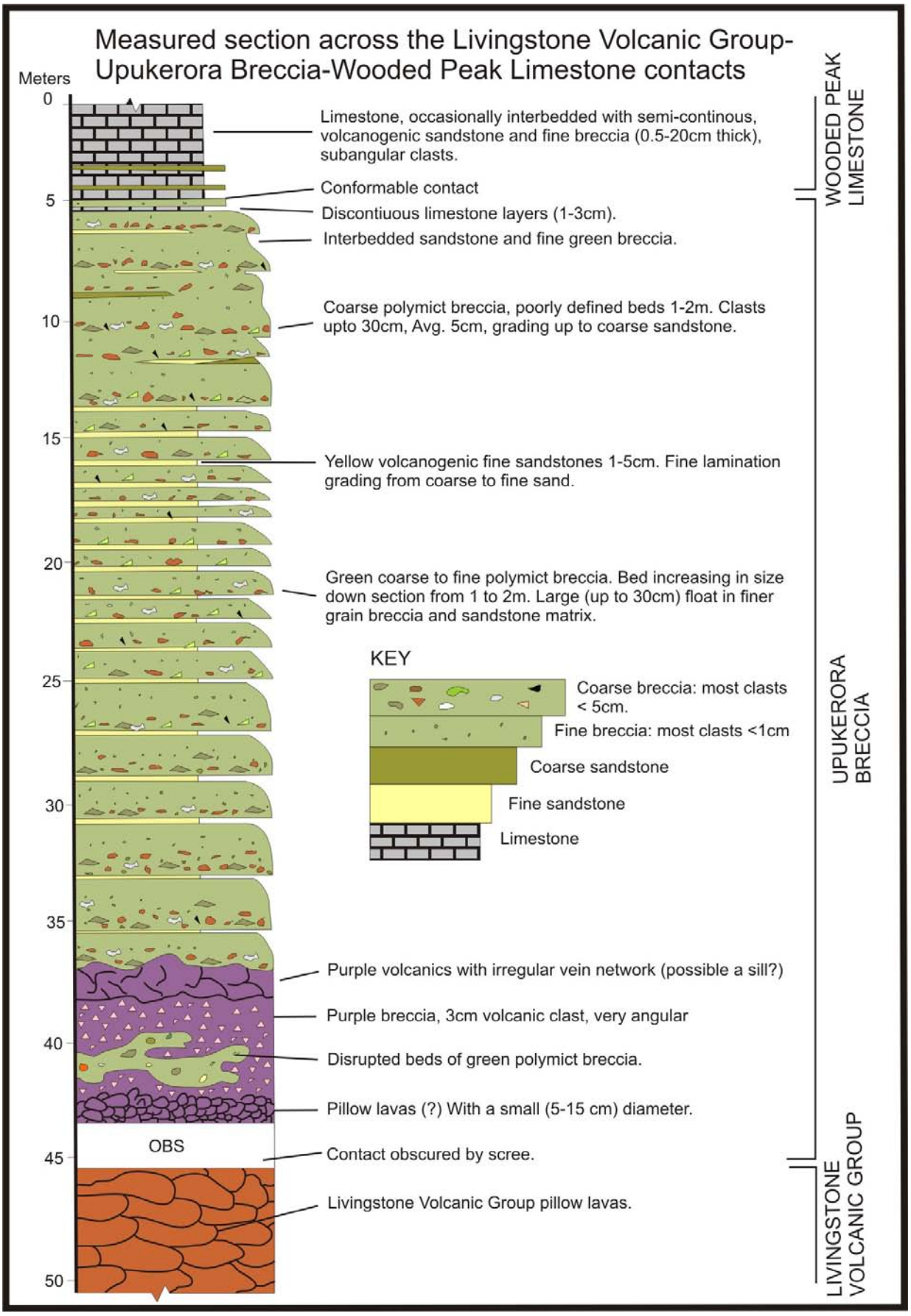

Fig. 3.29: Stratigraphic column showing the total thickness of the Upukerora Breccia as seen at CP6.

The lower third of the Upukerora Breccia is notably different from the overlying green Upukerora Breccia (Fig 3.29). Pillow lavas and basaltic breccia intercalate with green polymict igneous breccia (Fig. 3.30), possibly indicating volcanic activity during breccia sedimentation. After the contact with Livingstone Volcanic Group, pillow lavas intrude the first units of green polymict igneous breccia. These pillows are crudely formed and typically 20cm in diameter. Isolated ~10m wide pods had no clear feeder from the below and therefore may represent large slide blocks (Fig. 3.30a). Basaltic breccias are a distinctive purple colour and appear to have a close spatial relationship to the crudely formed pillow lavas. Basaltic breccias contain 75% basaltic clasts (fragments) in a hyaloclastite detritus (Fig. 3.30b). All clasts are extremely angular, averaging 2-3cm. Clast textures are porphyritic, containing phenocrysts of pyroxene, plagioclase and minor quartz. Hyslop (1978) attributed these basaltic breccias to mass flow units, originating from sills that broke to the surface as feeders to lava flows, Lava then flowed down slope and mixing with green, polymict igneous Upukerora Breccia (Fig. 3.30c). No rocks that could confidently be described as sills were seen at Courtney Peak, but have been reported in the lower Upukerora Breccia elsewhere (Hyslop, 1978; Kimbrough et al., 1992) and within metasediments near Red Mountain (Sinton, 1975).

The upper two thirds of Upukerora Breccia is bedded and a distinctive green colour. Clasts are usually angular to slightly rounded and average 5-15cm in diameter. Breccia units are 0.5-5m thick and extremely poorly sorted at the base and fine up-wards to moderately sorted sandstone. These characteristics suggest emplacement by mass flows. Clasts in the upper two thirds of the Upukerora Breccia vary from silt to boulder in size, with composition mainly being basalts and diorites. There are lesser amounts of gabbro and amphibolite. All clasts appear to be derived from the Livingstone Volcanic Group below. No pelagic intervals were observed.

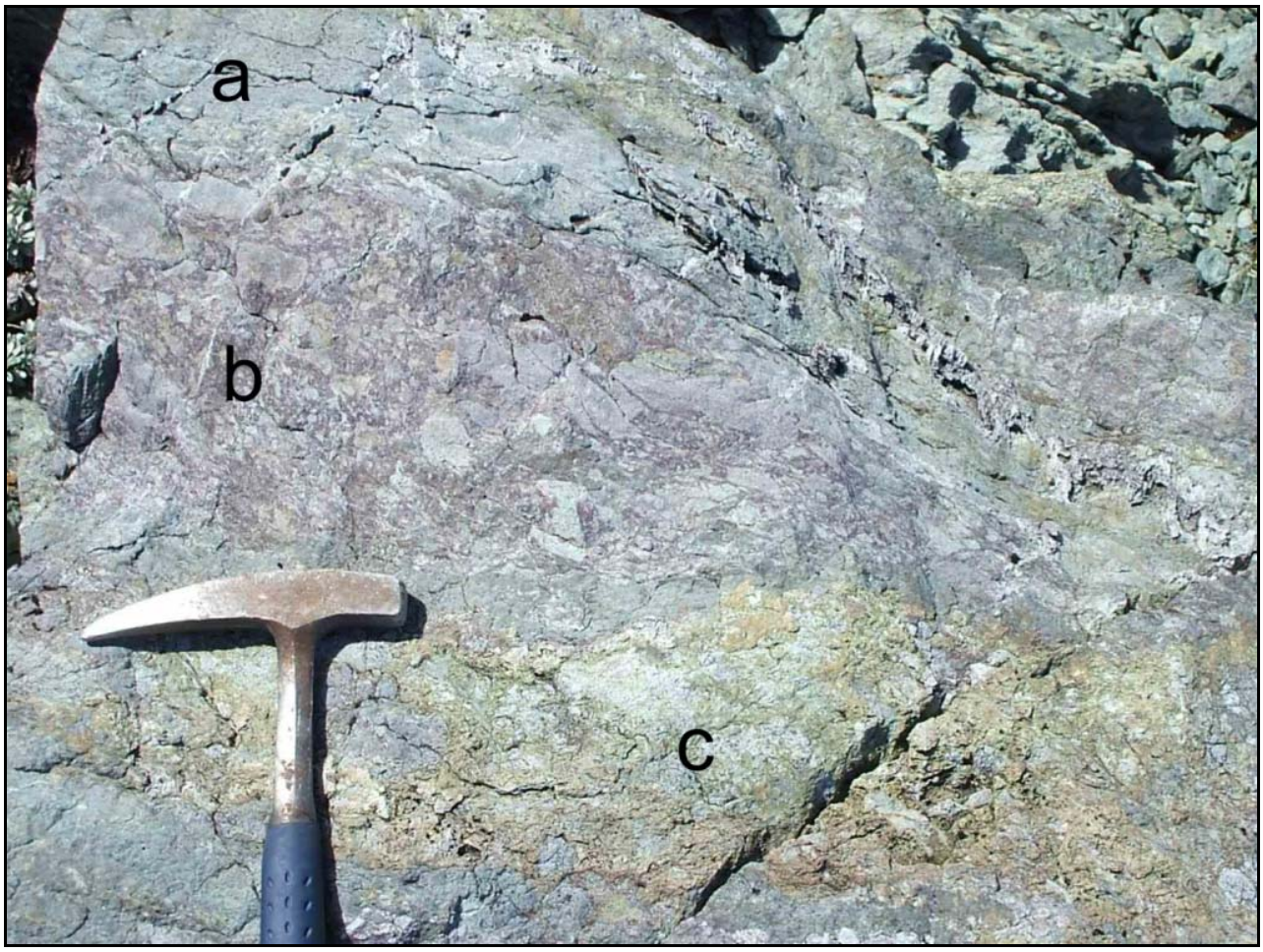

Fig. 3.30: A loose block originally from the lower stratigraphic portion of the Upukerora Breccia. **a)** Solid basalt clast possibly part of a sill or pillow lava flow. **b)** Purple breccia, made entirely of highly angular basaltic clasts in a hyaloclastite matrix. **c)** Recycled clast of green Upukerora Breccia.

The contact between the Upukerora Breccia and the overlying Wooded Peak Limestone is sharp. Before the contact, 1-2 cm bands of limestone are found within the last 30cm of breccia. After the contact thin breccia beds are spaced by 1-3m of limestone, beds may be present ~30m form the contact. This contact appears conformable, no evidence for a gap in deposition was seen (e.g. pelagic sedimentation), although, a slight angular discordance was measured (see section 5.2).

Chapter 4: Description of Structures

Mesozoic and Cenozoic deformation has greatly modified the Permian structure that this study investigates. This makes structural analysis of the DMOB difficult; which structures are relevant to Permian deformation of the Dun Mountain-Maitai terrane? A hard question, considering nearly all large faults in the study area show reactivation. To decipher this problem, this chapter is divided into three main parts, as follows:

1. **Regional scale structures:** Structures that boarder, completely cut or are extensive within the DMOB.

2. **Outcrop scale structures:** Small scale structures that occur extensively within the DMOB.

3. **Structure of intrusive sheets:** Investigation of distribution, form and morphology of intrusive sheets within the crustal portion of the DMOB.

Rotation by younger structures has changed the reference frame and therefore the nomenclature of older structures. To overcome this problem, structures described in the text are defined by the horizontal reference observed in the pseudostratigraphy at the time of their formation. Horizontal reference is given by paleo-horizontals (markers that recorded horizontal during the Permian formation of the DMOB, see section 5.1). For the purposes of this discussion, paleo-horizontal is parallel to the bedding of the Wood Peak Limestone (i.e. strike N-S, dip steeply). Therefore, if a fault is labelled as a “former normal fault”, it refers to its orientation when the Wood Peak Limestone was horizontal, irrespective of the current orientation of the structure. In situations where a recently formed or active structure is described, it is described as it is orientated today. For example a “normal fault” is a fault that shows a normal displacement with reference to today’s horizontal.

4.1 Regional scale structures

Regional scale structures are defined here as structures that border and/or cut through the Dun Mountain-Maitai terrane, in the Northern Bryneira Range. Many of these structures are regionally extensive, associated with Mesozoic terrane amalgamation. Others have local to regional significance, are seen in the Bryneira Range and neighbouring continuations of the terrane, and may also relate to Mesozoic to recent deformations.

4.1.1 Major Faults

The Alpine Fault as the active plate boundary is currently the driving geological structure in the South Island, cutting the entire length of the island and being very active. It strikes northeast-southwest and located ~16 Km to the northwest of the Northern Bryneira Range (Fig 3.1). The Alpine Fault probably has influenced on the some of the most recent deformations in the study area.

The Hollyford and Livingstone Faults border the Maitai-Dun Mountain terrane, to the east and west respectively. These large terrane boundary faults are the oldest major structures in the area, dating back to Mesozoic terrane closure. Accretion of the Dun Mountain-Maitai terrane and Caples terrane probably took place in the Early Cretaceous. Reactivation of the Hollyford and Livingstone Faults probably took place in the Cenozoic (Turnbull, 2000). Ridge rents (see section 4.1.5 below) and adjustment faults (cross faults, see section 4.1.4.3) showing recent movement are associated with both the Hollyford and Livingstone faults (Bishop, 1996; Turnbull, 2000).

4.1.2 Major Folds

The Key Summit Syncline is the only major fold in the study area. This tight isoclinal fold is truncated along its western limb by the Hollyford fault in the Pyke Valley, west of the Northern Bryneira Range (Turnbull, 2000). Steep dips of Maitai Group strata are the result

of the formation of the Key Summit Syncline and allow large stratigraphic sections to be observed over short horizontal distances.

4.1.3 Terrane bound Faults

A number of fault sets are confined with in the DMOB portion of the study area. The largest features appear to cut across large stratigraphic sections or the entire terrane, often showing considerable displacement. Regularly, minor faults show recent small displacements as scarps and breccia gullies.

4.1.3.1 Cross faults

Numerous cross faults cut at oblique angles to the DMOB trend, two sets are evident based on orientation. The first set is orientated northwest-southeast with vertical to steep southwest dips. Pseudostratigraphic offset indicate a possible former normal displacement but now shows a sinistral sense of motion. The amount of displacement is varied, but probably reaching a maximum of 200-300m based on the juxtaposition of pseudostratigraphic horizons. Direct observation of off-set was only made within the Livingstone Volcanics Group, it was unclear if these faults continued into the Maitai Group. Fault planes were best observed on ridge crests where cols and valleys follow the brecciated rock. Breccias extend 1-3m either side of the plane, with gouge at the trace being ~5-20cm wide. Foliation often forms parallel to the fault plane. Fault plane rock is highly altered. Spatial distribution is varied, south of Alabaster Pass and in the North Saddle area (Fig. 3.2a and b) where they are distributed at ~0.7-1.0km spacing. The Plateau area (see Fig. 3.2a and b) has fewer cross faults of this orientation. Timing of movement on these planes is not known, but some may be relic seafloor normal faults that have been reactivated several times since.

The second set of cross faults strike northeast-southwest, dipping steeply southeast. Only two of these faults were observed, both in the Lake Never area. The best exposed plane runs through Lake Never and the stream below to offset the Livingstone Group. Fault planes contain 0.5-1.0m of breccia and gouge (Fig. 4.1). Reactivation of these cross-faults is thought to be recent, as breccia appears fresh and minor scarps are evident.

Northeast-southwest striking cross faults may also have origin during Permian ocean floor spreading.

Fig. 4.1: Exposed fault plane of a northeast-southwest cross fault at P9. Scarps, unconsolidated breccias and gouge indicate recent movement on this plane. Photo is Approximately 1.5 m across.

4.1.3.2 Peanut fault

The Peanut Fault separates the Livingstone Volcanics Group from the Dun Mountain Ultramafics Group. It was named by Sinton (1975) from its outcrop in Peanut Stream in the Red Mountain area. It has been traced from the area north of Red Mountain south to the Barrier River (Sinton, 1975), and south from the Northern Bryneira Range where terrane thinning causes it to merge with the Livingstone Fault near Serpentine Saddle (Hyslop, 1978; Turnbull, 2000). In the study area, the trace is well exposed in the stream below Lake Never (P6), and can be followed southwest to where it intersects the Olivine River. From its intersection with the Olivine River, a splay probably follows the rivers

course to the Cow Saddle area (Turnbull, 2000). It seems probable that the Peanut Fault was once continuous from the Red Mountain area to Serpentine Saddle.

Brecciation and shearing affects wall rocks (forming discrete bands) in a ~100m wide zone as either side of the Peanut Fault trace. The Dun Mountain Ultramafic Group to the west side of the Peanut Fault is more disrupted. Persistent shear zones within the upper Dun Mountain Ultramafics Group are uniform in orientation, running parallel to the strike of the DMOB. These ~5-10m wide bands of highly sheared serpentinite, highlighted by gullies breccia and scree (seen at P7), repeated at 50-100m intervals down from the Crustal-Mantle transition, until more coherent serpentinite is encounted ~700m below. Joint sets and faults with slicken-sides are chaotic and no attempt was made to make sense of them. Sinton (1975) notes that slicken-sides indicate several directions of movement, but fairly consistently indicate some transcurrent displacement. Prominent shear zones strike north-south and dip moderately to the east. The timing and total amount of displacement along the Peanut Fault is unknown, but it is probably an early feature. There is good evidence for recent movement on the Peanut Fault in the slope flanking the study area above the Olivine River. Anti-scarps in these scree covered slopes have enabled ponds to develop (P13). Loose, breccia filled shear zones are also indicative of recent movement.

4.1.3.3 Terrane-parallel faults

Terrane parallel faults are the youngest faults seen in the study area. They form ridge rents up to ~5m high and strike NNE-SSW for 0.5-3km, sub-parallel to the Hollyford and Livingstone Fault systems. A large number of these faults are seen above the bush line on the western flanks of the Bryneira Range, as rents that form splays and sag ponds. Such well exposed topographic expression with little erosional modification suggests these are young features. Terrane-parallel faults are possibly related to recent movement on the Alpine fault or Hollyford and Livingstone Fault systems, where rock weakened by the relaxation of mountain slopes after deglaciation has failed during recent earthquakes (Bishop, 1996).

4.1.4 Schistosity

Schistosity is apparent in the Maitai Group and the upper units of the Livingstone Volcanics Group. In the volcanic, hypabyssal and upper plutonic sections have crude schistose planes that run parallel to the trend of the belt, and are most apparent along ridge tops. In the Maitai Group the schistosity is sub-parallel to the bedding planes. This is very apparent in the Wooded Peak Limestone where bedding and schistosity strike north-south.

4.2 Outcrop scale structures

An outcrop scale structure is defined here as a surface where brittle and/or ductile deformation has lead to displacement across a plane. ‘Outcrop scale’ gives reference to the spatial dimensions of these structures. Generally, their continuity is unknown and their ages being relative to crosscutting relationships with intrusive sheets. Only structures that demonstrated a similar age to intrusive sheets are considered here. All structures younger than OIS (Orange Intrusive Sheets) can not be constrained by crosscutting.

4.2.1 Extensional deformation

Extensional deformation is prevalent throughout the crustal portion of the DMOB. Most structures are fused and few contain interstitial fill between planes. Overprinting by subsequent episodes of deformation and magmatism is common. Types of extensional deformation are sub-divided below on the basis of morphology and scale. Often there is no one defining feature to characterise their structure, and a continuous spectrum from ductile to brittle deformation is recorded, sometimes within the same plan.

4.2.1.1 Microfaults

Microfaults are the smallest fault observed in the field. Displacements range from <1mm to 50cm. Microfault spacing is proportional to displacement, smaller offsets having closer spaced planes. Microfaults are sharp and healed, but can contain secondary vein fill. All crustal levels contain microfaults, but they are best developed in the middle and lower

gabbros. All are former normal faults that often developed as a conjugate as a pair. Half graben formation is common (Fig 4.2), horst and graben structures are subordinate (Fig. 4.3). Most conjugate sets intersect at 45-90 degrees. Displacement often develops on one of the two conjugate fracture planes (Fig. 4.2). This may be the result of progressive extension from one side, resulting in development of one dominant synthetic set of shears. This style of normal microfaults is seen displacing intrusive sheets older than OIS (orange intrusive sheets). Younger conjugate normal faults cut the Upukerora Breccia (Fig. 4.3), but these faults do not appear syn-sedimentary, and are of unconstrained age.

Fig. 4.2: Former normal microfaults seen here in layered gabbro. Note the conjugate to microfaults remain as a fracture.

Fig. 4.3: Conjugate former normal micro faults in the Upukerora Breccia, showing horst and graben structure**.**

Re-activation of microfaults by reverse-slip displacement is frequently observed (Fig 4.4). Reverse faulting may record a change from extension to compression in the middle and upper gabbros. Two types of examples are given; the first type is without relative timing constant by crosscutting intrusive sheets (e.g. Fig. 4.4). The second type records reverse-slip displacement prior to OIS of intermediate age (e.g. Fig. 4.5 and 4.6)

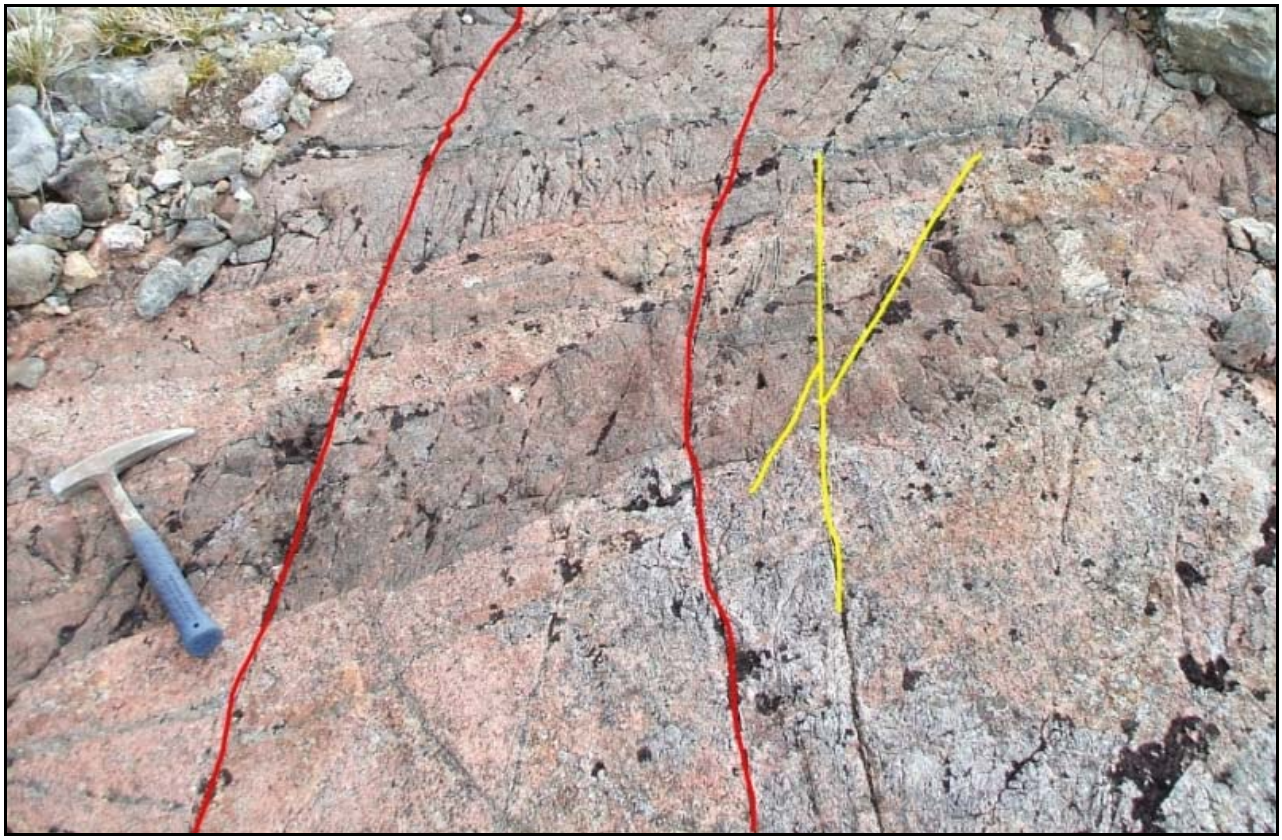

Fig. 4.4: Microfaults within the middle isotropic gabbros, displacing intrusive sheets. Yellow lines highlight a conjugate set of former normal faults, one of which shows reactivation to former reverse displacement. Red lines show former reverse faults, note the curved fault planes.

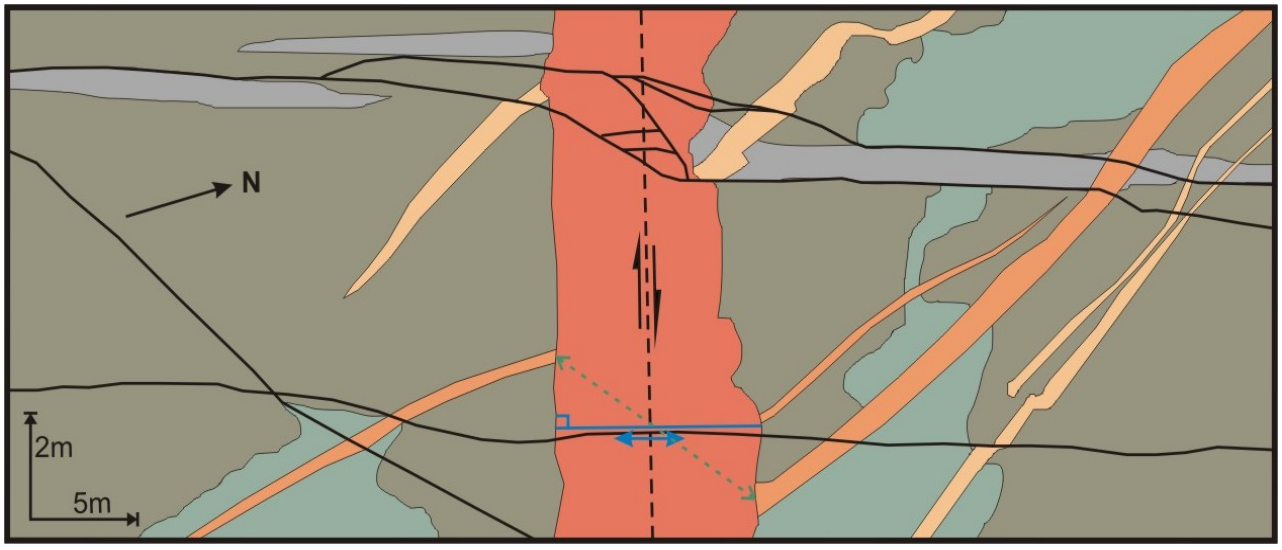

Fig. 4.5: Sketch showing crosscutting between OIS and GIS (see Fig. 4.6 for a relevant key). With respect to paleo-horizontal (Approximately N-S, with E being the way up), the displacement across the youngest intrusive sheet appears reverse (black arrows). Blue arrow indicates orthogonal dilation and the green arrow shows the resulting apparent offset. Sketch drawn at NS6.

Interpretation of reverse-slip on microfaults needs to be carefully considered, as it may be explained by both regional compressive and extensional stress fields. In figure 4.4, reverse-slip displacement can be explained by a change from extensional to compressive stress causing their reactivation. However, with no relative timing control by younger crosscutting dikes, broader implications concerning a change from regional extensional and compressive stress fields are inexplicable. In the second examples (Figs 4.5 and 4.6) two explanation need to be considered;

(1) Injection of younger OIS have taken advantage of pre-existing weakness in the rock, which already exhibit reverse-slip displacement.

(2) Apparent reverse-slip occurred by orthogonal dilation of a pre-existing fracture or normal microfault.

Without kinematic information from fault or intrusive sheet wall slickensides and flow direction, it is impossible to definitively solve this problem. Similar examples of reverse-slip displacement along intrusive sheets in modern extensional regions are explained as local kinematic adjustments to companion structures. Whereby intrusion along pre-existing fractures cause uplift of the hanging wall perpendicular to the intrusion direction, therefore inducing apparent reverse faulting via dilation of the fracture (Khodayar and Einarsson, 2004). This is very likely the situation shown in figures 4.5 and 4.6A, as the vertical displacement (indicated by the displacement of crosscutting intrusive sheets) is similar to the width of the intrusions, but cannot explain all revere offsets along intrusive sheets (e.g. Fig. 4.6B).

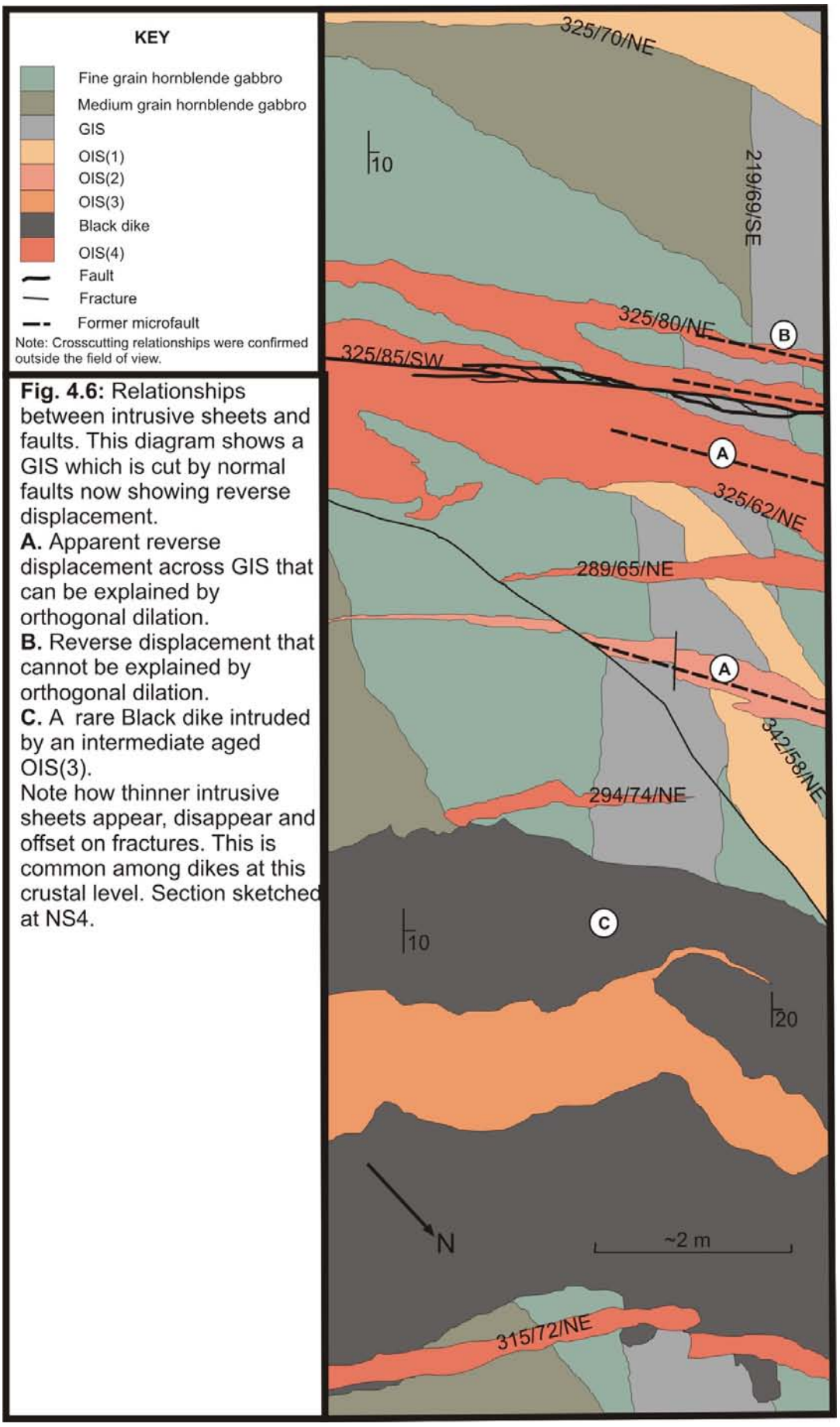

Fig. 4.6: Relationships between intrusive sheets and faults. This diagram shows a GIS which is cut by normal faults now showing reverse displacement.
A. Apparent reverse displacement across GIS that can be explained by orthogonal dilation.
B. Reverse displacement that cannot be explained by orthogonal dilation.
C. A rare Black dike intruded by an intermediate aged OIS(3).
Note how thinner intrusive sheets appear, disappear and offset on fractures. This is common among dikes at this crustal level. Section sketched at NS4.

4.2.1.2 Large scale ‘extensional’ faults

Large scale ‘extensional’ faults affect all crustal levels. These faults are tentatively labelled extensional, as their mode of displacement and relative age was often not known. Large variation in length, size and orientation makes identification and categorisation difficult (Fig. 4.7). They fill the scale range between microfaults and cross faults. Planes can be fused, contain recrystallsed cataclasites or veins. Others are open, due to recent reactivated. Spacing between planes is dependent upon size, with the largest faults spaced at approximately 100m intervals (Fig. 4.7), and smaller faults between them becoming progressively closer with less displacement. The smallest faults in this class were spaced 2-5 m apart, with offsets of 0.3-2 m.

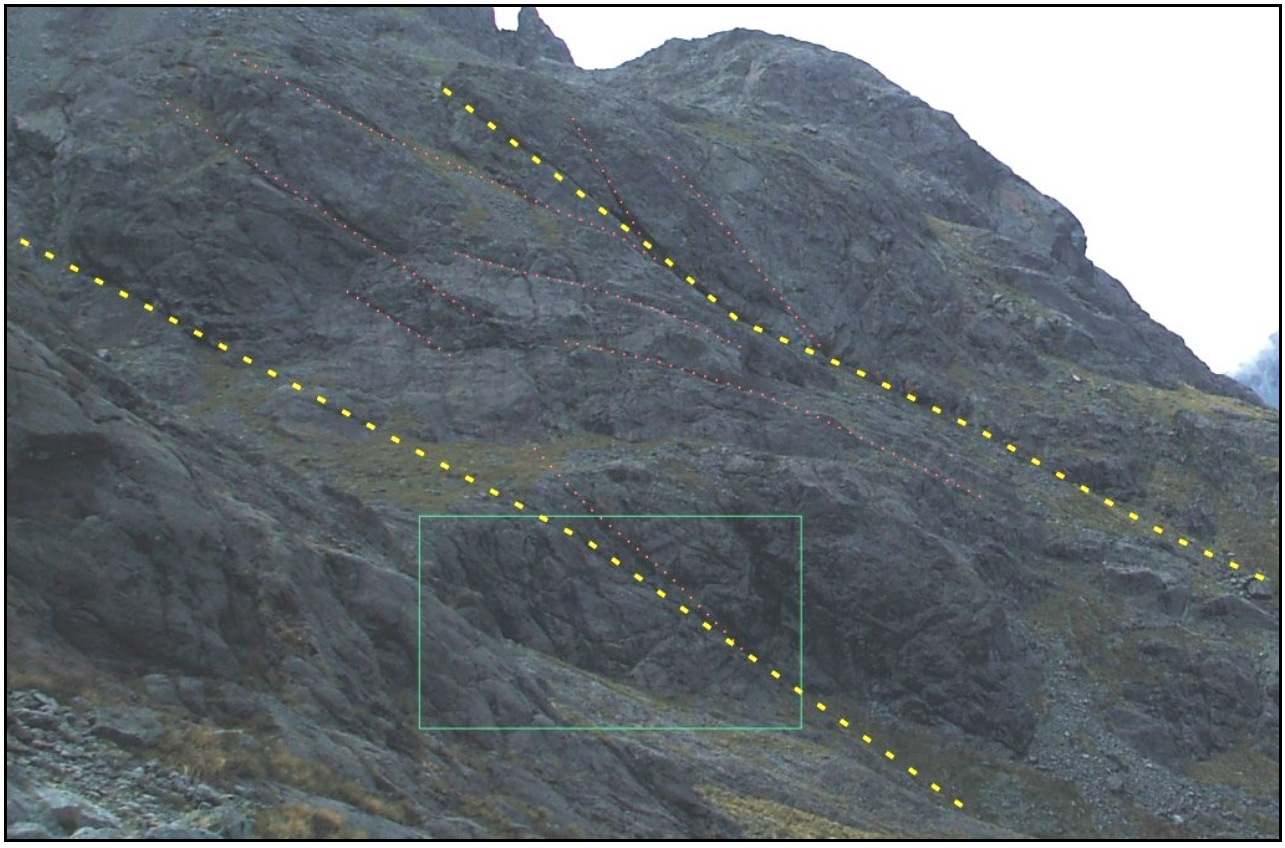

Fig. 4.7: Large former normal faults in the lower and middle gabbros. Yellow lines show the largest normal faults, faint red dotted lines show smaller faults. View in the middle distance is approximately 300m across looking towards P4. Green rectangle shows the position of figure 4.8.

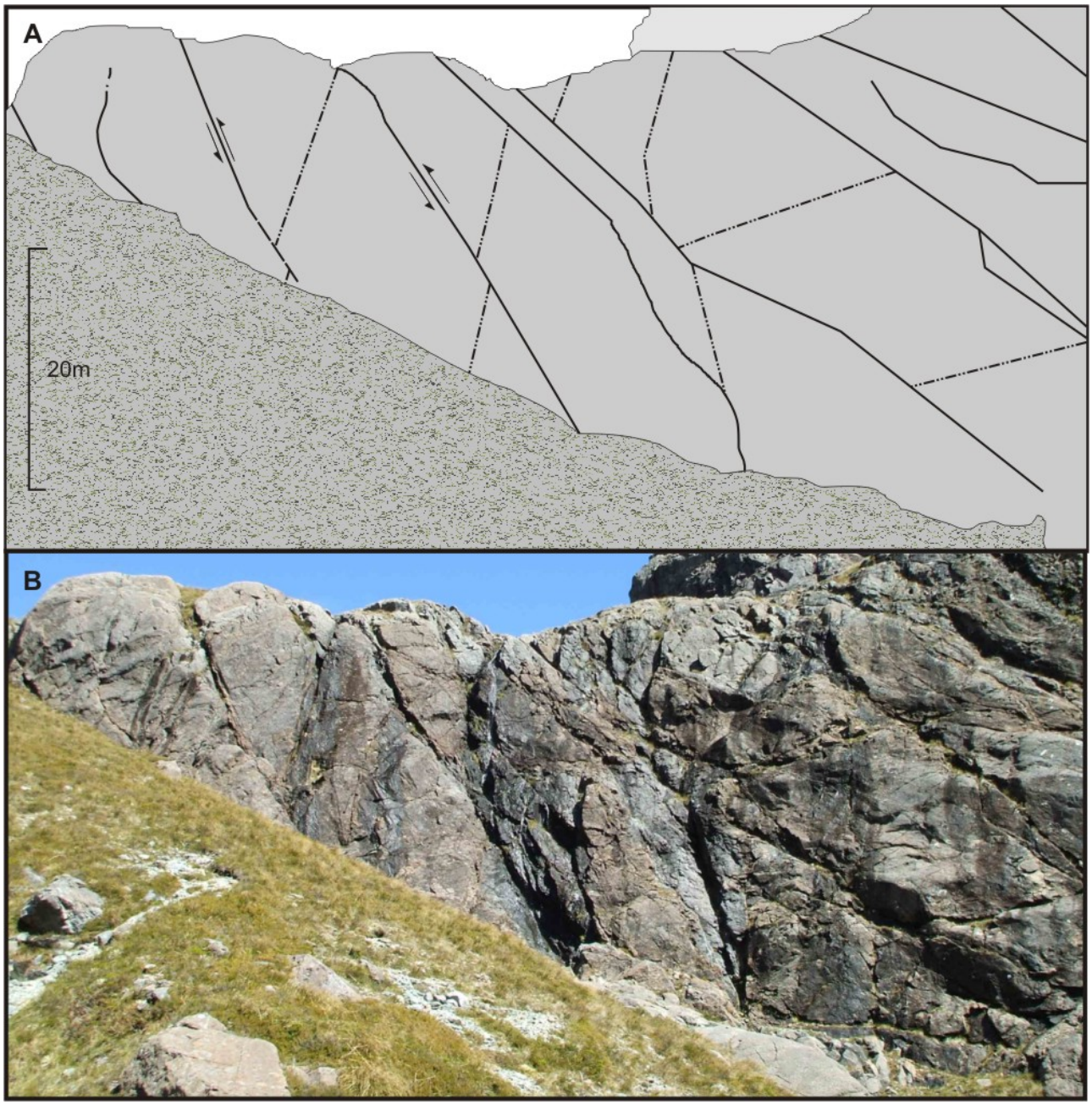

Fig. 4.8: A) shows a digitized version of B, a well exposed cliff below Lake Never (P6). Solid lines show younger, former normal faults with an unknown throw that are now has an apparent reverse displacement. Dashed lines show older faults that are offset, but were probable once normal faults. **B)** Shows a photograph of the outcrop.

Interpretation of these structures is not possible without control of their relative age, and only limited information can be deduced from them. It is unknown what structures in the large scale extensional fault class formed during the Permian or Mesozoic and which have been reactivated since. Large scale faults probably formed during numerous phases of brittle deformation in the DMOB basin development. Being an extensional environment most structures originally had a normal sense of movement, orientated with strike

perpendicular to extension direction. To visualise this, view figures 4.7 and 4.8 by rotating the page 90 degrees clockwise. Orientation information for large scale faults is presented in section 5.4.

4.2.1.3 Breccias

Breccias occur as isolated areas at all crustal levels. An isolated area of brecciated layered gabbro is observed at their contact with underlying ultramafic rocks of the Livingstone Peridotite. Clasts varied from cobble to gravel in size, surrounded in a secondary matrix possibly of hydrothermal origin. Crosscutting by and incorporation into younger dikes, suggests these breccias were formed during an early extensional episode.

Fig. 4.9: Brecciated, highly altered layered gabbro seen at P22

An isolated areas of magmatic breccia was encountered in the middle gabbros. Boulder to cobble size, well rounded clasts of gabbro are encased in finer grain gabbro of

unknown composition (Fig 4.10). These areas are closely associated with brittle faulting with normal sense of displacement. Faults contain gouge and breccias, and are now fused by veins.

Fig. 4.10: Magmatic breccias cut by a fault plain. Note the large round clasts of gabbro on the right and the envelope of normal shear breccias above the adze. Photo from P18.

4.2.1.4 Brittle-ductile deformation

Brittle-ductile deformation is seen in the lower and middle isotropic gabbros. This type of deformation is usually orientated sub-parallel to paleo-horizontal. There is large variability in morphology, resulting from different rheological conditions. Often variation is related to crustal level, structures in the lower crust showing more plasticity.

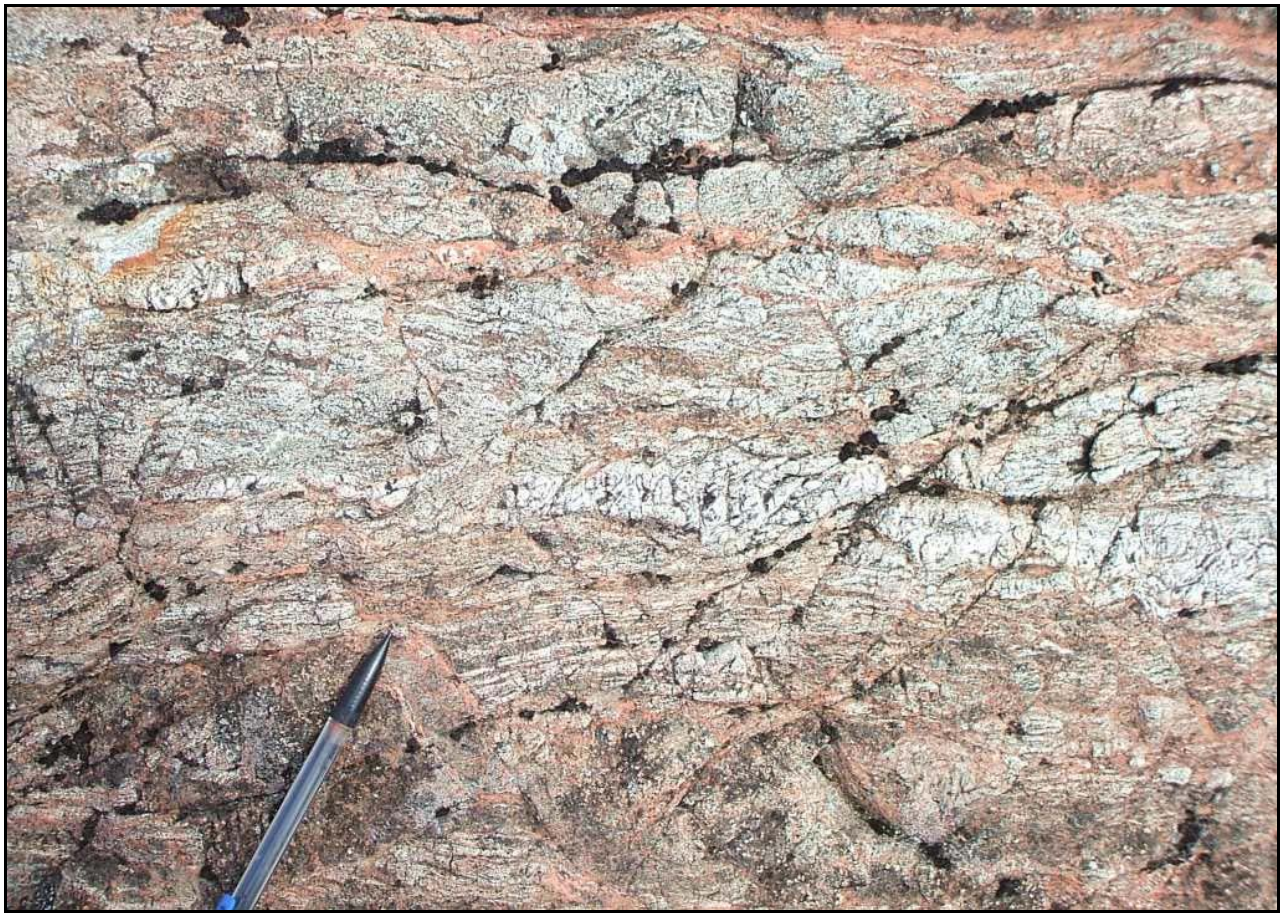

Fig. 4.11: A zone of extension associated with shearing. The ductile component can be seen in the development of foliation sub-parallel to horizontal. Later brittle deformations led to the development of conjugate normal faults and fractures. Photo taken at P15.

Clear examples of brittle-ductile deformation were rare, owing to its early formation. Only one outcrop was closely associated with a shear zone. Plastic extension via reduction in grainsize and formation of parallel fabrics precedes brittle failure. Brittle failure is first recorded in the development of a conjugate fracture pattern, that with continued extension records shear displacement with a normal sense of motion (Fig. 4.11). Associated shear zones (Fig. 4.12) form in response to ongoing extension. Shear zones are 1-2m wide, containing 5-10cm bands of cataclasites and breccias of various sizes. Cataclasites consist of very fine grain matrix containing <2mm fragments and individual grains of gabbro, all thoroughly recrystallsed. Breccias are surrounded in cataclasites, and form lozenge shapes that are often deformed asymmetrically by shear (Fig. 4.12). Synthetic riedel shears cut the original planar fabric and offset breccia blocks. Kinematic indicators such as riedel shears and deformed breccias indicate a true dextral sense of motion on the shear zone shown in figures 4.11 and 4.12. The orientation of this shear zone is at 20-

30^0 to paleo-horizontal, suggesting that this may have once been a low angle detachment fault. OIS cut across this shear zone, indicating an origin of GIS age. Brittle-ductile deformation is likely related to development of faults as magma cooled and moved away from the spreading ridge axis.

Fig. 4.12: Shear zone showing bands of gouge (orange) and lozenge shaped gabbro breccias. Photo taken at P15.

4.2.1.5 Ductile deformation

Ductile deformation was encountered as isolated patches within the middle and lower gabbros, often in close spatial association with amphibole rich intrusive sheets (ARIS). The surrounding gabbros are increasingly stretched parallel to the ARIS, forming planer and tabular segregation of mafic and felsic mineral (Fig 4.13), and pseudo pinch-and-swell like structures along isolated layers (Fig. 4.14). The boundaries between ARIS and affected gabbro are often blurred; mixing between the two is common. Enclaves of gabbros within the ARIS are variably melted and stretched. These areas are best

described as shear zones, where grain-size reduction has resulted in the development of foliation in a mylonitic fashion.

Fig. 4.13: Gabbros showing ductile strain. Near the hammer, concentrations of mafic minerals form a lineation in the rock.

This relationship between ARIS and surrounding gabbro is unclear. It may be that the ARIS where injected when gabbros were still in a “mushy’ state, stretching the gabbros as they were injected. Another possibility may be that ARIS were injected post-gabbro-consolidation and were hot enough to re-melt gabbro wall rock. The pseudo pinch-and-swell like structures are possibly the result of forceful intrusion (Price and Cosgrove, 1990) (Fig. 4.14).

Fig. 4.14: An ARIS cuts through gabbros dragging the wall and causing plastic deformation. Red dashed line shows the boundary between deformed and undeformed gabbro. Yellow arrows highlight the pinched areas of the pseudo pinch-and-swell like structure.

4.2.2 Fractures

Fractures are present in all exposures in the study area and their distribution is highly varied. It is rare to find an individual set to analyse and classify, as complex geometric relationships often hinder discrimination between sets. Fractures are discussed here with respect to their relevance to Permian deformation. Younger fracture sets are ignored. Fractures developed on multiple occasions probably in response to deformation and to cooling processes. Fractures and microfaults often have a genetic relationship. Evidence for shear displacement along fracture planes is common, in theory making them faults. For the purpose of this study this technicality is ignored as no clear-cut distinction can be made on outcrop observation.

The oldest fracture set forms parallel planar surfaces in the gabbro and intrusive sheets older than and including GIS (Fig. 4.15). Mineralisation is a ubiquitous property of the fractures and often sets them apart from younger sets. Mineralisation has caused the staining of wall rock and thin green amphibole crystalline veins ranging from 0.5-1cm in width. This type of mineralisation was only observed in the lower gabbros. These fractures are the first to record brittle deformation in the consolidated gabbro.

A younger fracture set is represented by a conjugate that is genetically and spatially related to the microfaults previously discussed (section 4.2.1.1). These fractures form a conjugate with an acute angle between 45^0 and 90^0. They are commonly barren, occasionally containing white veins. Conjugate normal faults and younger fractures have the same orientation (see section 5.4). It is unclear which formed first, but faulting probably propagated along pre-existing fractures. The activation of fractures by reverse faulting may also be applicable to the explanation given in section 4.2.1.1.

Fig. 4.15: The oldest fractures seen in the gabbros and early formed dikes.

4.3 Structure of intrusive sheets

Intrusive sheets are structure that record stress conditions within the crust during their propagation. The distribution, shape and morphology of intrusive sheets in the Bryneira Range, provides information about the physical environment in which they were injected. As the DMOB has no typical ‘sheeted dike complex’, the mechanisms for intrusive sheet emplacement have to be evaluated by observation of their structure. From the extensive literature on intrusive behaviour, information regarding buoyancy of magmas, degrees of strain with in the crust and physical condition of host rock can be ascertained.

Here the distribution, shape and morphological of GIS and OIS are discussed individually, providing a base to the orientation data introduced in chapter 5 and the discussion in chapter 6. No attempt was made to evaluate the characteristics of intrusive sheets in the mantle section.

4.3.1 Intrusive sheet segmentation

Intrusive sheets are more complex than the two dimensions observed in outcrop. When considered in three dimensions, a wealth of information concerning the mechanism of propagation and nature of the host rock can be collected. In outcrop an intrusive sheet is represented by a segment of unknown continuity. The morphological complexities of adjoining segments are indicative of their mode of injection. Relationships between intrusive sheets and the host rocks they intrude are divided into two parts. The first deals with **fracture dilation and resulting segmentation**, a process by which an existing fracture is dilated or newly formed by the propagation of an intrusive sheet. Morphology of adjoining segments can be indicative of the style of fracture dilation. The second section is concerned with **geometry of segmentation**; the classification of fracture dilation systems on the basis of their segmentation.

4.3.1.1 Fracture dilation and resulting segmentation

Intrusive sheets are best thought of as fractures which have dilated to accommodate magma. The style of fracturing and the resulting segmentation is in direct relation to the propagation system involved:

1. Pre-existing fractures (or faults) are dilated by intrusive sheet propagation when the magma pressure forces open an appropriately orientated weakness (Baer and Beyth, 1990; Delaney et al., 1986).

2. Newly formed fractures occur when magma pressures exceed the tensile strength of the host rock and causing hydraulic fracture (Delaney et al., 1986; Hoek, 1991).

A more detailed discussion about mechanisms for intrusive sheet propagation is given in section 6.2.6.

Pre-existing fractures:

As fractures are segmented (meaning they are discontinuous planes (Hoek, 1991)), the intrusive sheet propagating along fractures will also be segmented. Where intrusive sheets form a sharp angle this is called a **step** (Fig. 4.16A and Fig. 4.18). A step will form by the dilation of an existing fracture that has been previously offset. Whether this leads to the development of an attached or detached segment is dependent on the orientation of the crosscutting fracture relative to the dilation direction (Hoek, 1991). When two fracture segments run parallel and not connected, an **offset** geometry occurs (Fig. 4.16B and Fig. 4.17). At an offset, the two segments may have little or no overlap. Offset can also be joined to form segmented curves when a propagating sheet encounters a resistant layer (Fig. 4.16B). Offsets and steps may be geometrically and spatially related. **Branches** occur when intrusive sheets fork to run sub-parallel to each other (Fig. 4.16C). A **horn** is a small or failed branch off an intrusive sheet (Fig. 4.16C).

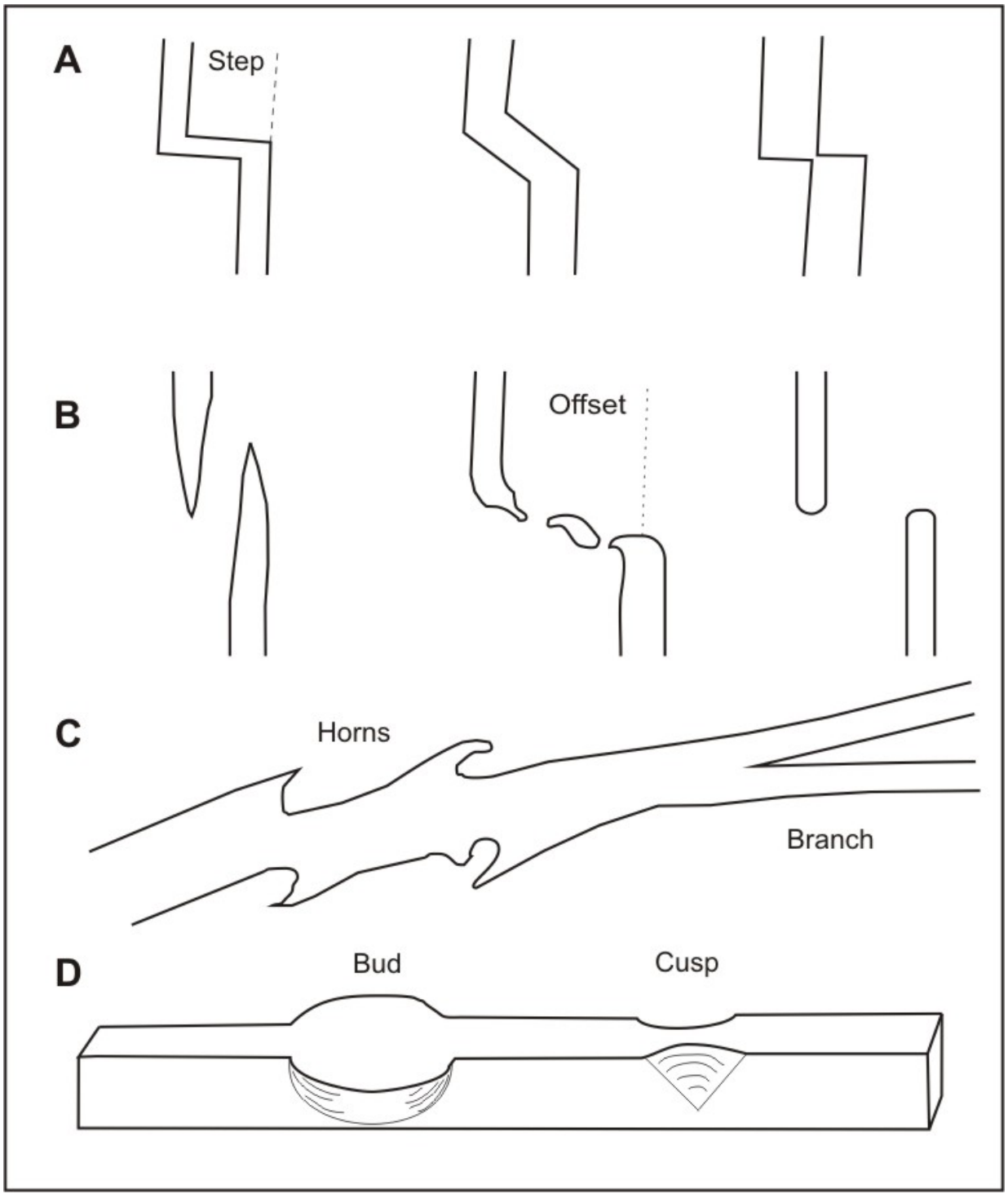

Fig. 4.16: Intrusive sheet segmentation terminology. **A)** Steps occur when a propagating intrusive sheet is forced to move along a cross cutting fracture to continue in it original direction. **B)** Offsets occur when a fracture segment is displaced and not connected. An offset must be spatially connected with a step somewhere on its plane. **C)** Horns formed by failed offshoots or step. Branches occur at intersecting fractures as divisions rather than conjugations. **D)** Block diagram of a hypothetical dike with a cusp and bud feature. These are related to morphology rather than segmentation. Nomenclature after Hoek (1991)and Rickwood (1990).

Hydraulic fracturing:

When there are no pre-existing fractures (or appropriately orientated ones) the propagating intrusive sheet is forced to generate its own fracture by hydraulic fracturing. The resulting intrusive sheet will be orientated perpendicular to the least compressive stress. Because there is no influence on this process by pre-existing weaknesses, intrusive sheets will have little or no segmentation.

Segmentation of the GIS was rarely encountered. Disturbance by younger intrusive sheets cutting GIS obscures much of the segmentation that is indicative of their intrusive nature. Offsets, horns and enclaves were occasionally seen in the upper gabbros and hypabyssal facies. These indicate that some GIS were influenced by the host rock. It is probable that in the lower crust GIS generated their own fractures in unconsolidated gabbros. In the upper crust propagation into more consolidated gabbros caused some segmentation.

Fig. 4.17 : A well preserved example of an offset with overlap and sinistral offset.

Segmentation is a common feature of the OIS, all types of segmentation described in figure 4.16 were observed. Offsets and steps were most commonly observed, likely the result of the pre-existing, segmented fractures in the host rock. Segmentation was better preserved on thinner intrusive sheets, probably due to proportionality between dike thickness and offset size, and possibly better preservation by lower flow volumes. Thick OIS often have **buds** and **cusps** (Fig. 4.16D), and enclaves of host rock. Feeder dikes that have channelled large amounts of magma often display buds (Gudmundsson, 1984). Enclaves also indicate the dilation of pre-existing fractures (Hoek, 1991).

Fig. 4.18: Partially connected offset or step where a ~1.5 m wide OIS intersects an older fracture or fault.

4.3.1.2 Geometry of segmentation

The geometry of segmentation describes the relationships between adjoining intrusive sheet segment. The morphology of an intrusive sheet will change with confining stress in the host rock and the existence of dilatable pre-existing weaknesses (Hoek, 1991). Classification is based on the type of segmentation formed along a singular or cluster of intrusive sheets. Geometry of segmentation is seen in the forms in the study area.

Irregular segmentation geometry (Fig 4.19A) forms when intrusive sheets move along pre-existing weaknesses and become segmented by crosscutting fractures and faults. Braided segmentation geometry (Fig. 4.19B) forms when there are low confining pressures; intrusive sheets may or may not follow pre-existing weaknesses. Planar segmentation geometry occurs under higher confining pressures where the intrusive sheet propagates its own fracture.

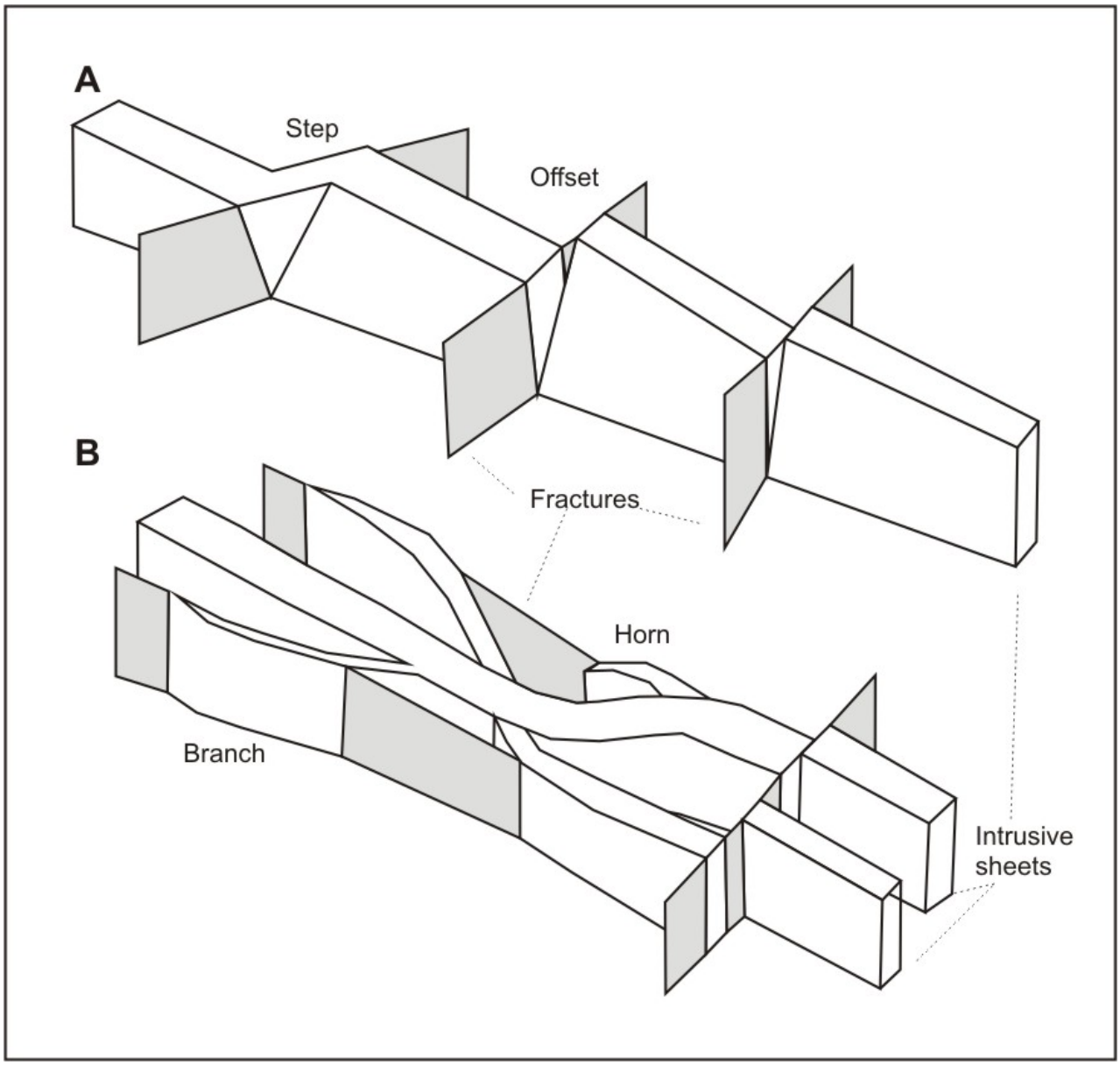

Fig. 4.19:.A) An Irregular segmented geometry. This system forms when an intrusive sheet propagates along a fracture and is segmented by crosscutting structures. Modified from Baer ((1990). **B)** Braided segmented geometry from when intrusive sheets branch and anasomose. Segments are often side-by-side and may or may not continue in three dimensions.

It was not possible to classify GIS geometry due to crosscutting by OIS, the preservation and continuity of GIS in any outcrop was inadequate.

In the lower crust, older OIS have an irregular segmented fracture system (Fig. 4.19A). Younger OIS show planar segmentation geometry, individual segments can often be traced for ~100m. In the upper crust (upper most gabbros and pillow lavas), there are slight changes in the geometry of segmentation of the OIS. Generally, segments are closely spaced and the intrusive sheets thinner displaying a mix of irregular and braided segmentation geometry. There is a greater abundance of branching in thin sheets parallel to larger sheets, steps and offsets are common (Fig. 4.21). Branching seen in the hypabyssal units and pillow lavas is sometimes anastomosing (Fig. 4.20), classifying them as a braided segmented fracture system (Fig 4.19B). The asymmetrical walls of these OIS suggest that they were formed relatively passively in rocks already near tensile failure (Price and Cosgrove, 1990). The precence of braided intrusive sheets in the upper crust are indicative of rapid, high energy fracture dilation (Hoek, 1991).

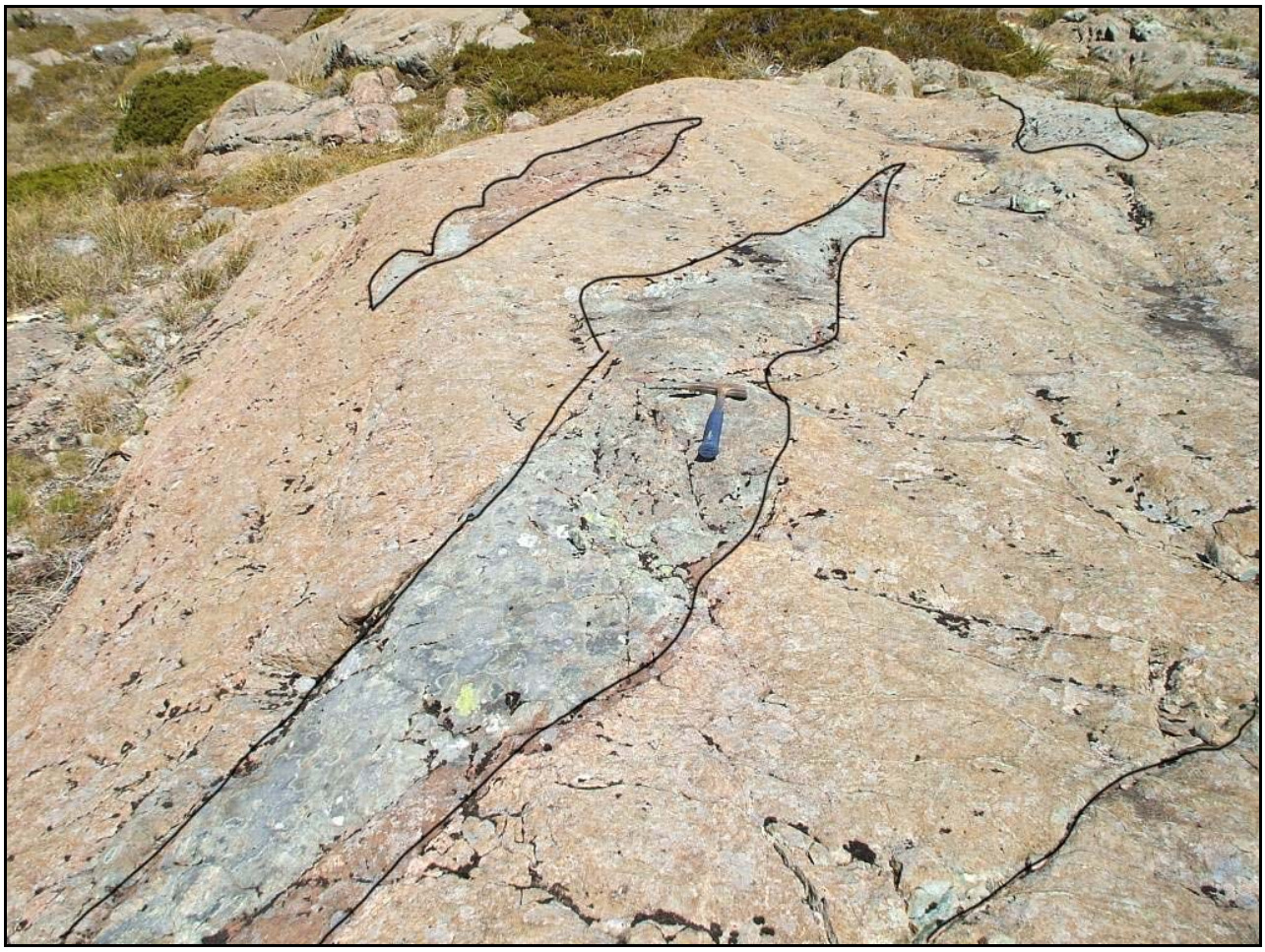

Fig. 4.20: Anastomosing OIS in the upper crust.

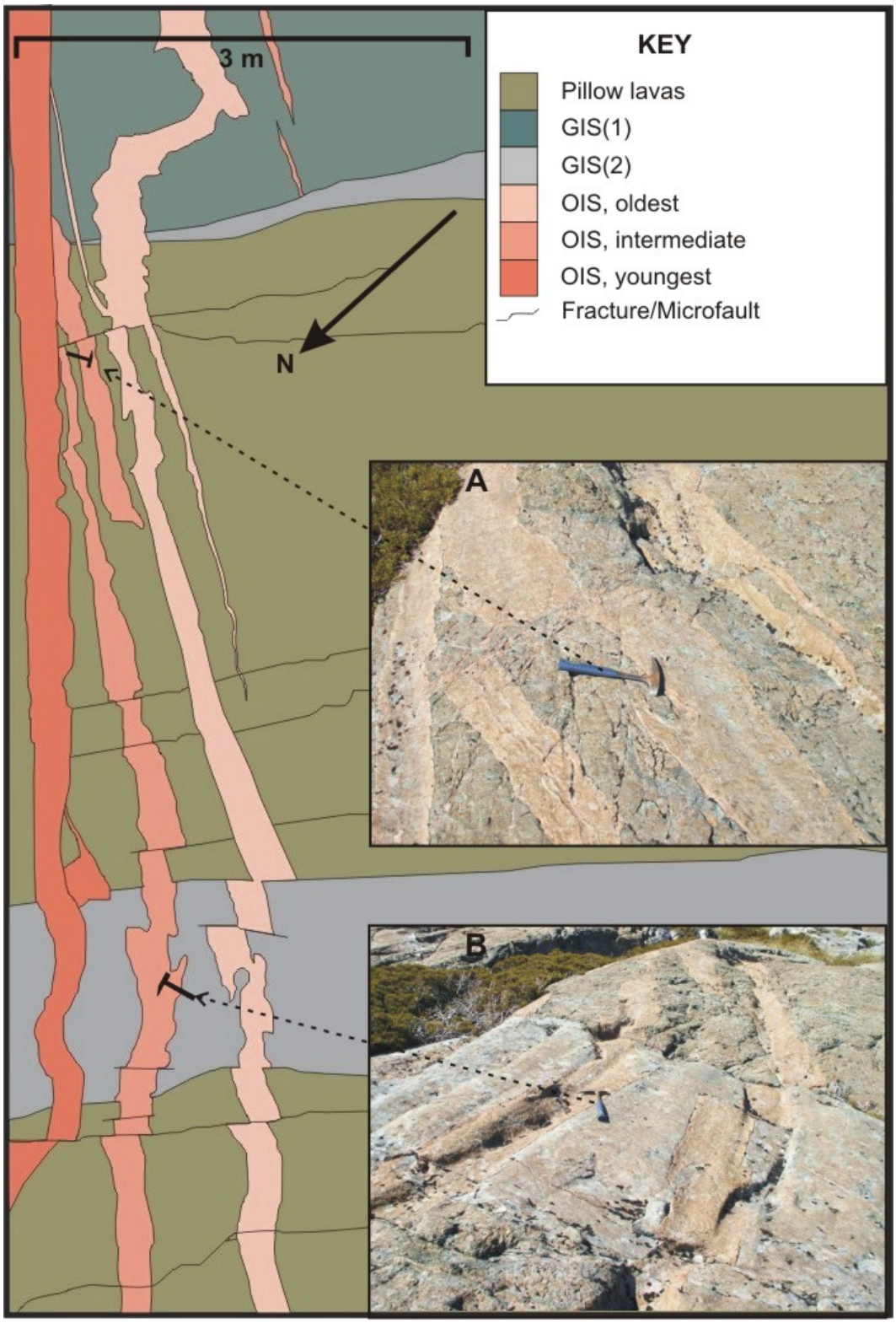

Fig. 4.21: Diagram and pictures illustrating the geometry of segmentation in the upper crust (pillow lavas). In this case progressively older OIS show less diverse segmentation. Picture A shows good examples of horns, branches, offset and steps. In picture B, the OIS cut a GIS, segmentation within the GIS may be caused by structures that run parallel to the GIS flow direction. These OIS are probably of similar age, but changing stress conditions forced the younger OIS to be less segmented. Section sketched at AP3.

4.3.1 Distribution of intrusive sheets

The physical distribution of intrusive sheets changes with pseudostratigraphic level in the Bryneira range. Intrusive sheet distribution changes in response to the physical conditions of the magma system and the stress systems acting on the host rock. Here, distribution of the intrusive sheets is assessed at all crustal levels. The clarity in preservation of OIS as opposed to GIS, means there is bias towards their distribution in the following discussion.

4.3.1.1 Distribution of intrusive sheets the Livingstone Peridotite and lower gabbros

At P22 OIS were followed from the lower gabbro into the Livingstone Peridotite below (Fig. 4.23). Their origin was obscured by serpentinite approximately 100m below the Livingstone peridotite-layered gabbro contact. Investigation up section and petrologic examination revealed that these dikes are young OIS. Spacing is around 10-50m, with thicknesses of 0.5-1.5m, and low angle crosscutting was observed. No other type of intrusive sheet is seen at this crustal level. The regular parallel sides of these dikes suggest they propagated through their own fractures (Fig. 4.22).

Fig. 4.22: Cross cutting OIS within the Livingstone Peridotite. Red line marks the boundary between the ultramafic country rocks, yellow between two crosscutting dikes.

4.3.1.2 Distribution of intrusive sheets in the middle gabbros

The GIS are first seen in the middle gabbros. At this crustal level GIS rarely form a defined parallel sided intrusive sheet. They are more commonly blob shaped bodies or amorphous horizons having poorly defined boundaries with little or no chilling (Fig. 4.24). Up section 300m of this, the first defined GIS are seen. Varied distribution and occasional cross cutting suggests that GIS were emplaced in the lower crust contemporaneously and slightly after the host gabbro, but part of the same magmatic system.

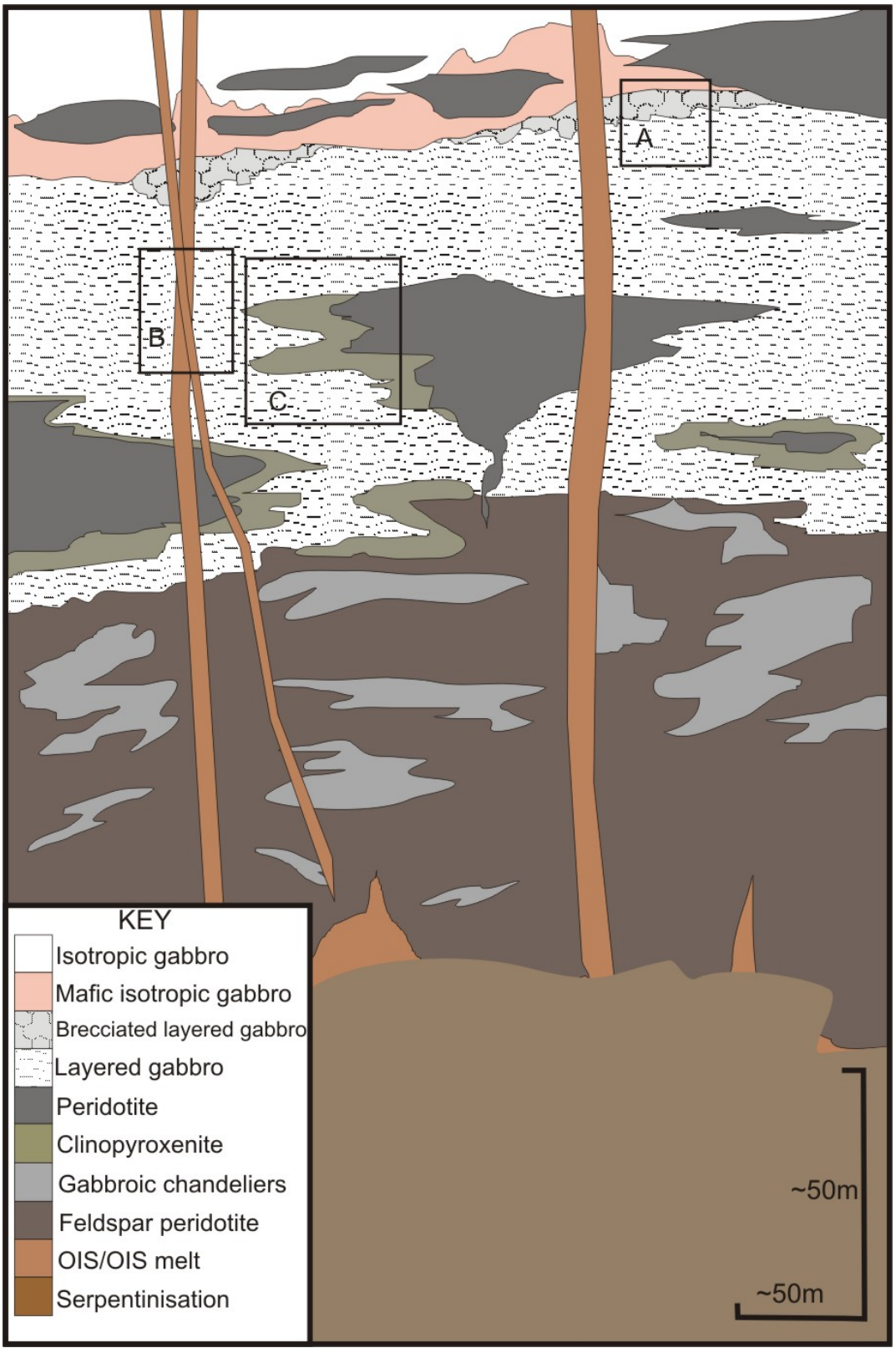

Fig. 4.23: Diagram showing the origin of OIS in the Livingstone Peridotite. **A)** is shown in fig. 4.9 **B)** is shown in fig. 4.22 **C)** is shown in fig 3.10. Note that the OIS are straight and continuous with no segmentation. The horizontal scale is half that of the vertical i.e. vertical exaggeration is two times.

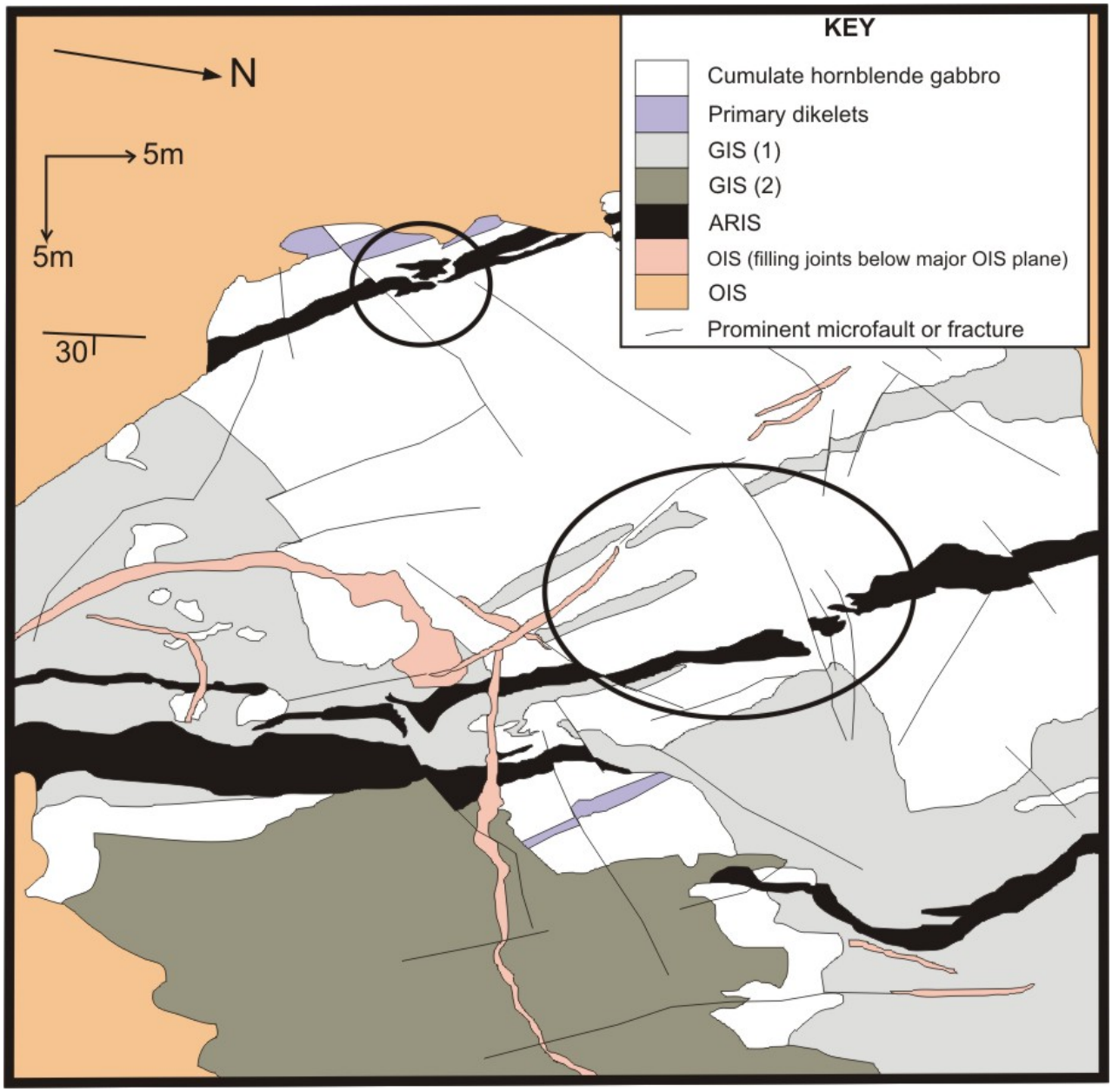

Fig. 4.24: A measured section of gabbro and intrusive sheet rocks that demonstrate the nature of the GIS in the (lower) middle gabbros at P4. Two ellipses highlight areas of unusually deformation, where GIS(1) and ARIS have been stretched until failure. In other places microfaults show both normal and reverse displacement. This is a particularly clean exposure of typical middle gabbro-intrusive sheet interactions.

In the lower part of the middle gabbros OIS distribution is orderly. They form continuous, sub-parallel sided sheets spaced ~10-30m, 0.3-2.5m wide (Fig. 4.25), cross cutting at low angles in common.

Fig. 4.25: Clear exposure of the lower crust, showing a variety of uniformly distributed intrusive sheets. OIS can be traced from left to right as well formed sheets. A bud can be seen on the left side of the large OIS that cuts the picture.

In the middle isotropic gabbros the distribution of intrusive sheets becomes more complex. Uniform distribution in the lower crust changes to distribution with no continuity in the middle crust. Change is particularly evident in the OIS, which changes from planar continuous sheets, to a mix of continuous and discontinuous sheet of varying thicknesses (Fig. 4.26). The volumetric distribution of OIS is also heterogeneous, particularly in older OIS. Areas of high OIS concentration are lie close to areas of low concentration. Sheets rapidly thicken to ~15m. All OIS still conform to the description of a planar intrusive sheet; no large bodies (laccoliths) were seen. It is possible that variation in distribution of OIS is the result of high fracture concentrations in the host gabbro allowing for lateral propagation, or a relationship between magma pressure and buoyancy (Price and Cosgrove, 1990). Younger OIS are less complex, often cutting the entire outcrop.

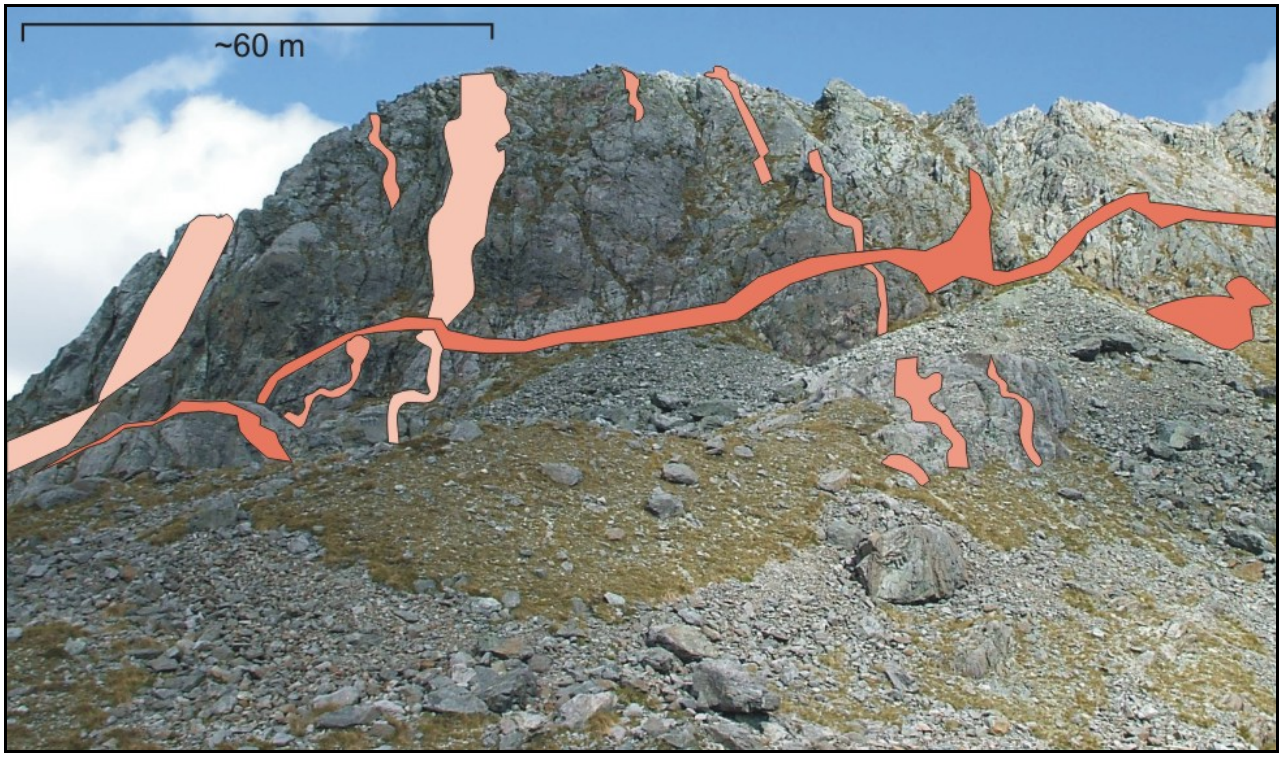

Fig. 4.26: Photo looking south at ridge north of Lake Never from P2. The large OIS have been highlighted to show their inconsistent relationships. Note that only the very large OIS are highlighted in this picture.

4.3.1.3 Distribution of intrusive sheets in the upper crust

The intrusive sheets of the upper crust are contained within the upper most gabbros, hypabyssal units and pillow lavas. Changes in distribution lead to a more uniform pattern in both OIS and GIS.

GIS in the upper crust are always consistently distributed. They are usually between ~0.5-1.5m thick with sub-parallel, straight or curved margins and evenly space by septa of host rock (Figs.4.21, 4.28A and B).

The distribution of OIS in the upper crust was disparate, major differences in spacing and concentration were observed. Commonly, clusters of three or more similarly aged OIS are separated by septa of host rock (Figs. 4.28 and B, Fig. 4.21). This pattern is described as pseudosheeting (after Hopson, 2007). In isolated areas OIS are closely spaced locally occupying 100% of the outcrop. These situations are seen at the transition between

hypabyssal rocks and pillow lava, possibly in a zone where the strength of the host rock rapidly decreases. It is often hard to trace individual intrusive sheets in these areas as intermingling and crosscutting between similarly aged segments is high. Within the pillow lavas OIS often have internal cooling ridges (Fig. 4.27), indicating pulses of magma incrementally opened sheets.

Fig. 4.27: Cooling ridges in an OIS, seen here cut a GIS.

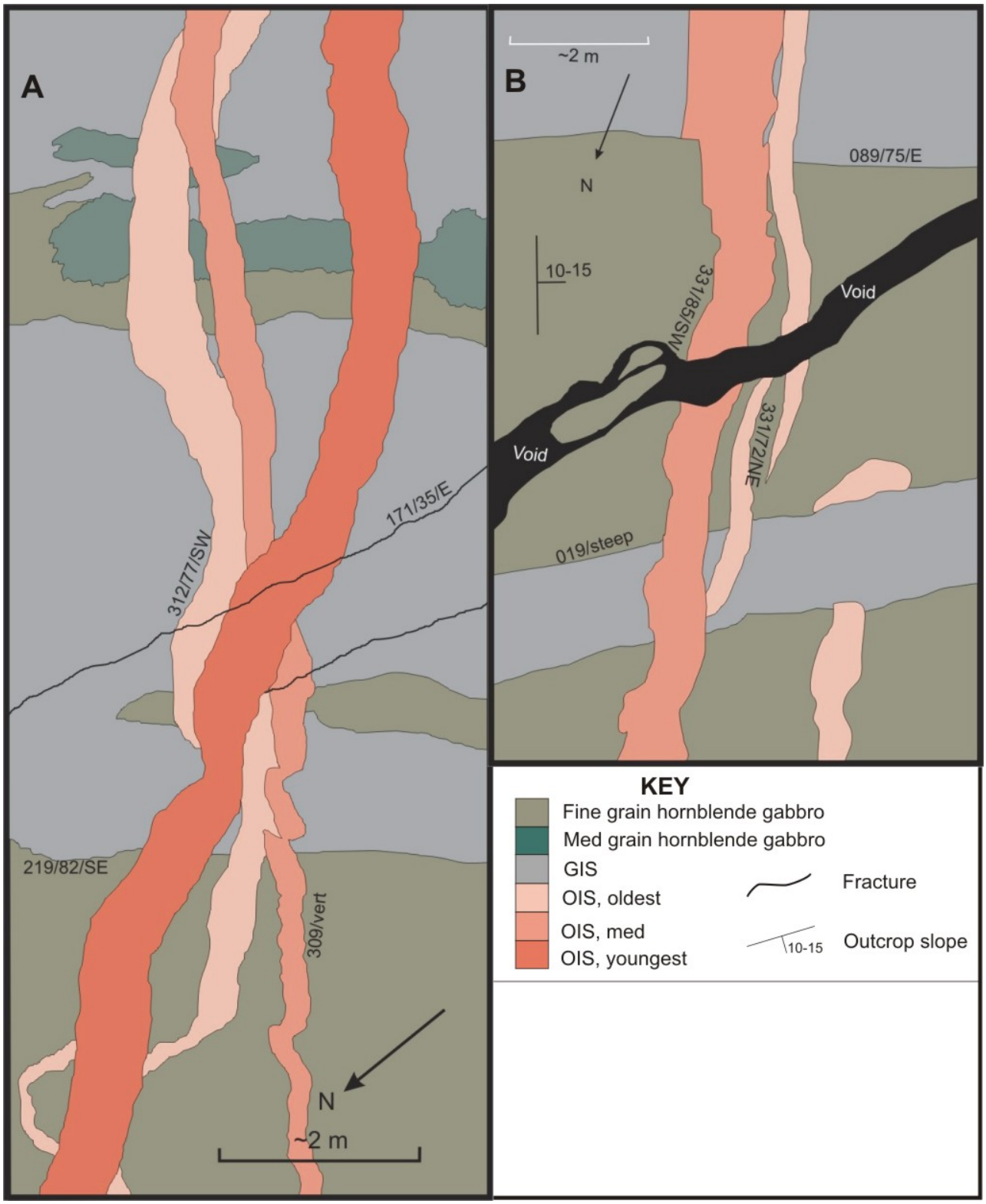

Fig.4.28: A) Three OIS following a similar route through the gabbros and GIS. **B)** A similar pattern where OIS are found close together. Both A and B show OIS displaying 'pseudosheeting' and spaced GIS, these patterns are typical of the upper gabbros. A and B were sketched at NS7 and NS4 respectively.

Chapter 5: Orientation of structures

5.1 Determining Paleo-horizontal

Paleo-horizontals are structural markers that represent a preserved horizontal with a known relative age. As ophiolite pseudostratigraph does not always record a horizontal reference during formation, paleo-horizontals are relied upon to retro-deform ophiolites to their original orientation. Paleo-horizontals are used in this study to return the DMOB to its original horizontal position, and further investigate the cross-cutting relationships between intrusive sheets (see later, section 6.2).

Most structural analyses of ophiolites have been conducted on relatively complete un-tectonised examples (e.g. Troodos Ophiolite in Cypress and Samail Ophiolite in Oman) and have been compared to observations and geophysical models of ocean crust (e.g. Dilek et al., 1998). From various studies, a number of potential paleo-horizontal indicators can be identified:

a) **Igneous layering** is observed in the plutonic portions of ophiolites and forms sub-parallel to the base of the magma chamber (Nicolas, 1989). Whether igneous layering always forms horizontally is not certain and this lead to ambiguity (see Harris, 2004). Igneous layering has been used in the Thetford Mines Ophiolite in Canada to establish paleo-horizontal in the Gabbroic zone (Schroetter et al., 2003).

In the Bryneira Range pyroxenite-gabbro rhythmic layering can be observed in the lower gabbros and layered gabbros at numerous locations (section 3.3.2.2), and is inferred to be a paleo-horizontal. Poles to igneous layering planes are presented as Igneous Layering A in Fig 5.1. A second type of igneous layering was measured by tentatively inferring that “pods” of Livingstone Peridotite were intruded as horizontal layers in the middle and lower gabbros. These are presented as Igneous Layering B in Fig 5.1.

b) **Pillow Lava Layering** is found in the volcanic portion of an ophiolite and is formed by the flow of lavas along the gently inclined ocean floor. Pillow lava layering has been used to demonstrate tectonic rotation of crustal scale block in the Josephine Ophiolite (California) (Alexander and Harper, 1992). In the Study area, well developed pillow lava

layering was found on the eastern flanks of Courtney Peak (CP4). Poles of these attitudes are shown in Fig. 5.1; these are overturned. It should be noted that because pillow lavas are extruded on to inclined slopes they were not strictly paleo-horizontal at the time of their deposition, but are unlikely to be more than 1^0-3^0 in error because seafloor gradients are typically low.

c) **Sedimentary layering** is commonly used as a paleo-horizontal in ophiolite studies to remove post-ophiolite rotation. In all cases, it is assumed that sedimentary beds were deposited almost horizontally.

In this study, two such paleo-horizontals are used:

1. Layering of the Upukerora Breccia is used as a syn-magmatic paleo-horizontal indicator. Intrusive sheets are recorded in the lower portion of the Upukerora Breccia (Hyslop, 1978; Pillai, 1989), indicating the Upukerora Breccia was paleo-horizontal during the final stages of magma injection (Fig. 5.1). Note that these beds are now overturned.
2. The Wooded Peak Limestone formed a conformable cap over the breccia and underlying oceanic crustal sequence. Layering records paleo-horizontal during its deposition (Fig. 5.1).

Both types of sedimentary layering was measured from the Courtney Peak area (CP4). Disparity in the orientation of the two sedimentary paleo-horizontals likely indicates ongoing deformation during their deposition.

5.1.1 Interpretation of paleo-horizontal orientations

All paleo-horizontal attitudes are shown as poles in figure 5.1. An apparent girdle is highlighted by a black great circle orientated E-W (Fig. 5.2). The presence of such a girdle indicates that nearly all paleo-horizontals have a similar strike of north-northeast, but very different dips to both the west and east. This symmetry in strike mirrors the trend of the Key Summit Syncline axial trace (trending north-northeast (Turnbull, 2000)) and the general strike of the DMOB.

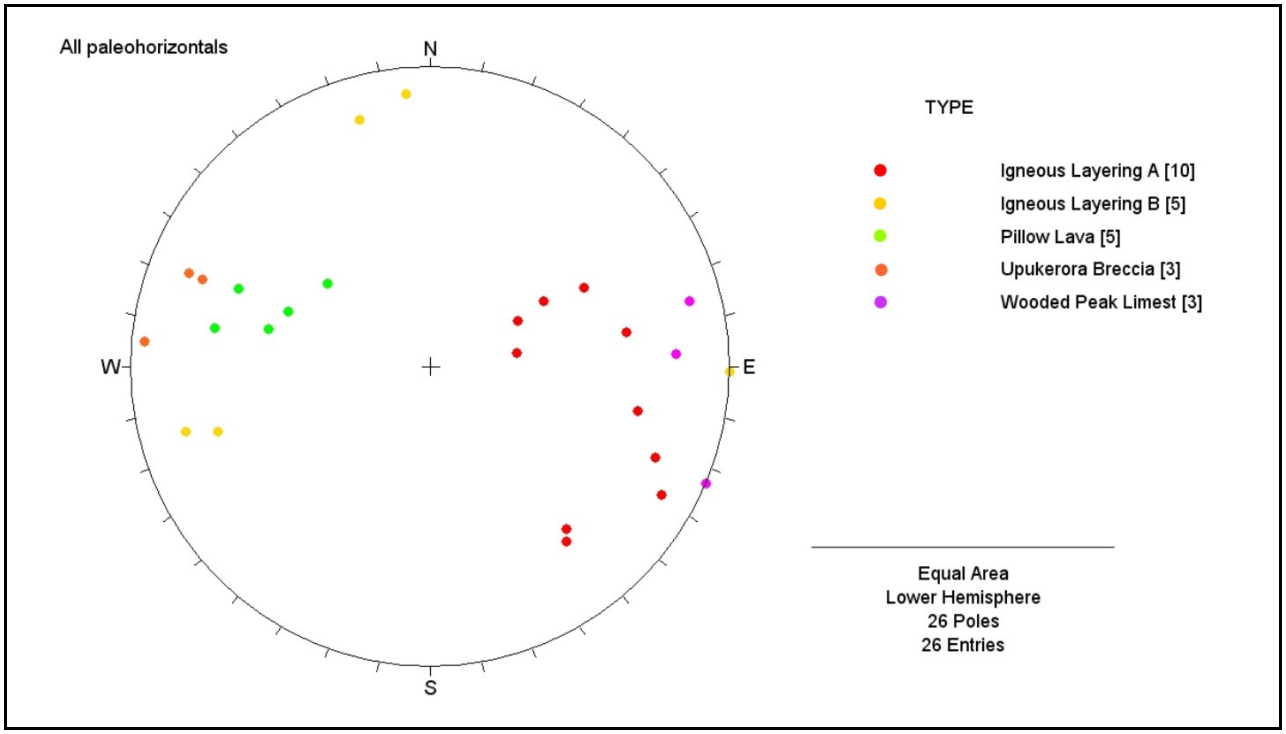

Fig. 5.1: Poles for all potential paleo-horizontals measured in the Northern Bryneira Range study area.

Relative age and validity of paleo-horizontals is related to their position in the DMOB pseudostratigraph and overlying Maitai Group stratigraphy. The age of paleo-horizontal markers increases with pseudostratigraphic and stratigraphic depth, and their validity as confident paleo-horizontals decrease with increasing age. Each type of paleo-horizontal is briefly summarised in order of increasing age and decreasing confidence:

1. Wooded Peak Limestone is the youngest paleo-horizontal. Bedding is assumed to have been horizontal and deposited on the DMOB after all magmatic activity had ceased. Wooded Peak Limestone provides the most convincing paleo-horizontal mark, hence is used to re-orientate the under-lying DMOB to a horizontal position of known relative age.
2. Upukerora Breccia is entirely composed of fragments of DMOB. Erosion of fault scarps has been sighted as a likely origin for these breccias (Kimbrough et al., 1992), indicating ongoing deformation during deposition. This, and the precence of rare intrusive sheet with in the breccia, indicates that the paleo-horizontal marker bedding of the Upukerora Breccia was synchronous with the end of DMOB magmatism.

3. Pillow Lava layering in less complex settings is commonly near-horizontal, therefore, they are a moderately good paleo-horizontal marker. They appear as layers that were sub-parallel during the extrusion of the lavas associated with the youngest OIS magmatism. This is illustrated in their similar orientations to the younger paleo-horizontals.
4. Igneous Layering B, does not fit with the west-east girdle highlighted (Fig 5.1). There is vague spatial similarity in orientation to the younger paleo-horizontals. The confidence and validity of Igneous Layering B, is therefore very low.
5. Igneous Layering A is thought to be the oldest potential paleo-horizontal, being coeval to the GIS magmatism. Orientations show a general strike that corresponds to the mean strike of the DMOB. In comparison with some younger paleo-horizontals (pillow lavas and Upukerora Breccia), Igneous Laying A has very different dips but has a similar orientation to the Wooded Peak Limestone. For this reason, the validity of Igneous Laying A must be treated with caution.

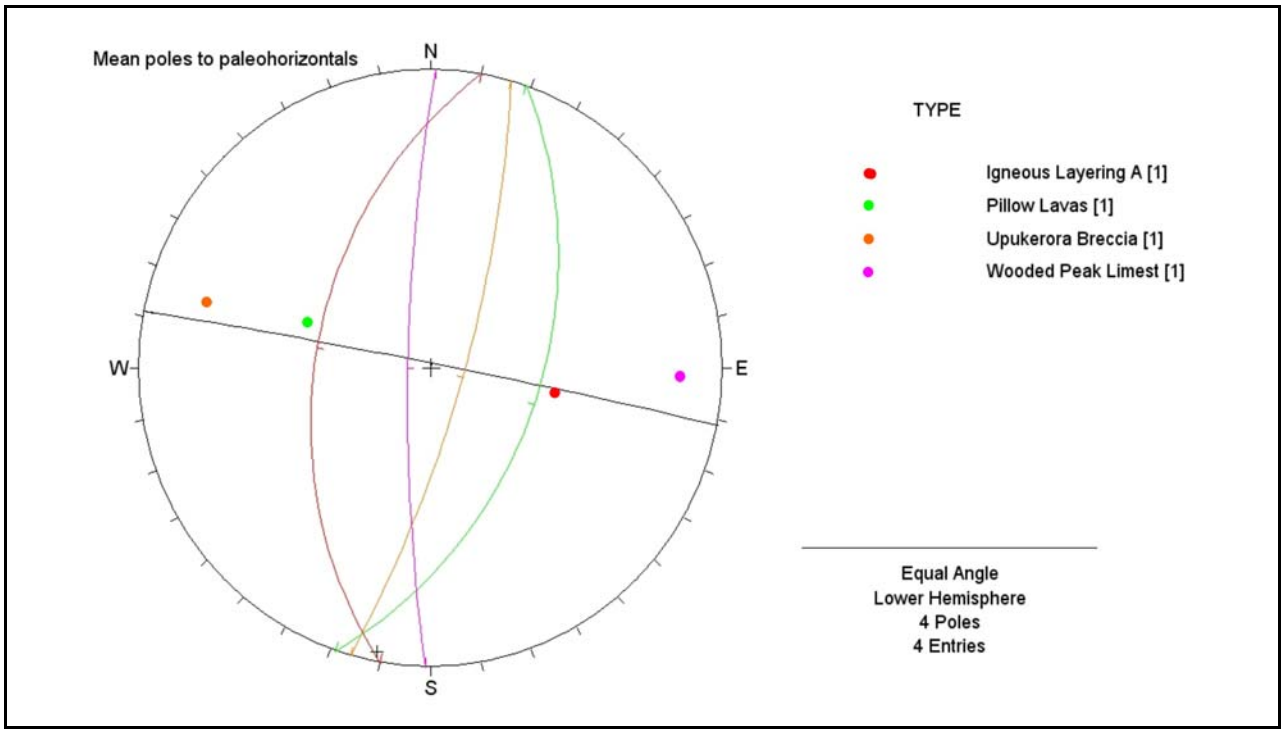

Fig. 5.2: Mean poles and corresponding planes (colour coded) for each type of Paleo-horizontal. The black great circle girdles all paleo-horizontals, indicating similar strikes but dissimilar dips. Igneous Layering B is not shown here, as no consistence in orientation was seen in figure 5.1.

Mean orientations were calculated by plotting each paleo-horizontal type as a set (shown in Fig. 5.2). Mean Wood Peak Limestone orientation is used in this chapter to re-

orientate the DMOB to its horizontal position during the Late Permian. In figure 5.3, the Wooded Peak Limestone is shown in its original horizontal position, the synchronous positions of older paleo-horizontals are also shown. Older paleo-horizontals are used later in the discussion chapter (chapter 6) to test the origin of cross cutting between intrusive sheets.

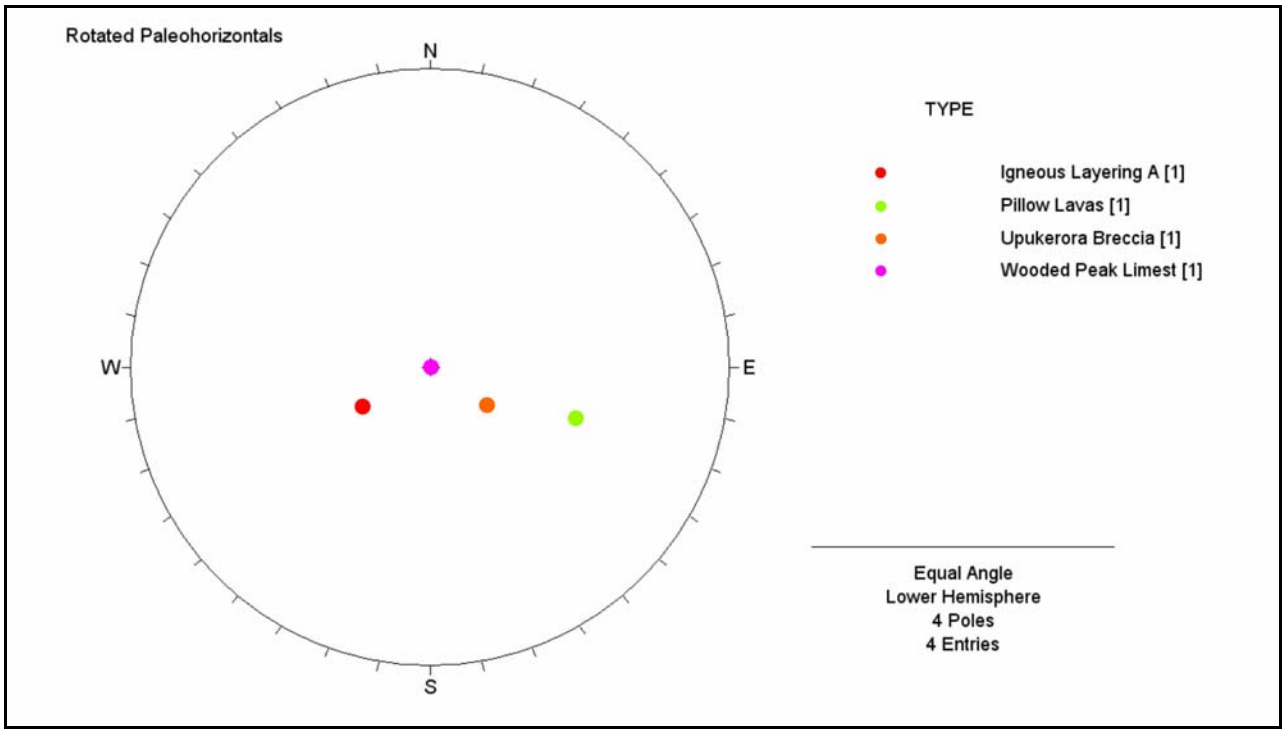

Fig. 5.3: Stereo net showing the position of paleo-horizontals when the Wooded Peak Limestone is in its original horizontal position. To do this, an 81 degree clockwise rotation around a trend of 002 degrees was performed.

5.2 Intrusive sheet orientation

The orientations of intrusive sheets were measured at all crustal levels within the Northern Bryneira Range. It was assumed that individual sheets propagated upwards or towards the west, this however was often unclear. The attitude of all types of intrusive sheet were measured, but the low number of minor intrusive phases (e.g. ARIS, Black dikes etc.) meant that it is not statistically viable to discuss their orientations. The large population of major intrusive sheet phases allows the orientation of grey intrusive sheets (GIS) and orange intrusive sheets (OIS) to be discussed separately in the following sections. Generally, the attitudes of intrusive sheets are consistently moderate to steep.

5.2.1 GIS Orientation

The GIS orientations are shown as poles in figure 5.4. They have no distinctive trend and show a broad distribution of poles in the northwest and southeast quadrant. Pole positions indicate that dips are highly variable to the northwest and southeast, with a minimum dip of ~40 degree in either direction. For easy reference, the GIS strike approximately parallel to the Bryneira Range.

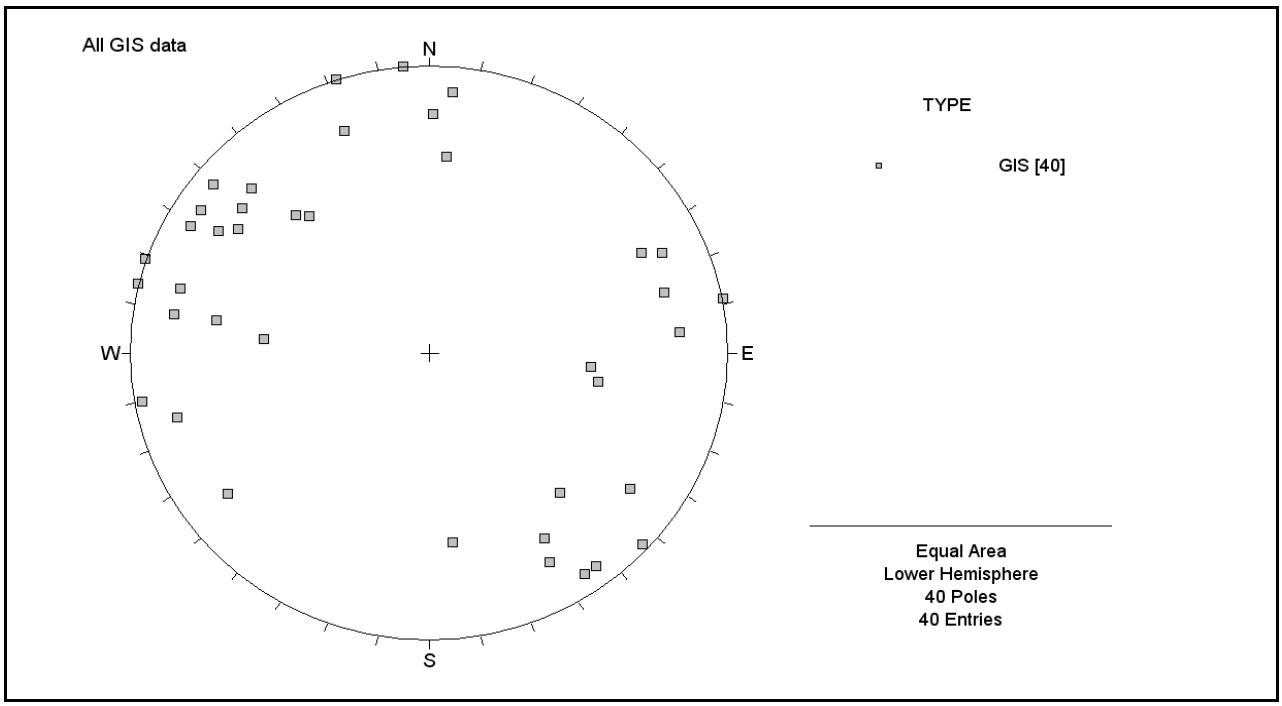

Fig. 5.4: Poles to GIS, showing all data collected in the study area.

5.2.1.1 Rotation of GIS data

Here, orientations of GIS are returned to their attitude during the deposition of the Wooded Peak Limestone. GIS in figure 5.4, displayed as poles, were rotated by the same amount as necessary to return the Wooded Peak Limestone to its original horizontal position. To do this, an 81 degree clockwise rotation around a trend of 002 degrees was performed (as in Fig.5.3). Re-orientated poles to GIS are shown in figure 5.5 as a contoured plot.

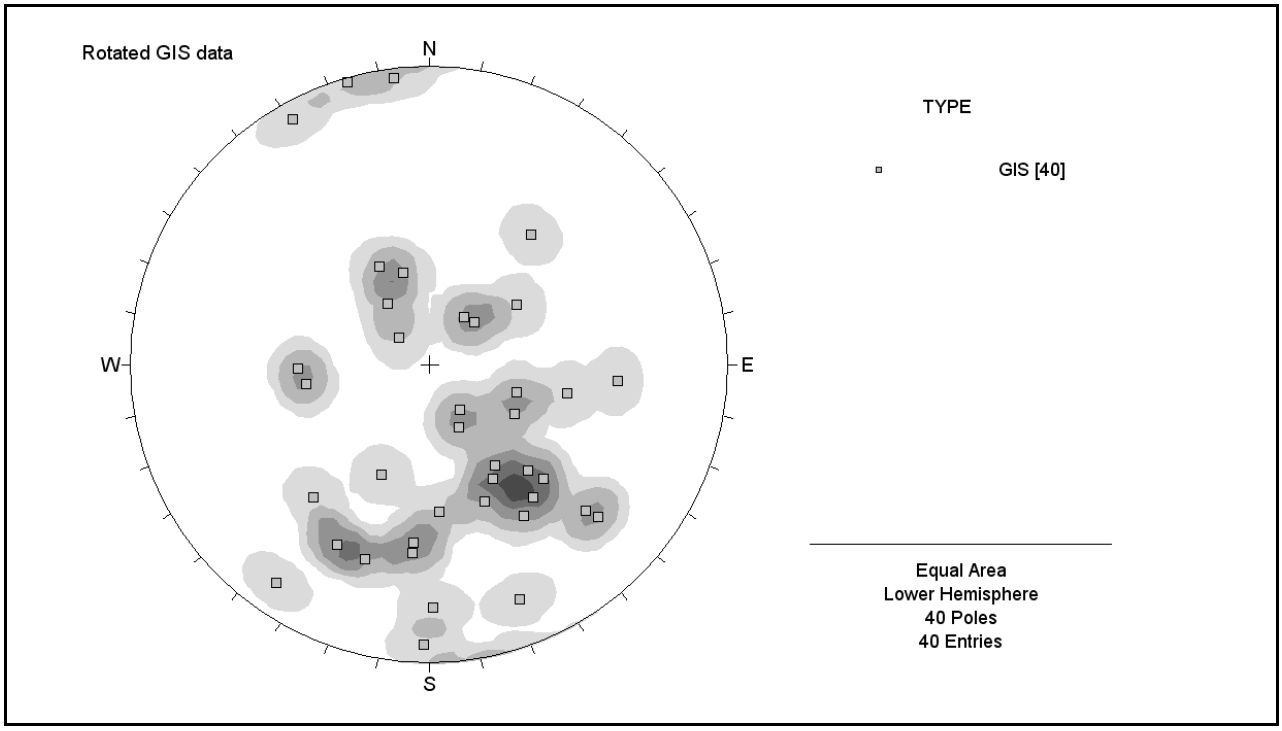

Fig. 5.5: Poles to GIS re-orientated to the position when the Wooded Peak Limestone was horizontal.

5.2.1.2 Interpretation of GIS rotated orientations

GIS poles are spread within a large central to southern zone of the stereo plot. Considerable scatter means that a unique interpretation and a unanimous orientation of propagation is not constrainable. It should be noted that there is large difference in age between the GIS and deposition of Wooded Peak Limestone. Therefore, the original orientations of GIS may have been altered by tectonism. Without additional information, the origin of scatter is only speculative (this is discussed in detail later in chapter 6). Regardless of scatter, there is a clear dominance of low inclinations for GIS. Orientations of near horizontal attitude are suggestive that GIS were injected as inclined intrusive sheets or sills. A subordinate number of sheets with high inclinations closer to vertical are spatially related to the central concentration. They connect dominant lower inclinations with the southern (and opposite northern) peripheries of the stereo net. Steeply inclined GIS were possible dikes acting as feeders to sub-horizontal sill-like sheets.

5.2.2 OIS Orientations

It was apparent in the Northern Bryneira Range that OIS did not occur as one discrete pulse of magmatism. Multiple or continuous pulses indicate ongoing intrusion over an unknown period, a fact illustrated by cross cutting relationships, chilled margins and changing composition between OIS at all crustal levels. This was recognised and taken into account when collecting orientation data. OIS data was collected by assigning each measurement to one of four sub-groups (OIS(1) (oldest) to OIS(4) (youngest)). Deciding which sub-group each sheet is part of, was done by individual assessment of:

- Weathering colour; younger OIS tend to be bright orange to orange–green, whilst older sheets are cream orange. Weathering colour may reflect increasing iron concentrations in younger OIS (Sinton, 1975).
- Crosscutting relationships with other OIS sheets.
- Segmentation and continuity; younger OIS are less segmented and can be traced further in outcrop.

Discriminating between individual OIS was made by judgement, some variation in the quality of this data is probable. The four sub-groups are best thought of as an attempt to subdivide the continuum from oldest to youngest OIS and should not be mistaken as representing four discrete pulses.

The sub-grouping in the orange intrusive sheets is shown in figures 5.6-5.9 below, as poles to sheet attitudes. In general, there were only just enough points measured to establish cluster for each sub-group. Stereo plots are arranged in order, from oldest to youngest sub-groups.

5.2.2.1 Orientation of OIS(1)

Figure 5.6 shows poles to intrusive sheets for the OIS(1) sub-group. There is no grouping or strong clusters evident in this plot. OIS(1) intrusive sheets have the lowest consistency in orientation of OIS sub-groups.

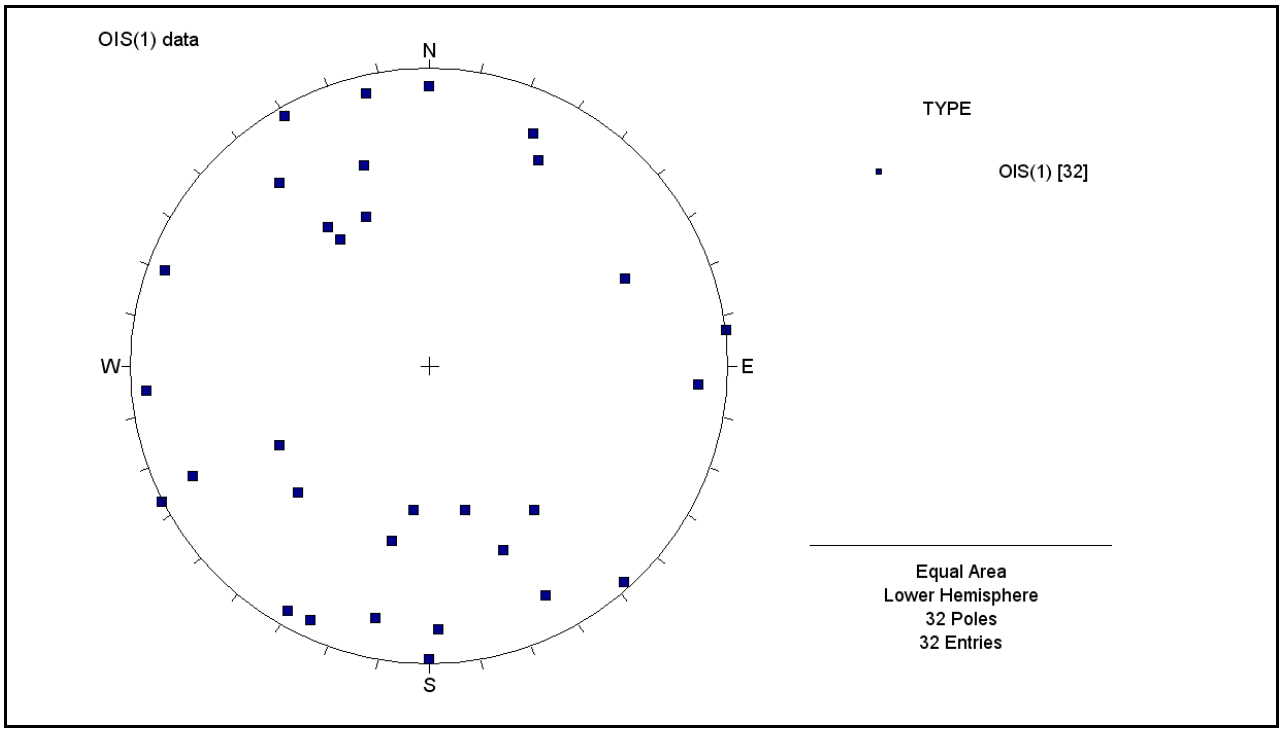

Fig. 5.6: Poles to the OIS(1) sub-group intrusive sheets. Showing all data collected in the study area.

5.2.2.2 Orientation of OIS(2)

Figure 5.7 shows the poles to intrusive sheets for the OIS(2) sub-group. This plot has significantly less data points than the other three sub-groups plots (Figs. 5.6, 5.8 and 5.9), this makes the extent of scatter harder to assess. A cluster of poles is evident in the east-northeast of the net. Poles in the northwest quadrant of the net form a close spatial association to each other, but are not dense enough to be a cluster.

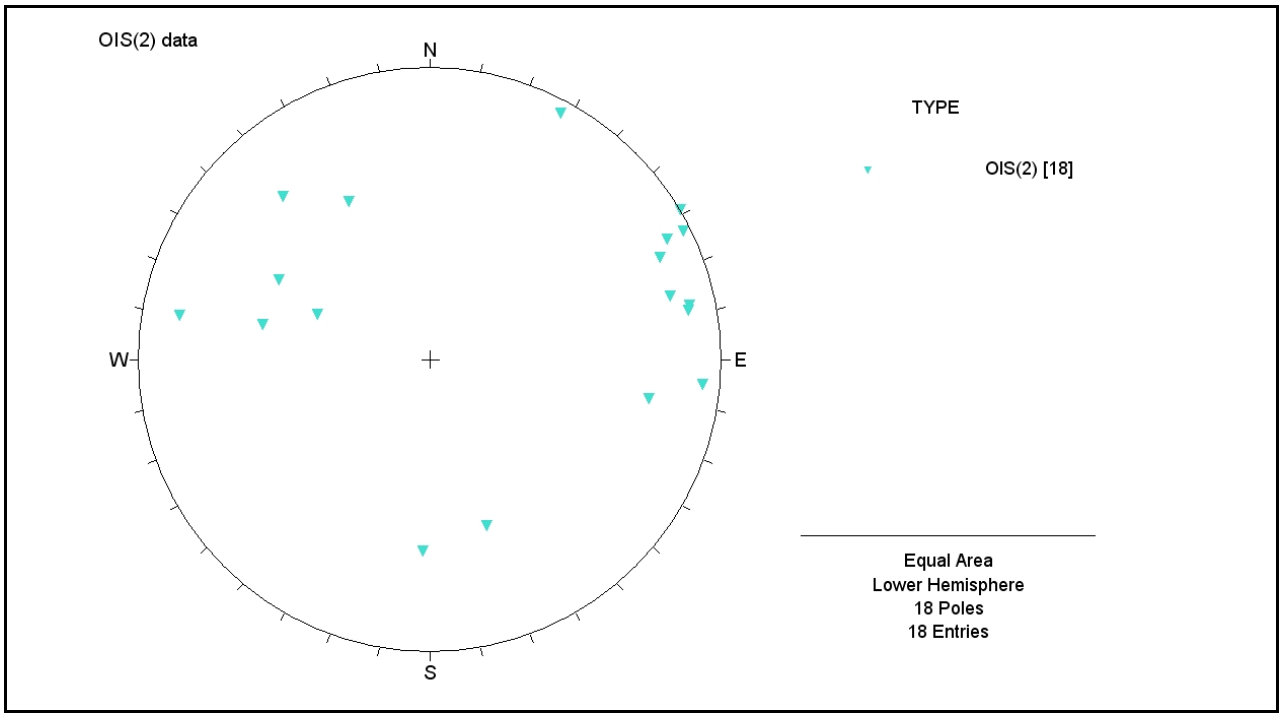

Fig. 5.7: Poles to the OIS(2) sub-group intrusive sheets. Showing all data collected in the study are.

5.2.2.3 Orientation of OIS(3)

Figure 5.8 shows the poles to intrusive sheets for the OIS(3) sub-group. The distribution of poles exhibits an inconsistent girdle from the northeast to the southwest quadrants, the strongest cluster being located in the west-northwest of the net. In terms of strike and dip, these poles represent a dominant northwest-southeast strike and highly variable dips.

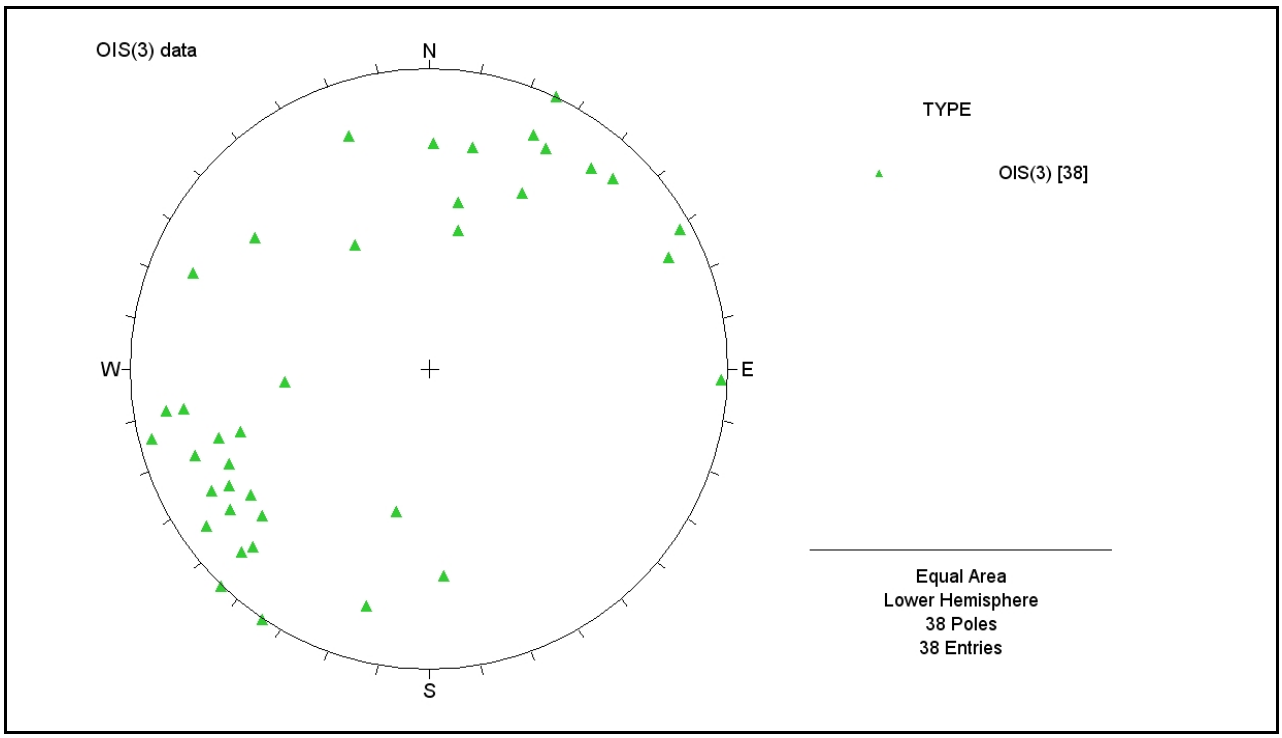

Fig. 5.8: Poles to the OIS(3) sub-group intrusive sheets. Showing all data collected in the study area.

5.2.2.4 Orientation of OIS(4)

Figure 5.9 shows poles to the OIS(4). This sub-group is particularly significant because they are some of the last intrusive sheets seen cutting the main ophiolite body, making them distinctive in outcrop. A strong cluster of poles is seen in the southwest of the net.

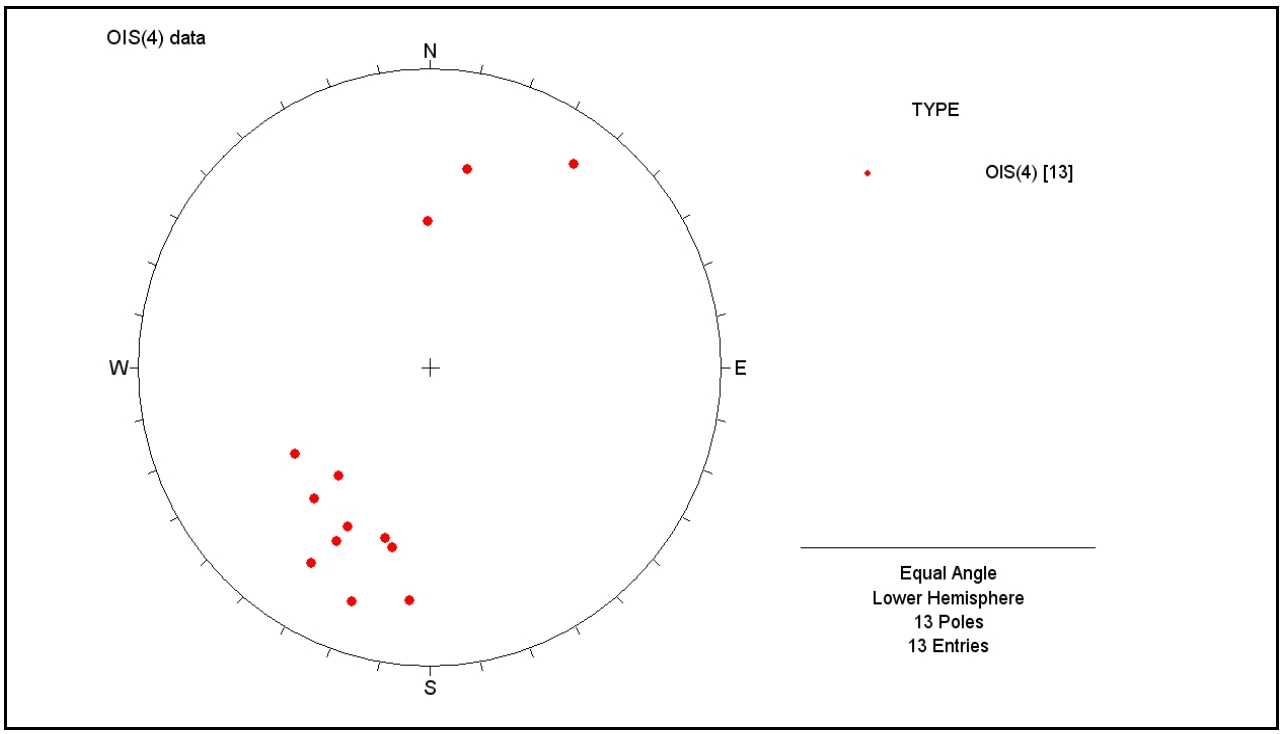

Fig. 5.9: Poles to the OIS(4) sub-group. Showing all data collected in the study area.

5.2.2.5 All OIS orientations

When all four sub-groups are overlain (Fig. 5.10), there is a fairly even distribution of poles over the stereo net. Most sheets have moderate to steep dips and fewer are seen in the centre and southeast quadrant (Fig 5.10).

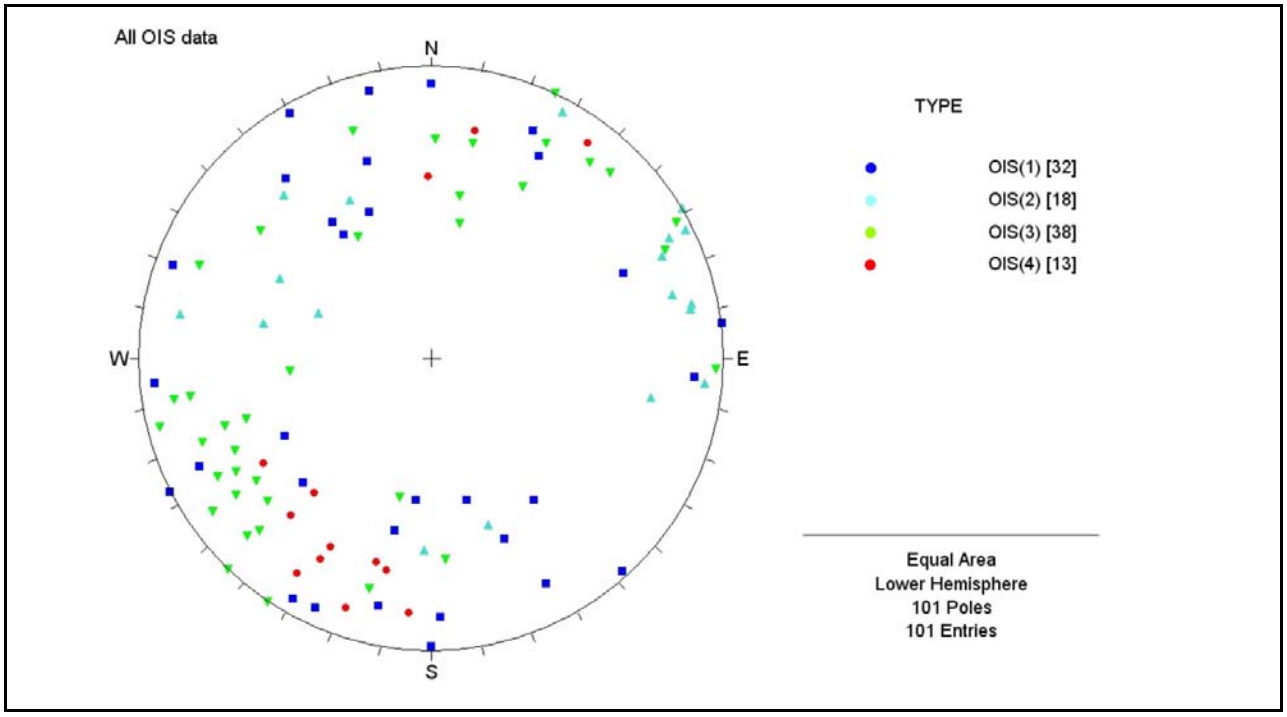

Fig. 5.10: All poles to OIS superimposed on one stereo plot.

5.2.2.6 Rotation of all OIS data

As for the GIS data, OIS data has to be returned to a known horizontal position before it can be interpreted. All OIS in figure 5.10, displayed as poles, are rotated by the same amount as necessary to return the Wooded Peak Limestone to its original horizontal position (Fig. 5.3). To achieve this, all poles are rotated 81 degrees clockwise, around a trend of 002 degrees. The re-orientated plots are shown in figures 5.11, contours are used to show where the dominant orientations lie.

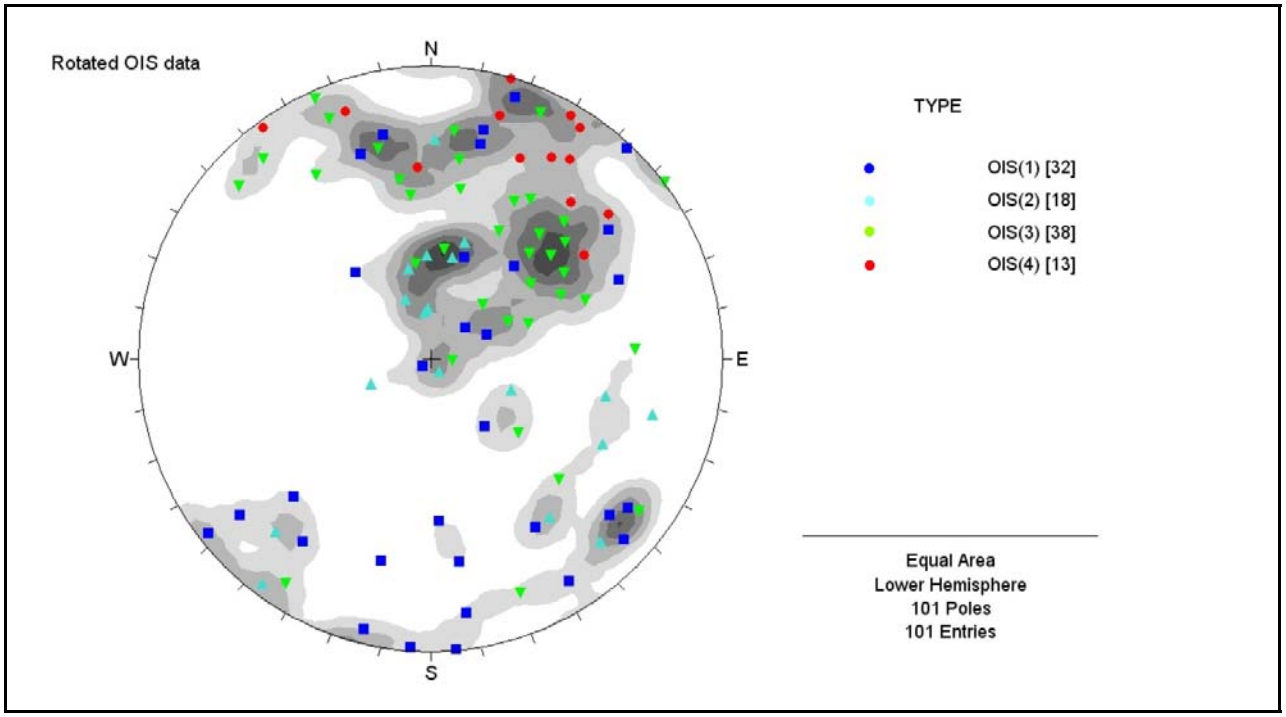

Fig. 5.11: Re-orientated, contoured poles to OIS showing all data rotated to the position when the first Wooded Peak Limestone beds were deposited.

5.2.2.7 Interpretation of all OIS rotated data

Poles to re-orientated OIS (Fig. 5.11) have a large scatter, yet show concentrations of common orientation in the northern quadrant. Variation in orientation does not allow simple assignment of conclusive intrusive sheet categorisation (e.g. dike or sill). OIS have propagated as sheets that span a spectrum of orientations through sills to dikes.

It is important to note here the distribution of OIS sub-groups. Scattered poles that lie around the periphery of the main northern cluster (Fig. 5.12B) are predominantly OIS(1), and to a lesser extent OIS(2) and OIS(3). Scattered poles indicate large a variation in orientation of older OIS. In contrast, the two younger sub-groups (OIS(3) and OIS(4)), dominate the area assigned as the northern cluster (Fig. 5.12 (A)). OIS(2) make up a concentrated area of this northern cluster.

The distribution of OIS in the northern quadrant cluster also has a relationship to the relative age of each sub-group. Moving out from the centre of the stereo net, poles generally belong to the younger sub-groups toward the margin (as indicated by the arrows in Fig. 5.12A). Sub-groups generally have lower variation in orientation with

decreasing age (as noted in Figs. 5.6-5.9). These observations are relevant to the next chapter (chapter 6) where age and orientation are discussed with relation to a tectonic model.

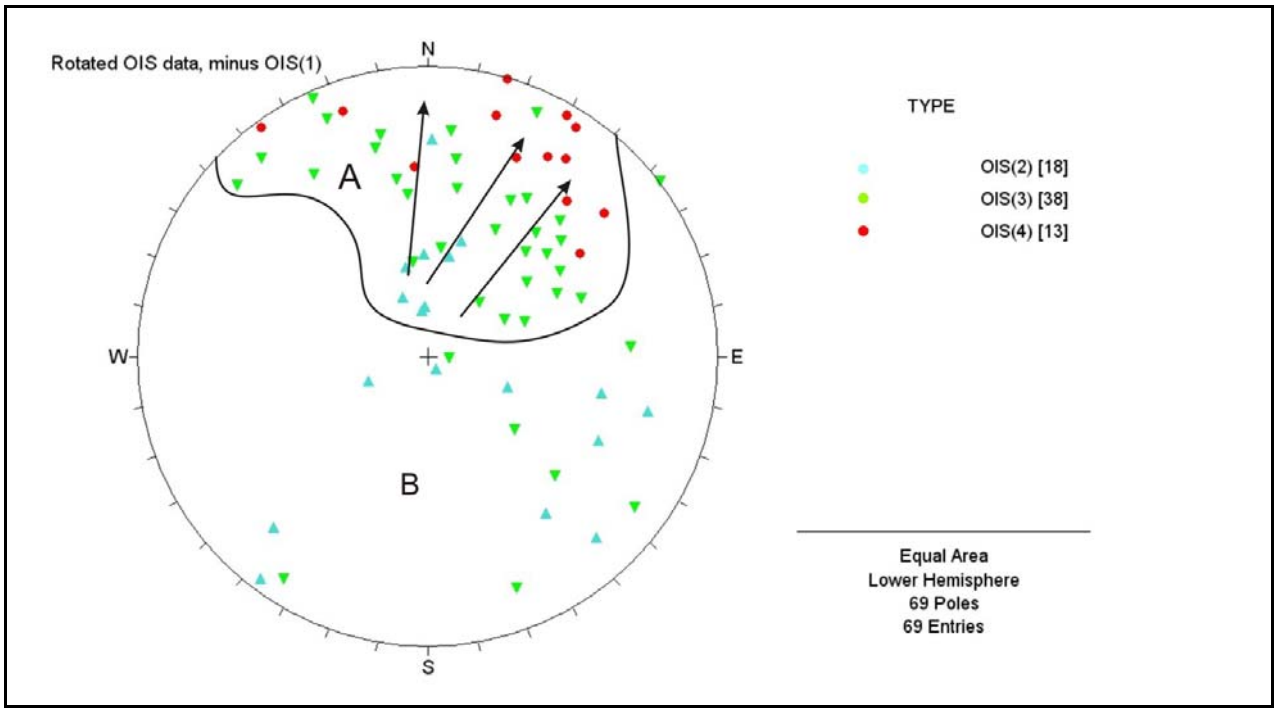

Fig. 5.12: A. Highlights the northern quadrant of the net where there is a cluster of poles of younger OIS. Arrows highlight a younging trend towards the periphery, from OIS(2) to OIS(4). **B.** Outlines the area of scatter. Note that the poles of the oldest OIS(1) have been omitted from this diagram to increase clarity.

5.3 Faults and Fractures

As has been shown in Section 4.2.2.1, it is hard to constrain faults and fractures to phases of Permian deformation. For this reason, little time was spent recording their orientation in the field. The data presented here was all collected from the Lake Never area at P6 (one outcrop is shown in Fig. 4.8B). Not all faults shown (Fig. 5.13) could be confidently confined to the Permian, but all fractures shown appear to have formed between GIS and OIS magmatism. It has also been shown that faults and fractures are both spatial and genetically related (section 4.2.1.1 and 4.2.2). All fault and fracture information is shown below in figure 5.13.

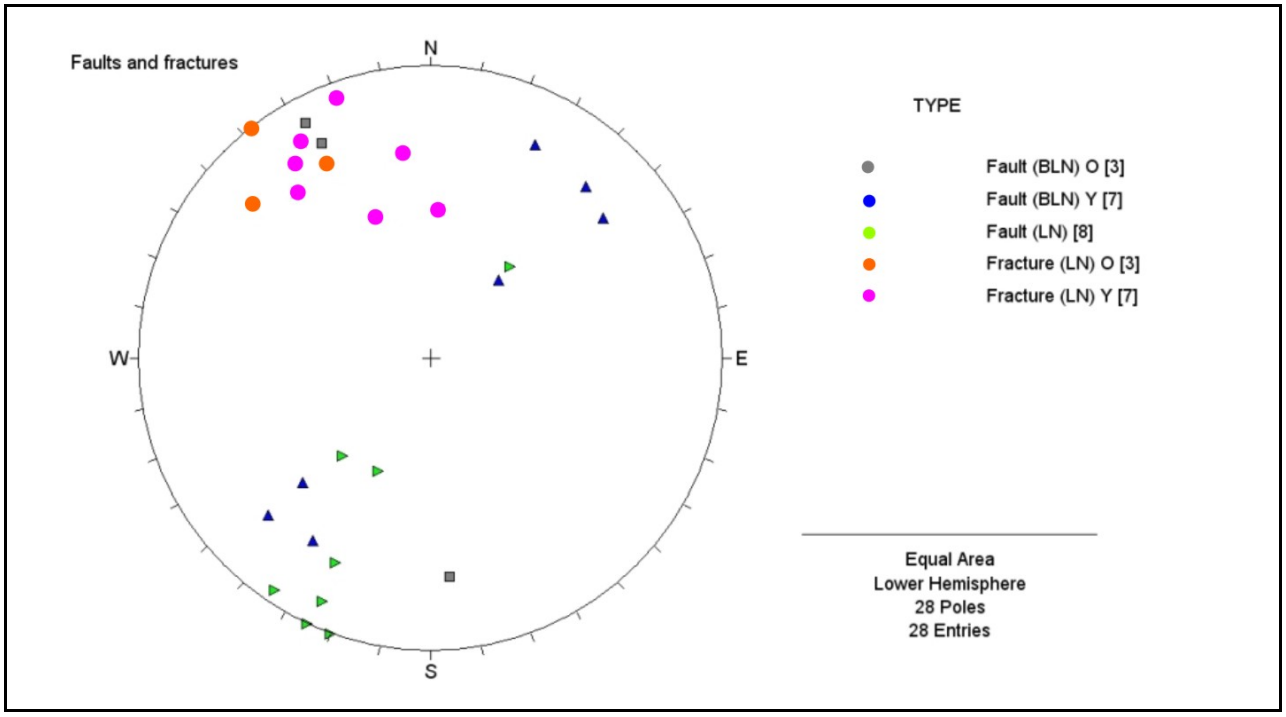

Fig. 5.13: Stereo plot of faults and fractures from the Lake Never area. LN= Lake Never, BLN=below Lake Never, O= older and Y= younger. The relative age of the 'Faults (LN)' is not known, they are most probably younger.

5.3.1 Interpretation of fault and fracture orientations

To interpret faults and fractures they have to be returned to their former orientation. The poles shown in figure 5.14, have been rotated by the amount necessary to return the Wooded Peak Limestone to its original horizontal position. As for the intrusive sheet orientations, this involved an 81 degree clockwise rotation around a trend of 002 degrees.

The results of re-orientation to former positions are shown below (Fig. 5.14). Two groups of poles are located in the north and south of the diagram and display considerable scatter. All have steep to moderate dips, as would be expected for normal faults. A mean great circle for all fault and fracture planes is shown and labelled in black, and demonstrates an east-west strike. As there is much variation in orientation between all groups of fractures and faults, it is difficult to draw conclusions. Important points to note from figure 5.14 are:

- Either side of the "mean plane" are two groups of planes with opposite dips. Possibly indicating the presence of a conjugate pair of normal faults.

- Poles in the south of the diagram are older faults (Fault (BLN)O) and fractures (Fractures (LN) O and Y). They have a consistent NE-SW strike and moderate dip.
- Poles in the northern part of the diagram are younger faults (Faults (BLN) Y and Faults (LN)). A large spread in orientation of these faults is demonstrated in their strike, but their dips are generally moderate to steep.

It has previously been shown in the structure section that faults and fractures intervening between the GIS and OIS magmatic phases are genetically related. The bi-modal distribution of faults and fractures (Fig. 5.14) may indicates that faults that followed fracturing formed on one of the conjugate pair. In general, these fault planes are orientated east-west, dipping moderately to steeply south.

The most significant observation to be taken from the orientation of faults and fractures is gained by comparing the pole positions of re-orientated faults and fractures (Fig. 5.14) with the pole positions of the re-orientated younger OIS sub-groups (Fig. 5.12). The positions of poles in both diagrams are located in the northern and southern areas. Poles to younger faults (Fault (BLN)Y and Fault (LN) in Fig. 5.14) and the main cluster of OIS (Fig. 5.12A) have similar distributions of attitudes. This possibly represents one or both of the following scenarios: a) The first being that younger OIS have preferentially followed faults when propagating through the crust. b) Orientations of both faults and similarly aged OIS have been influenced by the same stress field acting at the time of their origins. These are fundamental points argued in the following chapter, where tectonic models explaining the nature of intrusive sheeting are discussed.

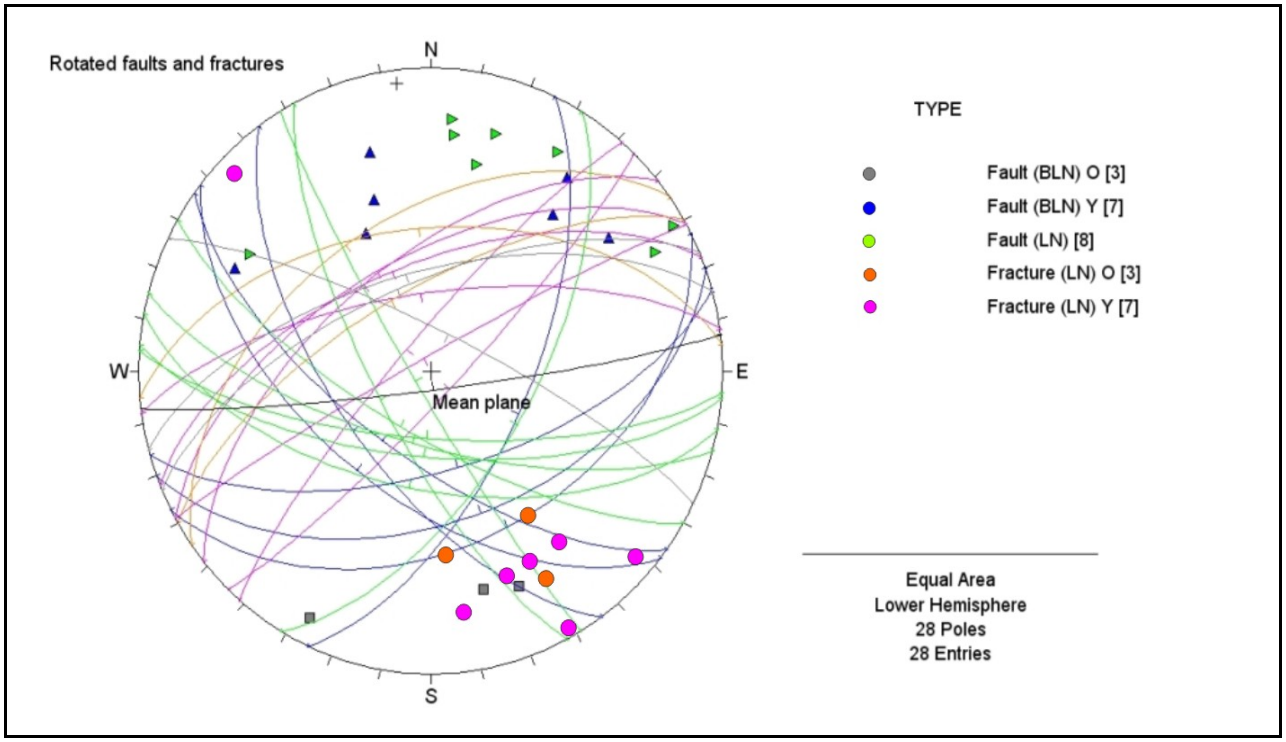

Fig. 5.14: Poles with corresponding planes labelled as above (Fig. 5.13). The black plane labelled 'Mean plane', is the mean plane for all poles shown.

Chapter 6: Summary, discussions and conclusions

6.1 Geological summary of the Northern Bryneira Range

The Northern Bryneira Range contains a relatively intact crustal portion (Livingstone Volcanics Group) and a highly deformed mantle portion (Red Mountain Ultramafics Group). These two components are separated by the Peanut Fault (a shear zone of unknown displacement and age) and together make up the DMOB. Overlying and in depositional contact with the crustal portion of the DMOB is the Maitai Group. Together the Maitai Group and the DMOB form the Maitai-Dun Mountain terrane.

6.1.1 Mantle portion of the Northern Bryneira Range

The preserved thickness of the mantle portion of the Northern Bryneira Range is ~1200m. Most of the mantle portion is variably tectonised serpentinite containing rare partially serpentinitised peridotite. Disrupted mafic dikes are found within the mantle portion. The mantle portion is truncated by the Livingstone fault on the eastern (lower) side.

6.1.2 Crustal portion of the Northern Bryneira Range

In the context of this chapter, the crustal portion of the DMOB is best summarised in three parts, respective of chronological order.

1. Crustal units that are associated with GIS (grey intrusive sheets) magmatism (oldest).
2. Crustal units associated with OIS (orange intrusive sheets) magmatism.
3. The Maitai Group units overlying magmatic crustal portion.

A period of deformation separates parts one and two.

6.1.2.1 GIS magmatism and resultant crustal units

The term ‘GIS magmatism’ is used in this chapter to describe all crustal growth during the injection of GIS. GIS magmatism represents crustal growth synchronous with the growth of the mantle portion of the DMOB. All crustal units formed by the end of GIS magmatism are shown in figure 6.1.

Amphibole rich intrusive sheets (ARIS) were injected some time after GIS magmatism. Their origin and timing is unresolved.

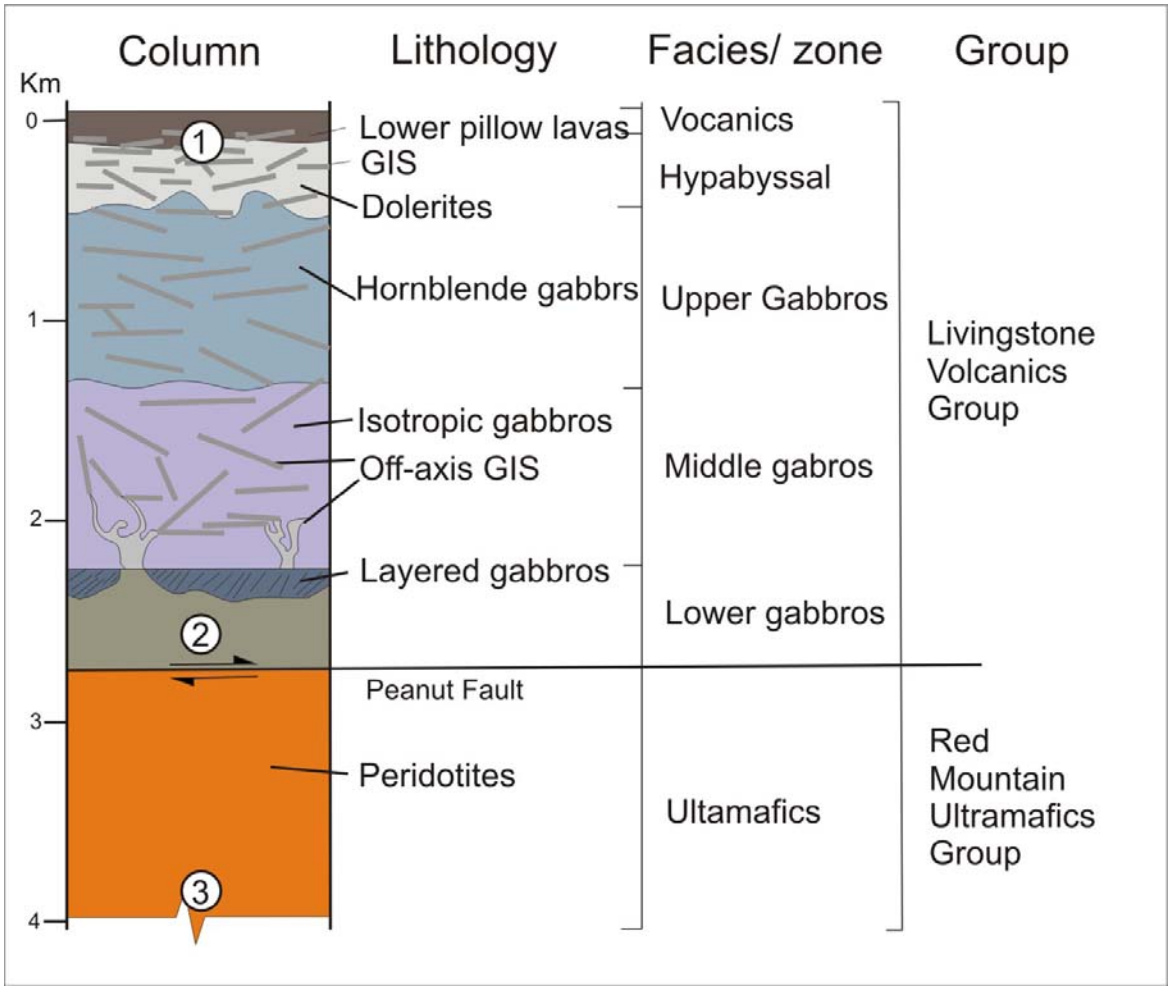

Fig. 6.1: Column showing the positions and nomenclature used to describe GIS magmatism (OIS magmatic portions are not shown). Circled numbers are shown to highlight areas of uncertainty within the column (discussed later in the text). **1**. The interface between the volcanic and hypabyssal facies and the original thickness of the extrusives. **2**. If the lower gabbros are complete or truncated by the Peanut Fault. **3**. The original thickness of the mantle section.

6.1.2.2 Between-magmatism deformation

Between the GIS and OIS magmatism, there was a period of deformation. Structures formed in this period are all extensional. During and after the cooling of crustal units, fractures and low angle brittle-ductile normal faults formed (section 4.2.2 and section 4.2.1.4 respectively). Continued cooling and extension allowed brittle failure, microfaults (section 4.2.1.1), large scale extensional faults (section 4.2.1.2) and possibly cross faults (section 4.1.3.1). These faults all had similar orientations (section 5.4). Faulting allowed hydrothermal circulation through the crust which altered the original mineralogy of rocks formed by GIS magmatism.

6.1.2.3 OIS magmatism and resultant crustal units

The term OIS magmatism is used here to describe rocks that have intruded through all GIS rocks and structures. It represents re-activation of magmatism within the DMOB. OIS magmatic units are shown in figure 6.2, superimposed on figure 6.1.

6.1.2.4 Maitai Group units

Only the lower units of the Maitai group are relevant to this study. The Upukerora Breccia is composed of clast eroded from the DMOB below and lies in sedimentary contact with the pillow lavas. Above and in sedimentary contact with the Upukerora Breccia is the Wooded Peak Limestone (Fig.6.2).

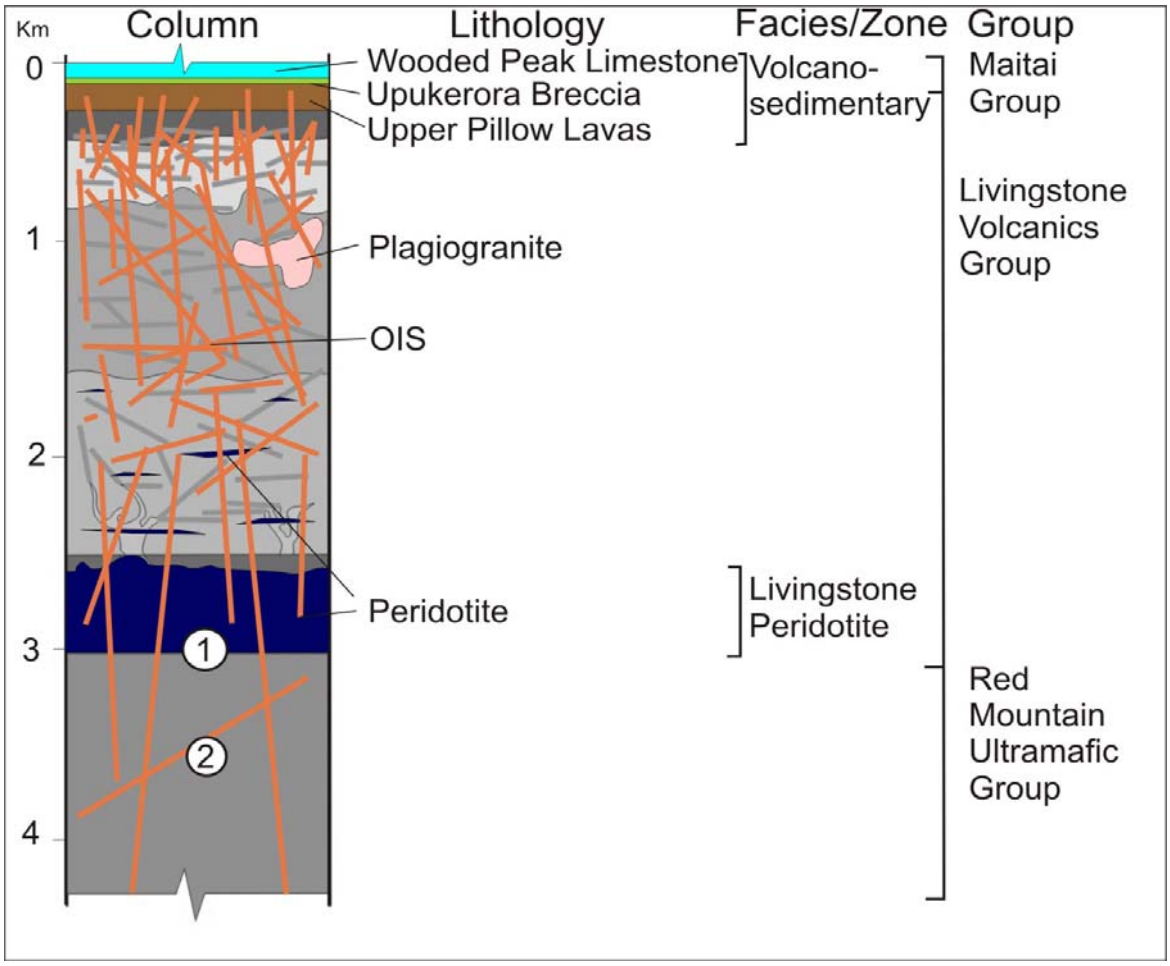

Fig.6.2: Column showing the positions and nomenclature used to describe OIS magmatism. Colour is used in the column to distinguish between GIS (greyscale) and OIS (coloured) magmatism. Circled numbers are shown to highlight areas of uncertainty within the column (discussed later in the text). **1**. The Peanut fault. **2**. The relationship of OIS magmatism and the original GIS magmatism in the mantle.

6.2 Discussion of the structural development of the Northern Bryneira Range

6.2.1 Initial DMOB crustal growth; GIS magmatism

The original DMOB crustal and mantle portions preserved in the Bryneira Range are attributed to GIS magmatism. The older rocks and structures of the DMOB rocks do not conform well to patterns seen on other well preserved ophiolites or in models of ocean crust. Key observations in the Bryneira Range are of episodic magmatism, extensive faulting, fault controlled hydrothermal circulation and thin crustal sequence. These

features are typical of crust formation at low spreading rates (Dilek et al., 1998). Slow spreading (< 5cm/yr) with intermittent magma supply results in a "cold" spreading environment where mechanical stretching predominates. Similarly, the complex and cyclic nature of the lower and mid-level gabbros is consistent with small ephemeral magma chambers with closed system crystallisation, gravity settling and the formation of crystal mush on the floor and sides of the magma chamber. A number of studies (see Dilek et al., 1998; Thy and Dilek, 2003) have shown these features to be common at slow spreading centres. Studies on slow-spreading oceanic crust (see Meurer and Gee, 2002; Schwartz et al., 2005), show that ~25% of magma emplacement occurs away from the spreading centre at a distance of ~ 3km over a period of > 0.3Ma.

Sill emplacement into the gabbros has been widely observed and is cited as the mechanism for transport of magma away from the spreading axis (Gee and Meurer, 2002; Meurer and Gee, 2002; Schwartz et al., 2005; Thy and Dilek, 2003). GIS in the middle gabbros exhibit crosscutting, and orientations suggest most formed as sills and inclined intrusive sheets (section 5.2.1.2). Low segmentation and asymmetric shapes suggest GIS were injected into still hot gabbros, over a period slightly after the main spreading phase in a slightly ‘off axis’ position.

Grain size changes rapidly from the upper gabbros in transition to the hypabyssal dolerites. The boundary with the extrusive volcanic sequence above is unclear. The hypabyssal facies does not contain a sheeted dike complex typical of most ophiolites. Instead, a thin sequence of dolerites and variable amounts of GIS forms a ~200m thick zone above the gabbros. The relationship between GIS and the hypabyssal dolerites was unclear, but they appear very similar outcrop. Again GIS dominantly form as nonsheeted sills and inclined intrusive sheets. Extrusive volcanic rocks associated with the GIS magmatism are thin and cut by GIS sills.

There are only a few examples of ophiolites that the GIS magmatic portion of the DMOB can be compared. GIS distribution and orientations make the Northern Bryneira Range particularly unique. Hopson (2007) sites examples in California, Tibet and Norway, all examples have nonsheeted dikes preceding sheeted sills as part of an evolving supra-subduction zone or back-arc settings. Hopson concludes that sheeted sills form as the result of imbalance between spreading rate and magma supply. Fast-spreading and low

magma supply causes sills to radiate out from a melt lens at the top of the magma chamber. Lateral propagation of magma forms a sheeted sill complex at the base or within the hypabyssal facies. Work by MacDonell (Macdonell, 1982) applies an earlier version of Hopson's ideas (Hopson and Fanco, 1977) to the DMOB in Red Mountain Area. Unfortunately, he did not distinguish between different magmatic stages, making his work difficult to compare with this study.

Hopson's model does not fit the Bryneira Range completely and has no explanation of non-sheeted sills as the primary intrusive phase. Only the Xigaze and Dazhuqu portions of the Yarlung Yangbo ophiolite (Girardeau et al., 1985) (Fig. 6.3) have similar crustal succession and intrusive sheeting as the Bryneira Range crustal portion related to GIS magmatism, but no details are provided about how the distribution and sill-like orientation formed. The Xigaze Ophiolite is thought to have formed during slow-spreading at a mid-ocean ridge, in a small basin near the paleo-Eurasian continent (Hebert et al., 2003). Heterogeneous crust sequences seen in the greater Yarlung Yangbo ophiolite are considered to be the result of protracted oceanic crust formation in a suprasubduction zone environment (Malpas et al., 2003).

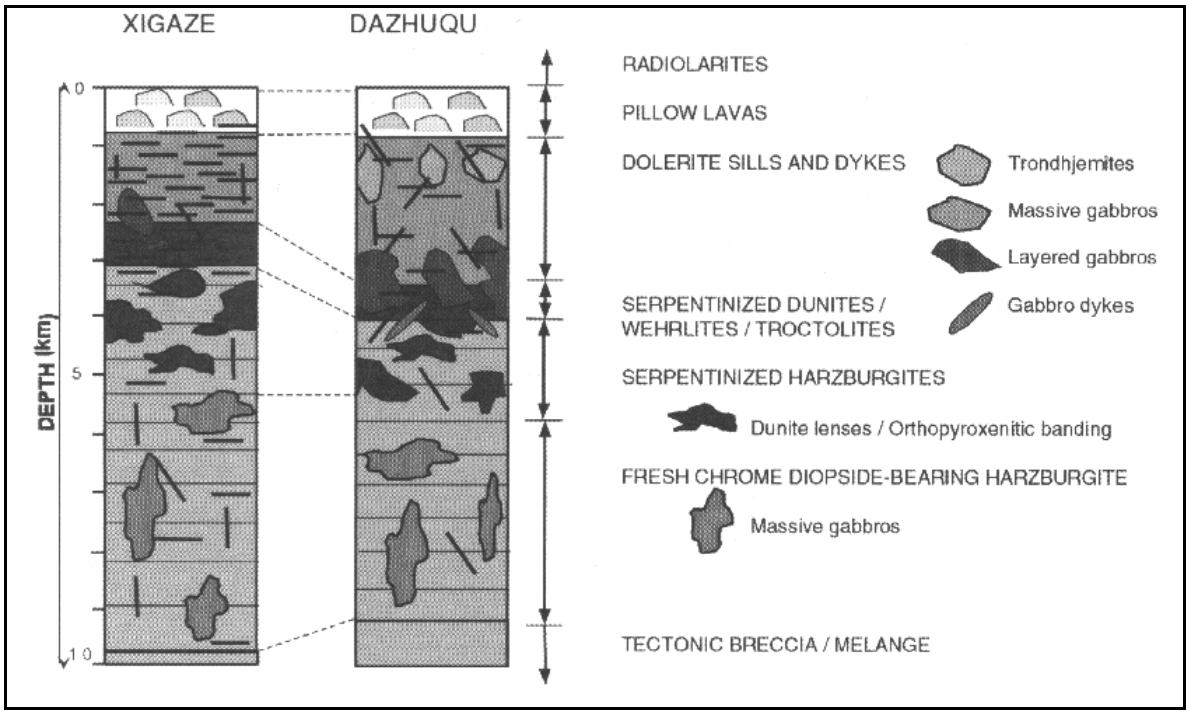

Fig. 6.3: Figure showing representative columns from the Xigaze and Dazhuqu segments of the Yarlung Yangbo Ophiolite. Originally from Girardeau (1985), modified by and from Hebert (2003).

The small ratio of extrusives to intrusives and a poorly developed dike complex in the Bryneira Range, and the DMOB in general, suggests an environment more complex than a simple spreading ridge (Kimbrough et al., 1992). The atypical crustal sequence formed during GIS magmatism may relate to slow-spreading where magma supply was quasi-continuous, keeping pace with tectonic extension. Proximity to a transform fault or other segmented boundary may also have influenced the crustal sequence seen in the study area (see Karson, 1998).

The geochemistry of the DMOB (see section 2.6) has been used to assign a range of tectonic settings to GIS magmatism of the belt, ranging from MORB to back-arc basin basalt (BABB). More recently, Nd isotopes, (Sivell and McCulloch, 2000) have been used and suggest early formed basalts have both MORB and BABB affinities, and that the assemblage is probably of back-arc origin.

6.2.2 Deformation synchronous with GIS magmatism

Initial stages of mechanical deformation probably took place at, or close to, the original spreading centre. There is little evidence by way of low angle faults and ductile deformation of movement that is strictly coeval with GIS magmatism. Indication of extension by ductile deformation was limited, confined to isolated areas within the gabbros. A single well-preserved example of plastic to brittle low angle faulting has been described (section 4.2.1.4).

The development of large normal faults, orientated parallel and dipping towards the spreading axis, commonly takes place at this time (Varga et al., 1999). It is possible that cross faults (described in section 4.1.3.1) are re-activated large normal faults. Early formed faulting may have facilitated downward penetration of water, establishing convection driven hydrothermal systems and hydrothermal alteration of rocks.

It is likely that most structures formed during GIS magmatism are re-activated, hence are poorly preserved.

6.2.3 Deformation post-GIS magmatic portion consolidation

The first post-GIS magmatic fractures are marked by the development of green veins containing amphibole (section 4.2.2). They probably developed during sub-solidus cooling and thermal contraction of the gabbro, as they cooled and moved away from the axis (Dilek et al., 1998).

Younger fractures developed as a conjugate set (section 4.2.2) and are marked by the development of white veins (possible feldspar and clay minerals). The change in vein mineralogy may reflect the progressive cooling gabbros during continuous hydrothermal fluid influx (see Dilek et al., 1997). Ongoing extension has led to some fractures changing to microfaults during the early stages of post magmatic crustal extension (c.f. Cyprus, Varga et al., 1999). Extension in the crustal portion was probably facilitated by the continual development of faults on all scales and these structures are thought to make a significant contribution to total tectonic extension (Dietrich and Spencer, 1993). Re-activation of most early faults has probably occurred during subsequent deformations.

Most faults and fractures would have welded and stabilised some time after moving away from the spreading axis. The first signs of renewed magmatism are the ARIS (amphibole rich intrusive sheets, section 4.2.1.5 and 3.3.3.1). The significance and the timing of ARIS injection is unknown. They may be associated with residual melt from the GIS magmatism, or may represent the onset of OIS magmatism.

6.2.4 Development of OIS magmatism

A significant amount of time elapsed before the initiation of OIS magmatism, during which the GIS magmatic portion had cooled and deformed. This time interval is indicated by ubiquitous chilled margins on OIS at all crustal levels. In the volcanic facies a thick layer of younger pillow lavas (~300m) caps the older pillow lavas associated with GIS magmatism.

The OIS display a diverse range of orientation throughout the crustal portion of the Bryneira Range. Crosscutting between, and chilled margins against other OIS, indicates injection over an extended period. Recognition of this (and other factors, section 5.2.2.7), led to collection of orientation data in four sub-groups (OIS(1)(oldest) to OIS(4)(youngest)). Sub-dividing the continuous phase of OIS magmatism enabled the recognition of an age related pattern within OIS sub-groups (section 5.2.2.7 and Fig. 5.). There is a progressive change in the OIS from no common orientation (the oldest OIS(1) sub-group), through 'sills' and inclined intrusive sheets (OIS(2) and OIS(3)) to closely grouped 'dikes' (the youngest OIS(4) sub-group). To investigate why the OIS have an age related distribution of orientation, two hypotheses need to be considered:

1. A **tectonic rotation**, where all intrusive sheets were once sub-vertical dikes that have been rotated into inclined positions during ongoing extension, synchronous with magmatism.
2. **Diverse primary orientations**, where during continuous injection of OIS, orientations have changed in response to a changing stress field in the pre-existing ophiolitic crust.

These two possibilities are discussed in detail in the following sections and are compared with similar examples in other ophiolites.

6.2.5 Are OIS orientations affected by coeval tectonic rotation?

To assess whether crosscutting relationships can be explained by tectonic rotation, a dynamic concept needs to be explained. In an extensional setting, tectonic rotation (or crustal tilting) affects oceanic crust by rotation of hanging-wall fault blocks over normal faults. The normal faults run parallel to the spreading axis and may merge in the lower crust (Agar and Klitgord, 1995; Dietrich and Spencer, 1993; Varga and Moores, 1985) or in the upper mantle as a basal detachment (Alexander and Harper, 1992) (Fig. 6.4A). Fault blocks rotate around a horizontal axis perpendicular to the extension direction. Synchronous magmatism and tectonism rotation will cause crosscutting at progressively

higher angles with time (Fig. 6.4B). Tectonic rotation is interpreted on the principle that all paleo-horizontal markers (see section 5.1) record a relative time reference, and the assumption that dikes were injected with sub-vertical orientations (ranging 15 degrees from vertical (Borradaile and Gauthier, 2006)) and have subsequently been tilted. Rotation angles are typically 30 to 50 degrees, but may locally reach 70 to 90 degrees (Verosub and Moores, 1981). It is important to note that rotation in excess of 20 to 45 degrees in a stable stress field requires more than one set of planar normal faults (Nur et al., 1986).

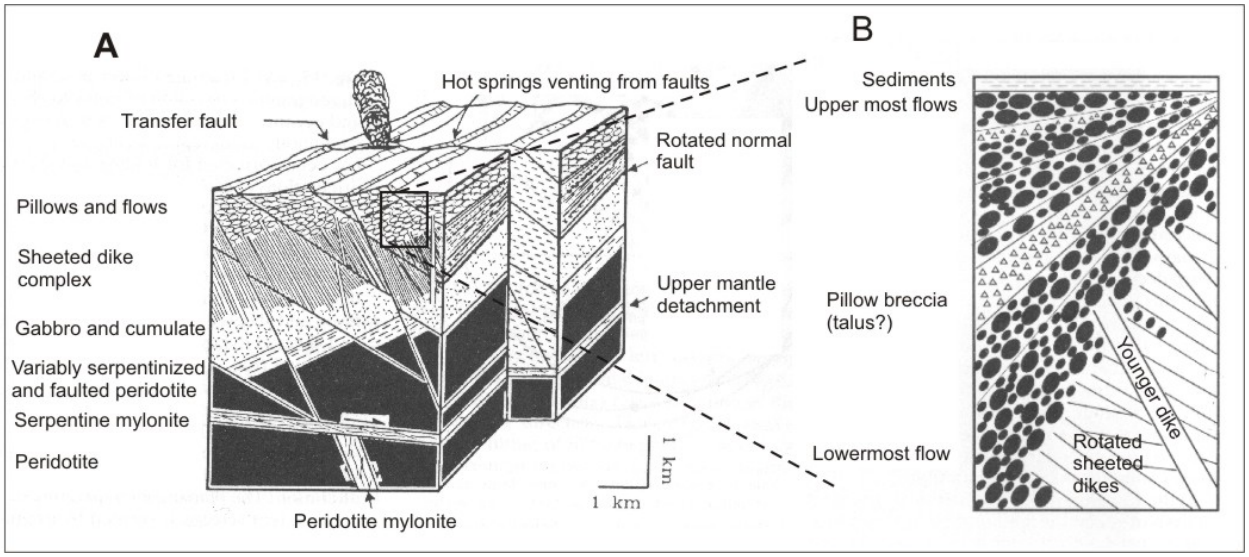

Fig. 6.4: A) Block diagram showing two sets of normal faults rotating a typical oceanic crustal sequence. Normal faults merge at an upper mantle detachment. Note that the once vertical sheeted dike complex is inclined, as are the once horizontal cumulates at the base of the gabbros. **B)** An enlarged diagram of the volcano-sedimentary facies and the top of the sheeted dike complex. Younger dikes pass through rotated sheeted dikes. Extrusives dip less as they young upwards, until horizontal sediments cap the oceanic crustal sequence. Modified from (Alexander and Harper, 1992).

Tectonic rotation during the formation of oceanic crust is well established in literature on some ophiolites and modern oceanic crust. The Troodos ophiolite in Cyprus has crosscutting of dikes that relate to the tilting of oceanic crust formation (Hurst et al., 1994; Varga et al., 1999; Varga and Moores, 1985; Verosub and Moores, 1981). Tectonic rotation affected the Josephine ophiolite, where crosscutting of dikes is the result of alternating amagamatic and magmatic phases (Alexander and Harper, 1992; Harper, 1982). Direct observation of active rotation has also been made at modern oceanic spreading centers (e.g. Karson and Rona, 1990).

The examples show that crustal extension in oceanic basins can result in rotation of dikes to lower inclinations, ultimately causing crosscutting. Crosscutting of “dikes” is seen in the Bryneira Range section and all other segments of the DMOB. To test if the DMOB has been affected by tectonic rotation, a reverse chronologic retro-deformation process must be applied to the OIS and paleo-horizontal orientations.

In section 5.1 it was noted that each type of paleo-horizontal is associated with a stage of development of the ophiolite below. If the relationships are correct, then progressively older (older than the Wooded Peak Limestone) paleo-horizontals can be retro-deformed to their original horizontal orientations, effectively removing tectonic rotation back through time (Fig. 6.2). Assuming most OIS were once dikes, and are also retro-deformed by the same amount as contemporaneous paleo-horizontals, they should move into their former vertical position (as represented in a stereo net by poles). If tectonic rotation has caused the age related distribution OIS sub-groups (section 5.2.2.7 and Fig. 5.12), progressively older poles to “dikes” should incrementally move into vertical positions when rotated by the same amount needed to restore paleo-horizontals to their original horizontal positions (i.e. poles will move towards the periphery of the stereo net). This process is worked through stepwise below. Bear in mind, the large distribution in OIS orientations (Fig. 5.11) suggests that most were never dikes, but rather a mix of sills, inclined intrusive sheets and dikes. The GIS will also move accordingly with this process but will not be discussed until the final interpretation.

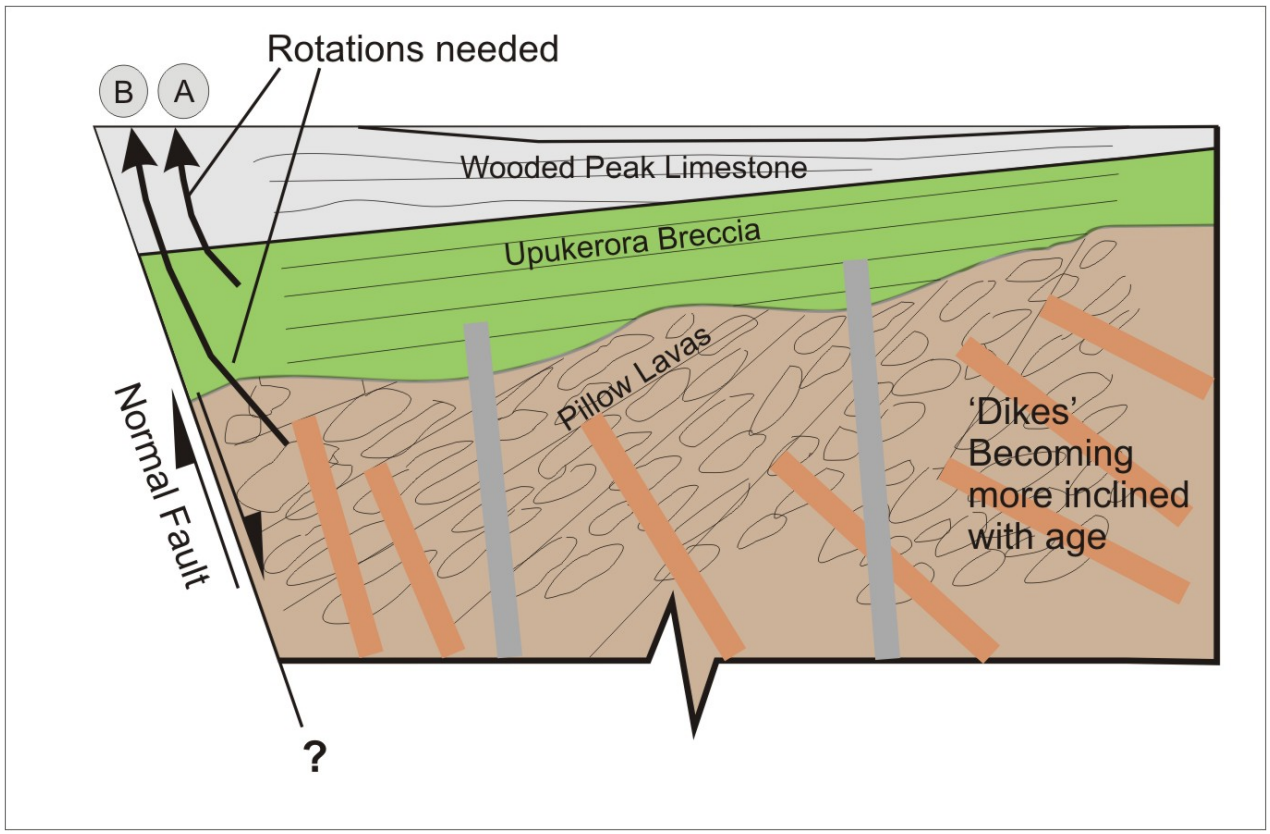

Fig. 6.5: Schematic diagram in the style of figure 6.4B, showing the relative positions of paleo-horizontals and inclined dikes when the Wooded Peak Limestone is in a horizontal position for the Bryneira Range. The lower crustal section is not shown. If the motion on the normal fault is reversed, the older paleo-horizontals will be returned to horizontal positions. The angle of rotation needed is shown by the arrow pointing to **A** for the Upukerora Breccia and the arrow pointing to **B** for the Pillow lava layering.

6.2.5.1 Removal of the Upukerora Breccia Paleo-horizontal

Intrusives from the underlying DMOB are found within the first ~100m of the Upukerora Breccia elsewhere in the DMOB (Hyslop, 1978; Pillai, 1989), therefore, magmatism finished during the Upukerora Breccia deposition. Hence, paleo-horizontal provided by the Upukerora Breccia will be the first removed. Figure 6.6 shows the pole to Upukerora Breccia restored to its original horizontal position and the synchronous positions of the other paleo-horizontals. Retro-deformed positions of poles to the OIS, when the Upukerora breccia is in its original horizontal orientation are shown in figure 6.7. This retro-deformation rotated OIS poles from their previous positions shown in figure 5.10 (when the wooded Peak Limestone was horizontal (Fig 5.3)), and was achieved by a 26 degrees clockwise rotation, around a horizontal trend of 034 degrees.

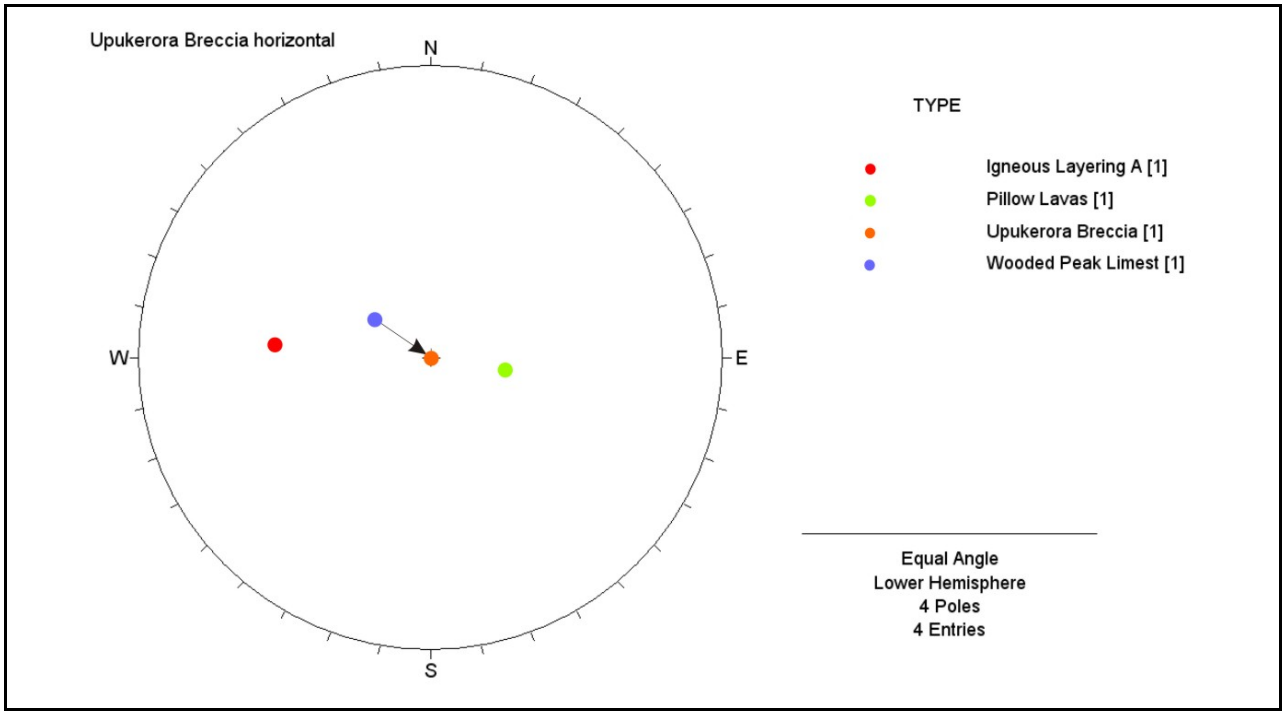

Fig. 6.6: Stereo net showing the Upukerora Breccia restored to former horizontal position. The arrow links the pole position of Wooded Peak Limestone with Upukerora Breccia indicating the rotation that was needed to return the Upukerora Breccia to its original horizontal. Note that the pole to the Wooded Peak Limestone is only representative and does not exist in this reference frame.

6.2.5.2 Interpretations of OIS orientations when the Upukerora Breccia lies in its former horizontal position

The poles to OIS shown in figure 6.7 are retro-deformed by the same amount as needed to return the Upukerora Breccia to its original horizontal position. When compared to their previous position (when the Wooded Peak Limestone was horizontal (Fig. 5.11)), the poles to OIS have moved towards the northern periphery (i.e. vertical orientations) of the net. Most significantly, the OIS(4) and OIS(3) sub-groups (the youngest OIS sub-groups) have moved into sub-vertical positions as indicated by their poles.

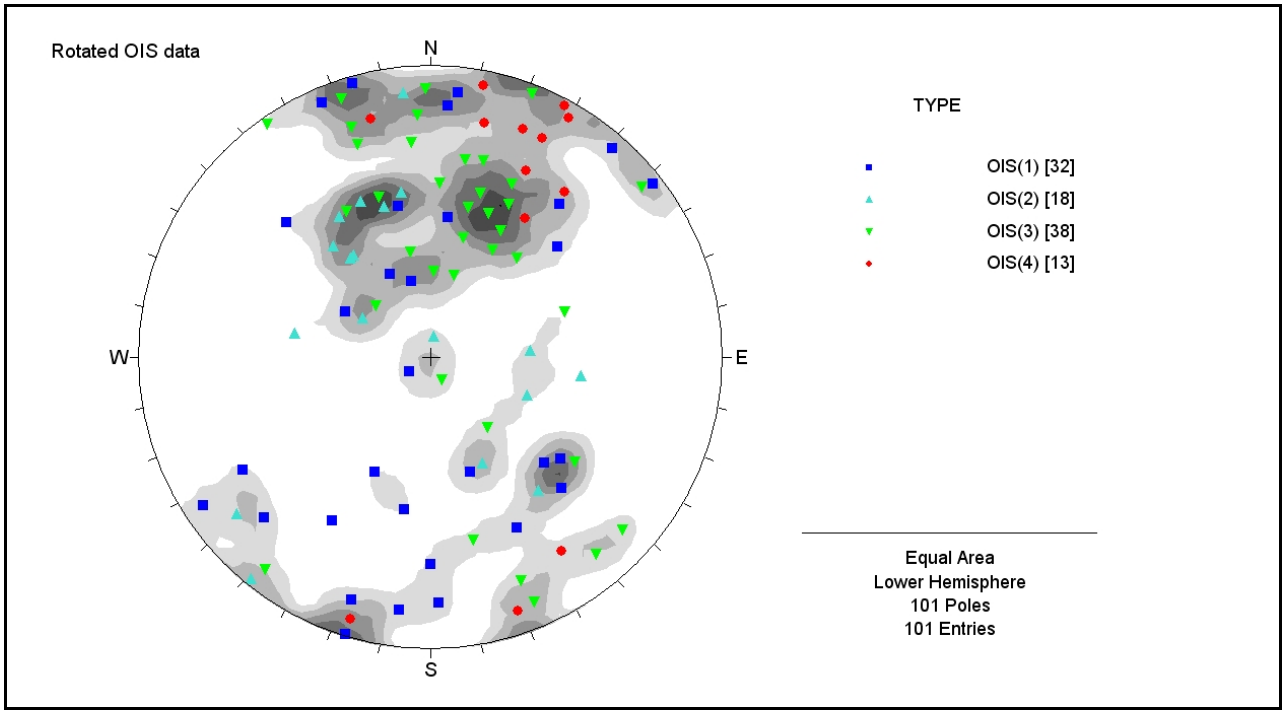

Fig. 6.7: Stereo net showing the poles to OIS, when the Upukerora Breccia is in a horizontal position. Note the poles to the youngest OIS(4) sub-group are representative of vertical to steep dips.

6.2.5.3 Removal of the Pillow lava layering Paleo-horizontal

Pillow lava layering was measured stratigraphically below the sedimentary paleo-horizontals, hence they are older. As Pillow lava layering was measured from the upper pillow sequence, they were probably extruded from OIS(4). At the time of extrusion OIS(4) must have been vertical dikes. Therefore, OIS(4) are omitted from the pillow lava paleo-horizontal retro-deformation (i.e. OIS(4) poles are not shown in figure 6.9). Retro-deformation of the pillow lava paleo-horizontal from their previous position (shown in Fig. 6.6) to their original horizontal position (and OIS to their synchronous position), was achieved by horizontal rotation of all poles clockwise 29 degrees around a bearing of 009 degrees. Figures 6.8 and figure 6.9 show the resolved position of the paleo-horizontals and OIS orientations respectively.

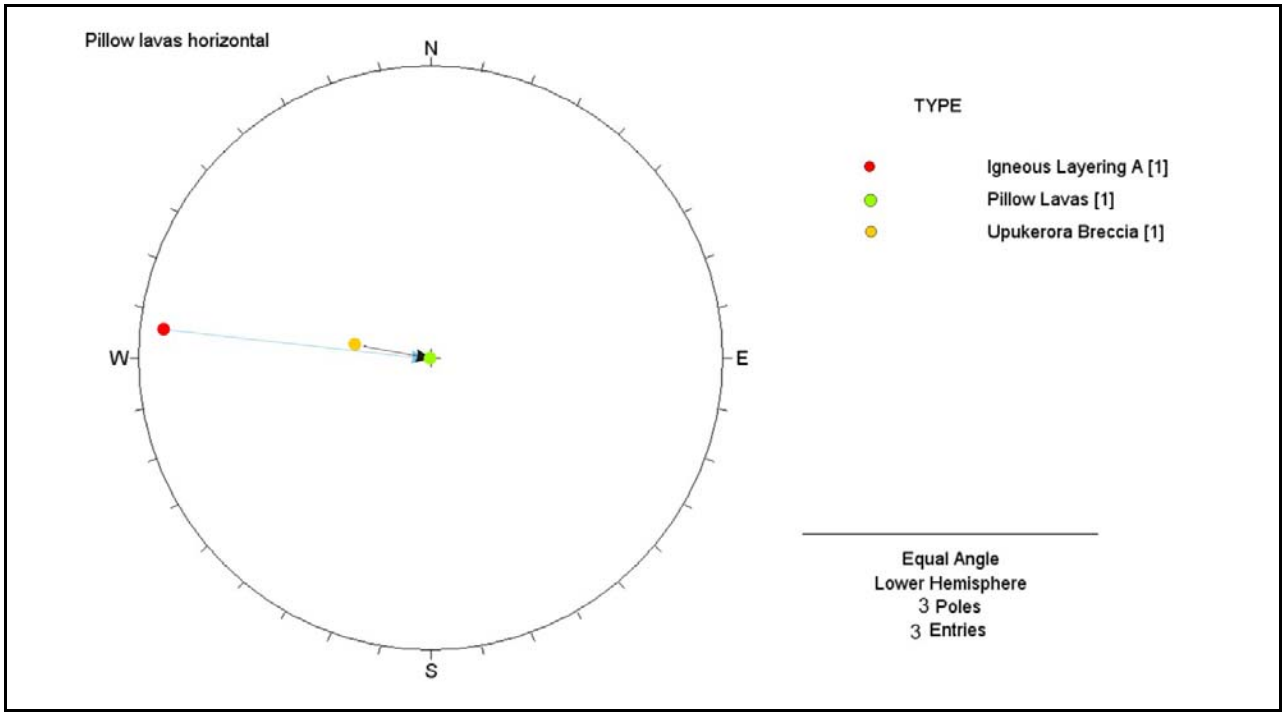

Fig.6.8: Stereo plot showing the Pillow Lava paleo-horizontal in its former horizontal position. The black arrow indicates the small circle rotation needed to achieve the pillow lava's original horizontal position from that shown in figure 6.6. Note the Upukerora Breccia pole is representative only and does not exist in this reference frame. The blue arrow shows the small circle rotation needed to return the Igneous layering paleo-horizontal to its former horizontal position (see section 6.2.5.5).

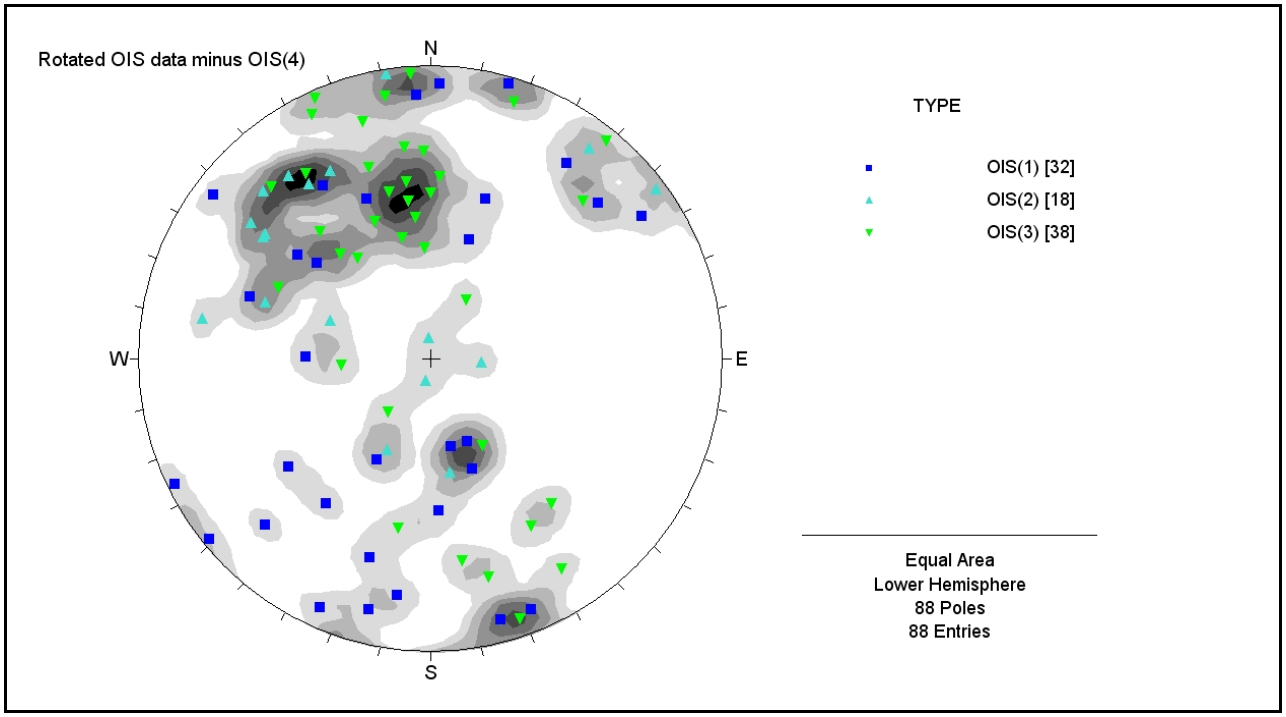

Fig. 6.9: Stereo plot showing the poles to OIS when the pillow lava paleo-horizontal is in its former horizontal position.

6.2.5.4 Interpretations of OIS orientations when the Pillow lava layering lies in its former horizontal position

The main clusters of poles to OIS shown in figure 6.9 have moved northwest. When compared to their last position in figure 6.7 however, few have moved into sub-vertical positions (as represented by poles close to the periphery of the net). The tectonic rotation hypothesis suggests OIS(3) “dikes” should now be in sub-vertical positions (as OIS(3) are known to be slightly older than OIS(4)), but, there is little change in the inclination of poles to OIS(3) when figure 6.9 and figure 6.7 are compared. In summary, the restoration of the pillow lava layering paleo-horizontals to its former horizontal position has moved few poles OIS into steeper inclinations and has failed to move the OIS(3) sub-group in to vertical ‘dike-like’ positions.

6.2.5.5 Removal of the igneous layering Paleo-horizontal

Igneous layering is the last paleo-horizontal marker bed to be retro-deformed to its original horizontal position. There is, however, major doubt with regard to the validity of this final rotation. To return the Igneous layering back to its former horizontal, after restoration of the Upukerora Breccia and Pillow Lavas, a counter-clockwise rotation of ~80 degrees is needed (see Fig. 6.8). Such a radical rotation in the opposite direction does not fit with the tectonic rotation model. This leaves two possibilities:

1. Igneous layering paleo-horizontals were not affected by tectonic rotation. Tectonic rotation only affected the upper crustal rocks.
2. Igneous layering was never paleo-horizontal.

Concerning the first point, tectonic rotation of intrusive sheets in the volcanic and hypabyssal facies has been shown to occur in the hanging wall of listric normal faults that merge at a low angle detachment zone in the upper gabbros (Dietrich and Spencer, 1993). There are, however, no low angle faults that post-date OIS, the observed low angle faults are related to older GIS magmatism. Thus there is no evidence that crustal tilting only affected the hypabyssal and extrusive components.

The second possibility suggests igneous layering was never paleo-horizontal. Igneous layering paleo-horizontal is related to crustal growth during GIS magmatism, and may have formed on the sides and base of a cooling magma chamber. This and subsequent deformation before and during OIS injection, substantiates the interpretation that igneous layering was probably not horizontal during OIS injection.

6.2.5.6 Summary of tectonic rotation

It has been shown that by returning the Upukerora Breccia and pillow lavas layering to their original horizontal positions respectively, and rotating OIS synchronously by the same amount, OIS can be brought closer to vertical orientations. It has also shown that the oldest paleo-horizontal, the igneous layering, cannot be used in this manner. Thus, tectonic rotation is possibly a mechanism by which some of the youngest OIS have become inclined as opposed to vertical. However, most OIS were injected as inclined intrusive sheets as opposed to dikes.

There must however be some degree of tectonic rotation within the upper crust. The significant difference in the dip of the sedimentary and pillow lava layering paleo-horizontal marker beds whilst a common strike is maintained is very important. The difference in dip between the Wooded Peak Limestone and the pillow lavas layering is ~55 degrees, so at least some of this change in dip must be due to tectonic rotation. It is reasonable to conclude that normal faults probably deformed the upper crust and possibly the lower crust, causing rotation of paleo-horizontal layers, synchronous with, and continuing after, the formation of the youngest OIS(4).

6.2.6 Do OIS have diverse primary orientations?

It has been concluded in section 6.2.5.6, that OIS were probably injected as inclined intrusive sheets and dikes. The term ‘diverse primary orientation’ implies that OIS (after retro-deformation) are close to their original orientation when injected. What remains unresolved is why there is a progressive change in the OIS from no common orientation (the oldest OIS(1) sub-group), through inclined intrusive sheets (OIS(2) and OIS(3)) to closely grouped ‘dikes’ (the youngest OIS(4) sub-group)? This question will be

addressed in this section by reviewing literature and making comparisons to the data sets measured in the study area. As a context to this discussion, the mechanisms by which dikes, inclined intrusive sheets and sills are reviewed. The following three sections (sections 6.1.7.1, 6.1.7.2 and 6.1.7.3) are summarised from Price and Crosgrove (1990) and are explained in a geological notation (as opposed to physical) where compression is a positive stress and tension is negative. So, a decreasing principle horizontal stress means the principle horizontal stress is moving towards zero and into the tensile negative stress.

6.2.6.1 Mechanism for the formation of a dike

A dike will begin to initiate when the magmatic pressure at its source exceeds the overburden pressure imposed by the overlying crust. Emplacement of a dike may occur by propagating along a pre-existing fracture or by forceful injection (hydraulic fracturing), propagating its own fracture. At depth in the crust both emplacement mechanisms must have an element of forceful injection. During hydraulic fracturing, the magma pressure must exceed the compressive component of the principle horizontal stress and the tensile strength of the host rock. To open a pre-existing fracture, the compressive component of the principle horizontal stress acting normal to the fracture must be exceeded by the magma pressure. Therefore, a dike will preferentially propagate along a vertical fracture which is orientated perpendicular to the principle horizontal stress.

6.2.6.2 Mechanism for the formation of an inclined intrusive sheet

In order for an inclined intrusive sheet to form, as opposed to a vertical dike, the tensile component of the principle horizontal stress must increase (i.e. the principle horizontal stress moves further into the tensile negative stress). This is directly related to the hydraulic fracture process in which a hybrid extension/shear fractures. Alternatively, an intrusive sheet may propagate along an existing fault or fracture that is suitably orientated where magma pressure is in excess of the normal stress acting across its plane. Further complications occur when fractures that are not preferentially orientated and a component of shear must also be considered ((see, Ziv et al., 2000).

6.2.6.3 Mechanisms for the formation of a sill

A sill will be emplaced when the magmatic pressure is roughly equal to the overburden pressure. A sill needs a horizontal weakness to intrude and will begin to do so if any cohesive component (if there is any) is exceeded by the magma pressure. A sill will be emplaced along a weak plane when the difference in magnitude of the horizontal and vertical stresses is very small compared to magma pressure. Sills need to be fed from below by a dike or inclined intrusive sheet. A dike or inclined intrusive sheet will turn into a sill when horizontal weakness is intersected and the overburden pressure and magmatic pressures are equal. Sills may also form in response to rapid injection of dikes that temperately alter the normal stress field in such away that at a certain level in the crust a sill will form (Gudmundsson, 1990). Or, in a response to a local change in the stress where the orientation of the least and most compressive stresses switch orientation (i.e. the least principle stress acts vertically) (along pre-existing weaknesses, Delaney and Gartner, 1997) (by hydraulic fracturing, Motoki and Sichel, 2008).

6.2.6.4 Interpretation of the stress evolution during OIS formation

An interpretation with regard to the possible stress conditions during OIS propagation is presented here. In the context of mechanisms for formation of dikes, inclined intrusive sheets and sills outlined above, comparison between structural significance of intrusive sheets (section 4.4) and orientation information (this chapter) is made. Assessment will be made using the orientations of OIS when the Upukerora Breccia is in its original horizontal position (Fig. 6.7). These OIS orientations are used because they are thought to be more representative (than the orientations when the Wooded Peak Limestone is in it original horizontal position) of the final orientations for OIS before magmatism ceased. In using this horizontal reference frame, a known component (26 degrees) of tectonic rotation is incorporated into the final interpretation. Below, each of the OIS sub-groups are interpreted individually with regard to changing inclination (not trend). Each of the numbered bullets below corresponds to the same numbers on figure 6.10.

1. The oldest OIS(1) sub-group has the biggest spread in orientation (Fig. 6.10). OIS(1) were injected into the GIS magmatic portion of the crust that contained

numerous pre-existing weaknesses. This is seen in the highly segmented nature of the early OIS (section 5.3.1.2). A large spread in intrusive sheet attitude indicates there was little preferentially orientated principle horizontal stress in the crust (meaning the intermediate and minimum stresses were almost the same) (Delaney and Gartner, 1997).

2. The more confined distribution of OIS(2) sub-group poles indicates a defined orientation for the principle horizontal stress (Fig. 6.10). A defined principle horizontal stress forces the propagating intrusive sheets to be preferentially orientated. Inclined intrusive sheets took advantage of pre-existing faults and fractures with the appropriate orientation. This resulted in the development of segmentation and irregular segmentation geometry. The low inclination of poles to OIS(2) indicates that the tensile component of the principle horizontal stress was large.

3. A slow increase in the principle horizontal stress (resulting in a decrease in differential stress), forces OIS(3) to intrude faults and fractures with steeper attitudes. This is seen in the distribution of poles for OIS(3) in figure 6.10.

4. In the final sub-group, OIS(4), the principle horizontal stress in the crust has increased to the point that the magma pressure has hydraulically fractured the host rock. As it is most efficient to propagate a new fracture on a plane normal to the principle horizontal stress, OIS(4) poles are closely spaced and represent sub-vertical dips (Fig.6.10). Forceful injection is seen in the lack of segmentation of young OIS and their wider spacing in outcrop (section 5.2.1.2). The geometry of segmentation was also noted to have changed near the hypabyssal-volcanic contact from irregular anatomising segmentation geometry, as the result of high energy injection (section 5.2.1.3).

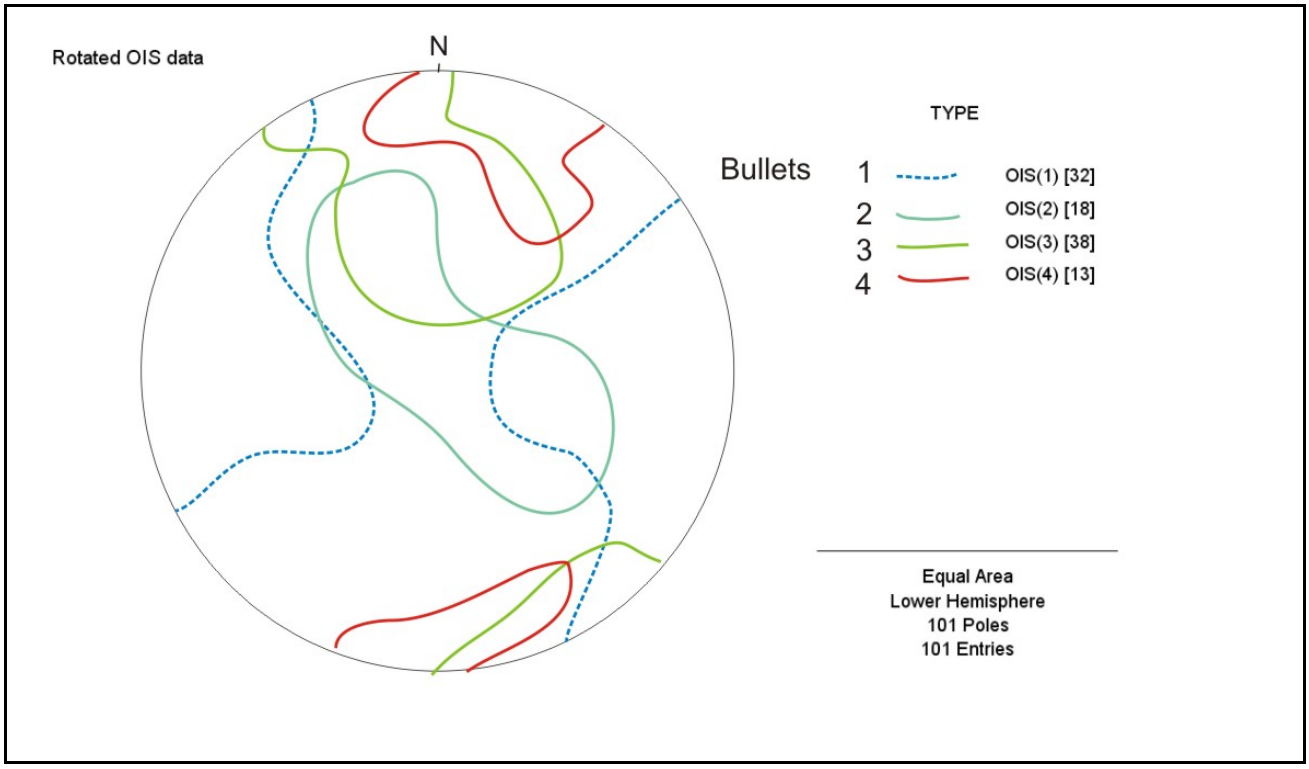

Fig.6.10: Stereo net of OIS distribution when the Upukerora Breccia is in its original horizontal position. Instead of poles, colored outlines are plotted that encompass all poles for each group minus a few outliers (poles with extremely different orientation). Note that OIS(1) (oldest) has a large spread, the three younger sub-groups have similar spreads but the inclination of the spreads become progressively steeper (as pole closer to the periphery of the net indicate steeper dips on corresponding planes).

The distribution of poles in each sub-group (Fig.6.10) not only corresponds to a change in inclination (represented in the plunge in OIS poles), but also trend. This becomes clearer when a representative great circle is plotted on the net for the mean pole to each OIS sub-group (Fig. 6.11). When the normals to representative great circles are projected outside the net, a change in ‘strike’ for the mean poles to OIS subgroups is evident. This angle ø is therefore indicative of a changing orientation of the dictating principle horizontal stress.

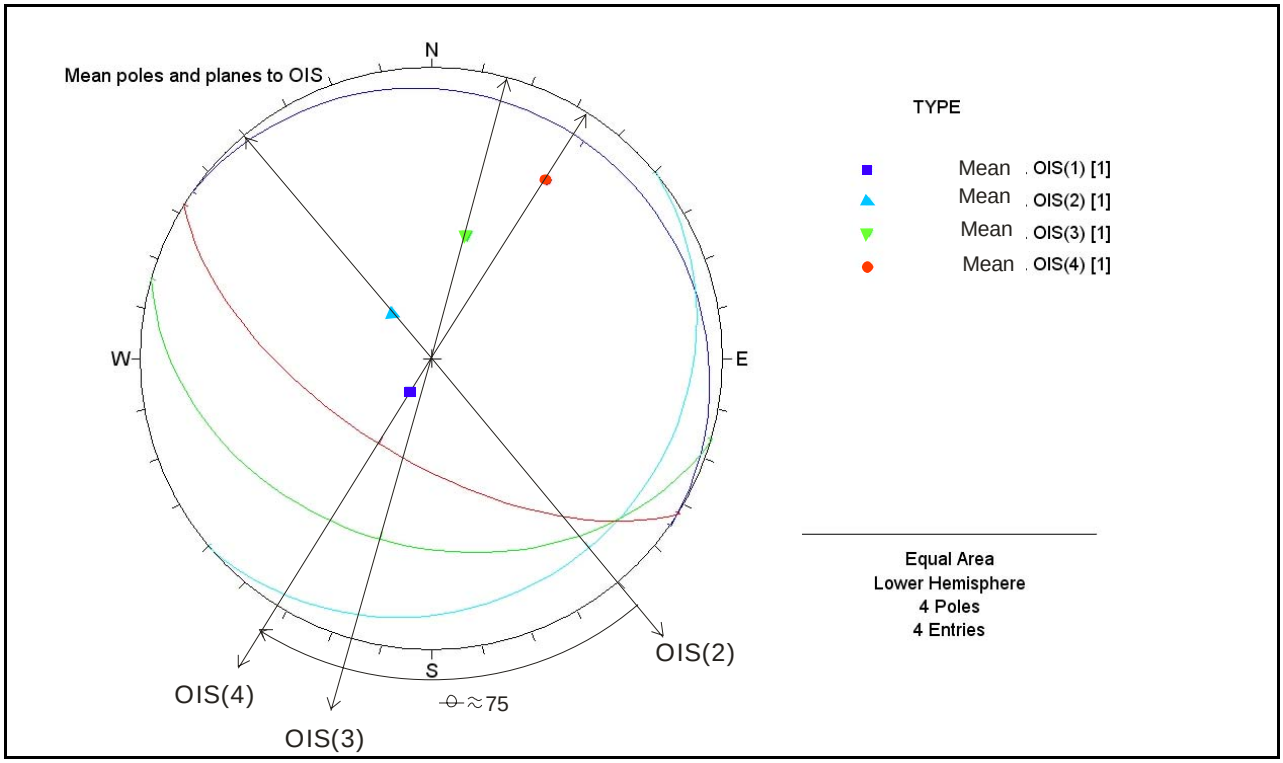

Fig. 6.11: Stereo net showing mean poles to each OIS sub-group and corresponding planes. The normals to the youngest three planes (as it is apparent that they have defined stress fields) are projected outside the net and the angle ø is indicated at ~75°.

As OIS(1) has no dictating principle horizontal stress the mean great circle is almost horizontal (Fig. 6.11). The principle horizontal stress is defined during OIS(2) propagation, where a low inclination great circle is representative of the principle horizontal stress. The younger OIS(3) and OIS(4) sub-groups are represented by steeper great circles and a changing angle of principle horizontal stress. The overall rotation in principle horizontal stress must be ~75 degrees (Fig. 6.11).

6.2.6.5 Final OIS orientation conclusions

The first OIS were injected into deformed, cold oceanic crust of the earlier GIS magmatic episode. Pre-existing weaknesses from earlier brittle deformation were abundant and horizontal stresses poorly defined, allowing OIS to propagate over a wide range of attitudes. As the principle horizontal stress became defined, OIS(2) and OIS(3) took advantage of pre-existing weaknesses within the deformed GIS portion of the crust. Many of these weaknesses were inclined due to previous and possibly contemporaneous extensional faulting. Preferentially orientated fractures and fault

became dilated by older OIS magmas that, on cooling, welded them together. Consolidation of older OIS possibly inhibited the propagation of younger sheets. The limited capacity for the existing crust to expand laterally forced younger OIS to inject under higher magma pressures. Youngest OIS(4) are less likely to follow pre-existing weaknesses. Over time, an increase in the principle horizontal stress required OIS to become preferentially orientated with progressively steeper dips. A probable explanation for this increase in principle horizontal stress, directly relates to volumetric expansion. OIS make up a large volumetric component of the crust and probably absorbed a large component of extension through dilation during their injection. Normal faults that show reactivation by reverse dip-slip (section 4.2.1.1) may be a direct product of local increase in horizontal stress and were probably reactivated as companion structures.

Coeval to the change in intrusive sheet inclination (the product of intensification of horizontal principle stress), was a rotation in principle horizontal stress. It is very difficult for an intrusive sheet to intrude along a pre-existing weakness that is not orientated nearly perpendicular to the least compressive stress (with respect to magma pressure, Ziv et al., 2000). It therefore seems necessary to rotate the least compressive stress direction in order to keep it perpendicular to the mean orientations of OIS through time. This rotation appears to be clockwise, ~75 degrees around a vertical axis (Fig. 6.11). Stress field rotation however, may be a synthetic product of the assumed amount of tectonic rotation experienced by the OIS orientations (this amount being the 26 degrees needed to return the Upukerora Breccia to its original horizontal position from its previous position when the Wooded Peak Limestone was in its original horizontal). A greater or lesser amount of tectonic rotation will drastically change the rotation angle needed to maintain the least horizontal stress perpendicular to the mean OIS orientations. Regardless of this proposed syn-magmatic rotation in the least horizontal stress, the final least horizontal stress must be orientated **northeast-southwest** as dictated by the youngest OIS(4) orientations (Fig.6.11).

On the decline of magma supply the extending basin must have changed from volume expansion (intrusive sheeting) to brittle faulting as a mechanism to accommodate the extension. It seems highly feasible that this transition occurred toward the end of OIS injection when magmatism is known to be contemporaneous with tectonic rotation.

In review of the tectonic rotation hypothesis, there must have been some component of tectonic rotation. The evidence for tectonic rotation is most apparent in the difference in dips between the Wooded Peak Limestone and pillow lava layering. As all poles to paleo-horizontals lay on a common great circle orientated east-west, it is geometrically probable that the normal faults responsible for their rotation were perpendicular to that great circle. Normal faults will **form** perpendicular (north-south) to the least principle horizontal stress which, for that reason, must be orientated **east-west** during tectonic rotation.

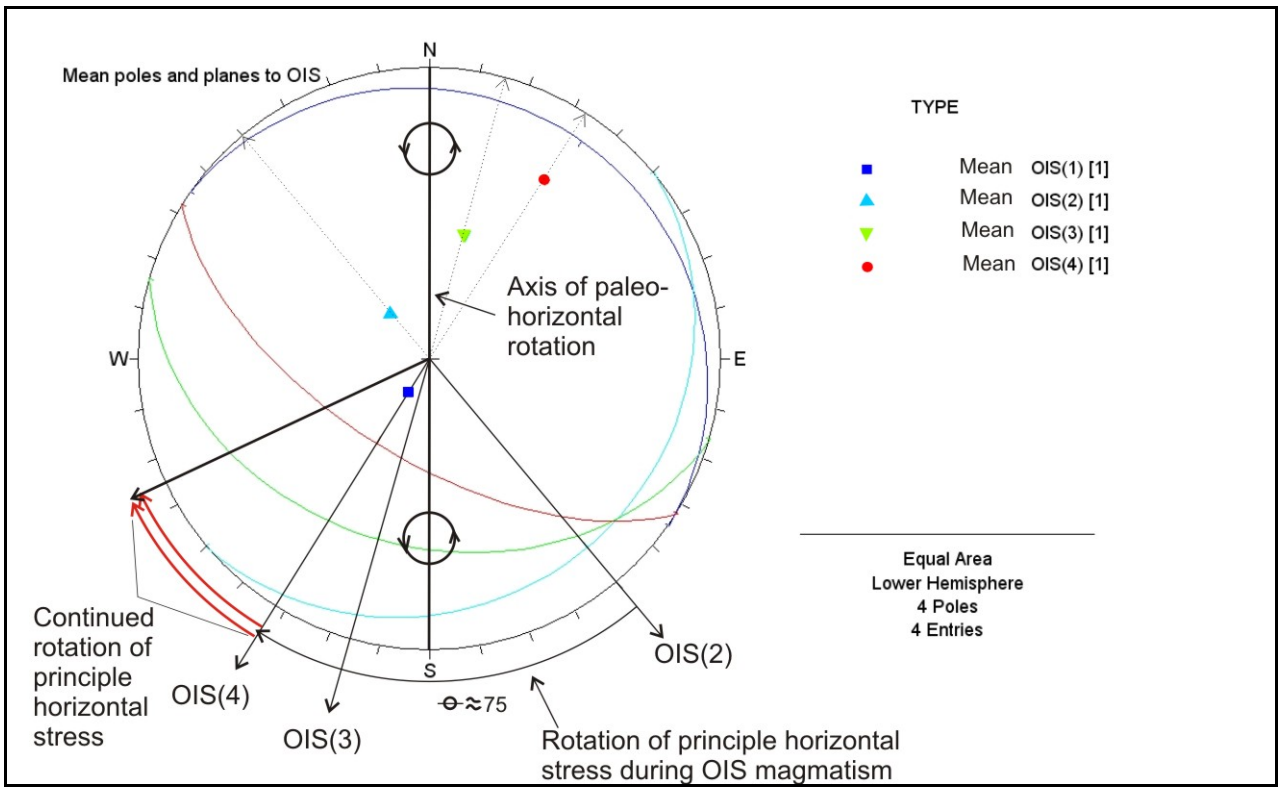

Fig. 6.12: Stereo net showing the rotation of the principle horizontal stress during OIS magmatism (as in figure 6.11) and during continued rotation of sediments (indicated by the double red arrow). The final arrow indicative of the principle horizontal stress is oblique to the axis of paleo-horizontal rotation. Anticlockwise rotation about this axis (as indicated), rotated lower Maitai Group sediments above normal faults.

A paradox between the two hypotheses (tectonic origin and diverse primary orientation models) is now apparent. If these two models were to be coeval during the final stages of magmatism, then the controlling minimum principle horizontal stress should be parallel, not oblique as concluded (the OIS(4) needs a principle horizontal stress orientated northeast-southwest and the tectonic rotation mole needs a principle horizontal stress orientated east-west). This apparent difference in principle horizontal stress orientation can be ignored if the normal faults responsible for tectonic rotation are

reactivated older normal faults formed earlier. Movement on a pre-existing fault plane with low cohesion can occur when the fault plane is orientated parallel to the least principle horizontal stress (Price and Cosgrove, 1990). However, it is unlikely that the 26 degree difference in dip (caused by tectonic rotation) between Wooded Peak Limestone and the Upukerora Breccia could develop in such a situation. Continued clockwise rotation of the principle horizontal stress past the normal to the great circle representative of mean OIS(4) orientations, would soon lead to oblique extension (Fig.6.12) Graben formation and the resultant tectonic rotation of paleo-horizontals probably happened during and after development of oblique extensional faulting. Large scale rotation and basin extension may have occurred on a master faults with many kilometers of displacement, or on pre-existing transform faults (summarised in Fig 6.13).

Throughout this orientation discussion GIS orientations have not been applied to the two hypotheses tested. GIS orientations have probably been affected by multiple episodes of deformation, resulting in an unknown amount rotation. The lack of constraint on these rotations meant that the two hypotheses could not be applied to GIS orientations.

6.2.7 Origin OIS magmatism

The OIS were seen cutting all of the crustal units in the Bryneira Range, and were also seen emerging from serpentinised Livingstone Peridotite (Fig. 4.3.1.1), suggesting a link between the ultramafic units of the DMOB and the OIS. Unfortunately, intrusive sheets in the Dun Mountain Ultramafics Group of the Bryneira Range were poorly exposed, highly deformed and difficult to interpret. Elsewhere, a geochemical link has been made between the intrusive sheets in the Dun Mountain Ultramafics Group and the Island Arc Tholeiite (IAT) magmas (Sano et al., 1997) (see later). Intrusive sheets within the Red Mountain Ultramafic Group have chilled margins against previously serpentinised mantel rock (Sinton, 1980). The above facts strongly suggest that OIS melts move through cold, previously formed mantel rock en route to the crustal portion of the DMOB. The origin and relative timing of the Livingstone Peridotite and associated middle gabbro ‘pod’ intrusion remains unconcluded.

6.2.8 Chronology and geochemistry of OIS magmatism

Crosscutting relations between different types of intrusive sheets and deformation structures indicates that tectonic events and magmatism events are episodic, and alternate through time with some overlap (Dilek et al., 1998). This is certainly the case for the Bryneira Range section of the DMOB. Second stage OIS magmatism is the result of a change in geodynamics in the Permian DMOB basin. Geochemical investigations strongly suggest change in tectonic setting from the initial development of the GIS magmatism, to later OIS magmatism (see later). The gap between these two magmatic episodes is not well constrained. The dates currently available for the DMOB lie in the range 270-280Ma (Jugum, 2008; Kimbrough et al., 1992; Sivell and McCulloch, 2000). These are mainly U-Pb ages from plagiogranite contemporaneous with OIS magmatism. Relationships of GIS and OIS magmatism in the Bryneira Range suggests a significant pause between these two magmatic episodes, and a tentative age from ~295-308Ma (Late Carboniferous) for the older magmatism (Sivell and McCulloch, 2000) is very interesting.

Re-activation of magmatism in the Bryneira Range was almost certainly related to a change in position relative to the plate boundary. The felsic association of the Lintley-Otanomomo segment of the DMOB comprises of subduction related melts, but does not have an exposed mafic section equivalent to the GIS magmatic portion of the Bryneira Range. It seems likely however, that the Lintley-Otanomomo segment is related to the OIS magmatism in a suprasubduction zone setting. New U-Pb geochronology (Jugum, 2008) from the Lintley-Otanomomo segment at Otama gives ages of 270+/- 2.5Ma compared with ~276 +/-2.5 and ~277 +/- 2.5Ma in the Livingstone Mountains-Bryneira Range area. These dates are sufficiently close to suggest they are part of the same arc.

The geochemistry of OIS related basalts has widely been identified as IAT. The tectonic affinity IAT magma indicates the original GIS magmatic portion of the DMOB had moved into a position above a subduction zone probably adjacent to an island arc (Fig. 6.13). Various similar tectonic models have been proposed for the geochemical evolution of the DMOB, of which Sivell (2000) is the most recent. They propose that pre-existing BABB crust (GIS magmatic portion) was trapped in the fore-arc region of a newly developed

subduction system. IAT intruded the pre-existing BABB crust at ~278Ma, forming a slow-spreading extensional regime in a fore-arc setting during nascent arc activity. The formation of oceanic crust in a supra-subduction zone setting, that later becomes trapped in orogenic belts as an ophiolite, is now believed to be the origin of most ophiolites (Hawkins, 2003). Supra-subduction zone setting is consistent with diverse geochemistry in magmas, as seen in the DMOB.

6.2.9 Waning of magmatism and continued extension

Magmatism lessened in the Northern Bryneira Range as the OIS magmatic front moved away. Continued extension caused tectonic rotation during the final stages of magmatism, and probably continued for some time after. Uplift and erosion of foot-wall block is recorded by the denudation of upper crustal units, as seen elsewhere in the DMOB (Coombs et al., 1976) and the wide range of thickness of Upukerora Breccia probably relates to wedge shaped basins. The Upukerora Breccia records a period of erosion of unknown length before deposition of the Wooded Peak Limestone. This period may have been as long as ~20Ma (Kimbrough et al., 1992). Wide variation in the thickness of the Wooded Peak Limestone also suggests extensional faulting may have continued long after magmatism ceased.

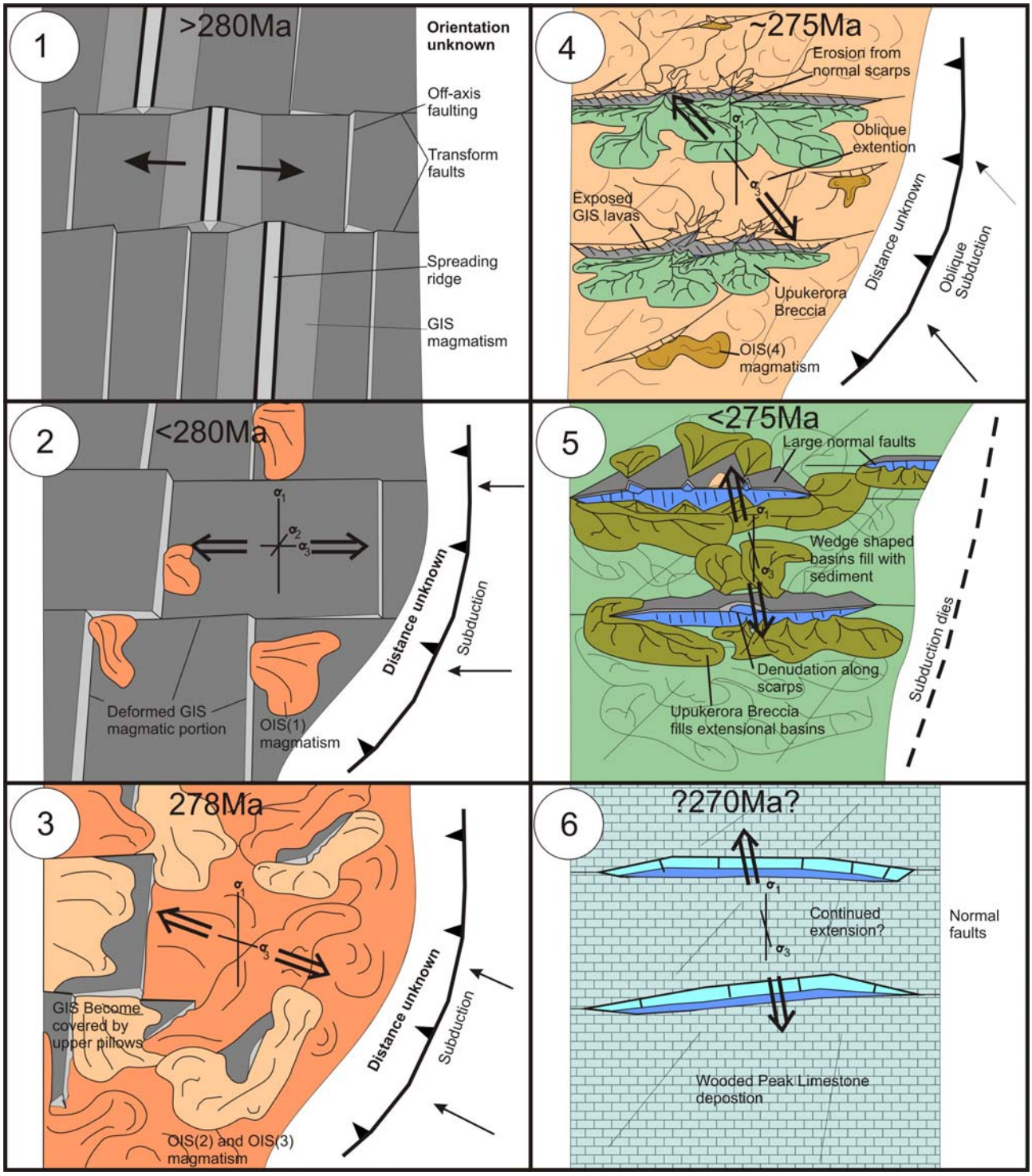

Fig. 6.13: Palinspastic diagram showing the Dun Mountain-Maitai terrane oceanic basin development during the Permian. **1.** Initial GIS magmatism forms at a spreading ridge in a back-arc basin. Pervasive brittle deformation forms structures in an off-axis position during and after magma cooling. **2.** Subduction initiates and the first OIS magmas are injected into the deformed, pre-existing crust with no dominate principle horizontal stress orientation. **3.** Continued subduction and injection OIS(2) and OIS(3) intrusive sheets covers GIS extrusives with OIS related lava flows. **4.** Waning magma supply (OIS(4)) and continued extension leads to oblique normal faulting (possibly on pre-existing transform faults) synchronous to the final magmatism. Upukerora Breccia begins to fill grabens by erosion of scarps. **5.** Continued extension and erosion denudes the upper crustal units of the DMOB along scarps and Upukerora Breccia fills wedge shaped basins. **6.** Wooded Peak Limestone deposition begins, possible during continued extension.

6.3 Conclusions

The Northern Bryneira Range records multiple periods of magmatism and deformation. It does not have a typical ophiolite sequence and notably lacks a sheeted dike complex. Initial oceanic crust was formed in a slow-spreading environment, resulting in a thin crustal sequence. Subsequent cooling and extension lead to the development of pervasive brittle deformation and hydrothermal alteration. A second period of magmatism started after a pause of unknown duration, being recorded by intrusive sheets cutting the entire crustal sequence and associated extrusives. The new magmas have a supra-subduction zone geochemistry, and are dated by synchronous intrusions of plagiogranites with U-Pb ages of 276+/-2.5 and 277+/- 2.5Ma (Early Permian). Change in OIS attitudes and orientations indicate rotation and intensification of the controlling stress field. The DMOB is characterised by pervasive extensional deformation during and after periods of crustal growth. Paleo-horizontal surfaces record rotation during the final stages of OIS magmatism. Wedge shaped sedimentary breccias and denudation of parts of the belt suggest large scale normal faulting continued after magmatism ceased in the Early Permian. Mesozoic deformation has rotated the Bryneira Range through ~90 degrees during the formation of the Key summit Syncline, and Cenozoic deformation may have rotated the Bryneira Range through more than 45 degrees about a sub-vertical axis.

6.3.1 Further study possibilities

Further studies on the evolution of the DMOB may include:

- Paleomagnetic sampling. This data would accurately determine the changing intrusive sheet orientation and therefore give inference to the changing stress dynamic of the greater DMOB basin.
- Geochronology of intrusives. As there is a well defined order of intrusive sheeting in the belt, it would beneficial to determine definite age relationships.
- Structural data. Any structural study would benefit form more orientation data, possibly from a wider area.

Geology of the Northern Bryneira Range

Map location

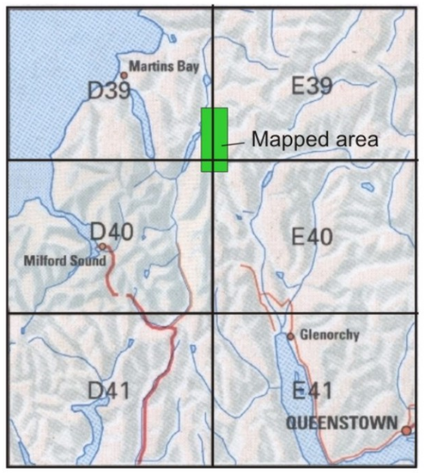

SCALE ~ 1:33,000

0Km 1 2 3

Geological symbols

	Accuate	Approximate	Inferred
Contacts			
Faults			
Fault (tick on downthrown side)			
Major regional faults			
Active faults			
Fold			
Syncline			
Antiform			

Structure	Dipping	Vertical	Overturned
Bedding			
Foliation/shistosity			

Mapping boundaries

- This study
- Turnbull (2000)
- Bishop (1994)

Column location C1

(See figure 3.7, in thesis)

GRID NORTH, G-M Angle, MAG. NORTH

MAGNETIC NORTH on this map is 19.5 degrees east of grid north.

Map Units

HOLOCENE

Gravel, sand, mud; modern to post glacial flood plains, may be terraced (Q1a).

Gravel and sand alluvial fan, grading into valley allivium (Q1f).

Holocene landside deposits (Q1t).

Q1f, Q1t, Q1a

TRIASSIC

249Ma

PERMIAN

Dun Mountain-Maitai terrane

MAITAI GROUP

- LITTLE BEN SANDSTONE: Bedded volcanoclastic sandstone (Tml)
- TRAMWAY FORMATION: Well bedded sandstone and siltstone (Ymt).
- WOODED PEAK LIMSTONE: Bedded limestone, minor sandstone and siltstone (Ymw).
- UPUKERORA FORMATION/BRECCIA: Igneous Breccia with minor silt and sandstone (Ymu)

Tml, Ymt, Ymw, Ymu

LIVINGSTONE VOLCANICS GROUP

Undifferentiated volcanics, dikes and gabbros (Yl); pillow lavas (Ylv); dolerites and dikes of the hypabyssal facies (Ylh); isotopic hornblende gabbros and dikes (Yli); cumulate gabbros of various composition (Ylc); gabbro and pyroxenite, variably serpentinised (Ylp).

Yl, Ylv, Ylh, Yli, Ylc, Ylp

DUN MOUNTAIN ULTRAMAFICS GROUP

Variably serpentinised, extensivly sheared ultramafics, cut by dikes (Yds).

Yds

Brook Street terrane

BROOK STREET VOLCANICS GROUP

MANTLE VOLCANICS FORMATION: Pyroclastic sediments intruded by basic dikes and sills

Ybm

290Ma

Caples terrane

CAPLES GROUP

- CRESENT FORMATION: Schistose green sandstone and black mudstone (Yce).
- MOMUS FORMATION: Massive sandstone (Ycm).
- HARRIS SADDLE FORMATION: Andersitic flows, pillow lavas and hyaloclastic breccias (Ycr).

Yce, Ycm, Ycr

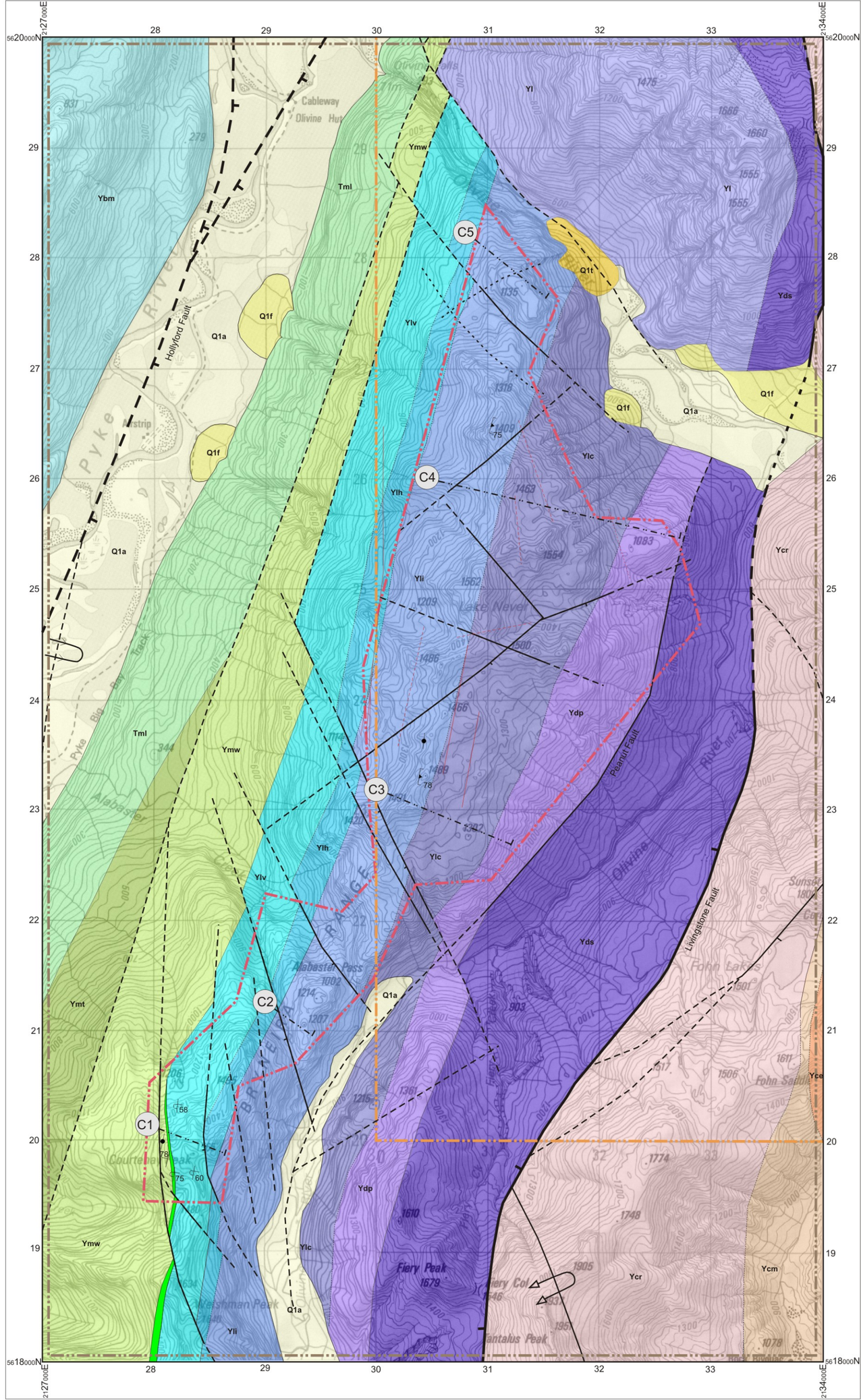

References

Agar, S.M. and Klitgord, K.D., 1995. A mechanism for decoupling within the oceanic lithosphere revealed in the Troodos Ophiolite. Nature, 374(6519): 232-238.

Alexander, R.J. and Harper, G.D., 1992. The Josephine ophiolite: an ancient analogue for slow- to intermediate-spreading oceanic ridges. IN Parson, L.M., Murton, B.J. & Browning, P. (eds), 1992, *Ophiolites and their Modern Oceanic Analogues.* Geological Society Special Publication No.60: 3-38.

Anonymous, 1972. Penrose field conference on ophiolites. Geotimes, 17: 24-25.

Baer, G. and Beyth, M., 1990. A mechanism of dyke segmentation in fractured host rock. Mafic dykes and emplacement mechanisms: Proceedings from the second international dyke conference. A.A. Balkema Publishers, Adelaide/South Australia.

Ballance, P.F. and Campbell, J.D., 1993. The Murihiku arc-related basin of New Zealand (Triassic-Jurassic). Sedimentary Basins of the World., 2. Elsevier, Amsterdam, 21-33 pp.

Bishop, D.G., 1996. Geology of the Forgotten River Area: Sheet E39AC. Institute of Geological and Nuclear Sciences, Lower Hut, New Zealand.

Blake, M.C. and Landis, C.A., 1973. The Dun Mountain ultramafic belt-Permian oceanic crust and upper mantle in New Zealand. U.S. Geological Survey Journal: Research, 1: 529-574.

Borradaile, G.J. and Gauthier, D., 2006. Magnetic studies of magma-supply and sea-floor metamorphism: Troodos Ophiolite dikes. Tectonophysics, 418: 75-92.

Bradshaw, J.D., 1993. A review of the Median Tectonic Zone: terrane boundaries and terrane amalgamation near the Median Tectonic Line. New Zealand Journal of Geology and Geophysics, 36: 117-125.

Bradshaw, J.D., 2007. The Ross Orogen and Lachland fold belt in Marie Byrd Land, northern Victoria Land and New Zealand; implication for the tectonic setting of the Lachlan fold belt in Antarctica. U. S. Geological Survey-Open-File Report:, Report: OF 2007-1047, Short Research Paper 059,.

Bradshaw, J.D. et al., 1997. New Zealand Superterranes Recognized in Marie Byrd Land and Thurston Island. The Antarctic Region: Geological Evolution and Processes; proceedings of the VII international symposium on Antarctic earth sciences. Terra Antarctica Publications, Siena, 1995, 429-436 pp.

Campbell, H.J., 2000. The Marine Triassic of Australasian and its interregional correlation. Permian-Triassic Evolution of Tethys and Western Circum-Pacific. Elsevier, Amsterdam, 235-255 pp.

Cawood, P., 1986. Stratigraphic and structural relations of the Southern Dun Mountain Ophiolite Belt and enclosing strata, northwestern Southland, New Zealand. New Zealand Journal of Geology and Geophysics, 29: 179-203.

Cawood, P.A., 1987. Stratigraphic and structural relations of strata enclosing the Dun Mountain ophiolite belt in the Arthurton-Clinton region, Southland, New Zealand. New Zealand Journal of Geology and Geophysics, 30(1): 19-36.

Coombs, D.S., Cook, N.D.J., Kawachi, Y., Johnstone, R.D. and Gibson, I.L., 1996. Park Volcanics, Murihiku Terrane, New Zealand; petrology, petrochemistry, and tectonic significance. New Zealand Journal of Geology and Geophysics, 39(4): 469-492.

Coombs, D.S. et al., 1973. The Dun Mountain ophiolite belt, New Zealand. Ophiolites in the earths crust. Nauka Press, Acad.Sci., USSR.

Coombs, D.S. et al., 1976. The Dun Mountain ophiolite belt, New Zealand, its tectonic setting, constitution, and origin, with special reference to the southern portion. American Journal of Science, 276(5): 561-603.

Cooper, R.A. and Tulloch, A.J., 1992. Early Paleozoic terranes in New Zealand and their relationship to the Lachlan Fold Belt. Tectonophysics, 214: 129-144.

Craw, D., 1979. Mélanges and associated rocks, Livingstone Mountains, Southland, New Zealand. New Zealand Journal of Geology and Geophysics, 22: 443-454.

Delaney, P.T. and Gartner, A.E., 1997. Physical processes of shallow mafic dike emplacement near the San Rafael Swell, Utah. Geological society of America Bulletin, 109(9): 1177-1192.

Delaney, P.T., Pollard, D.D., Ziony, J.I. and McKee, E.H., 1986. Field relations between dikes and joints: Emplacement processes and Paleostress analysis. Journal of Geophysical Research, 91(B5): 4920-4938.

Dickins, J.M., Johnston, M.R., Kimbrough, D.L. and Landis, C.A., 1986. The stratigraphic and structural position age of the Croisilles Mélange, East Nelson, New Zealand. New Zealand Journal of Geology and Geophysics, 29(3): 291-301.

Dietrich, D. and Spencer, S., 1993. Spreading-induced faulting and fracturing of oceanic crust; examples from the Sheeted dyke complex of the Troodos Ophiolite, Cyprus. Geological Society Special Publications, 76: 121-139.

Dilek, Y. et al., 1997. Structure and petrology of hydrothermal veins in gabbroic rocks from sites 921 to 924, MARK area (Leg 153): Alteration history of slow-spread lower crust. Proceedings of the Oceanic Drilling Programs, Scientific Results, 153: 155.

Dilek, Y., Moores, M.E. and Furnes, H., 1998. Structure of modern oceanic crust and ophiolites and implications for faulting and magmatism at oceanic spreading centers. In: W.R. Buck, P.T. Delaney, J.A. Karson and Y. Lagabrielle (Editors), Faulting and magmatism at mid-ocean ridges. American Geophysical Union., Washington, D. C., pp. 219-265.

Eccles, J.D., Cassidy, J., Locke, C.A. and Spoerli, K.B., 2005. Aeromagnetic imaging of the Dun Mountain ophiolite belt in northern New Zealand; insight into the fine structure of a major SW Pacific terrane suture. Journal of the Geological Society of London, 162(4): 723-735.

Gee, J. and Meurer, W.P., 2002. Slow-cooling of the middle and lower oceanic crust inferred from multicomponent magnetization of gabbroic rocks from the Mid-Atlantic Ridge south of the Kane fracture zone (MARK) area. Journal of Geophysical Research, 107(B7): EMP3-1.

Girardeau, J., Mercier, J.C.C. and Xibin, W., 1985. Petrology of the mafic rocks of the Xigaze ophiolite, Tibet. Contributions to Mineralogy and Petrology, 90: 309-321.

Gudmundsson, A., 1984. Formation of dykes, feeder-dikes and the intrusion of dykes from magma chambers. Bulletin Volcanologique, 47-3: 537-550.

Gudmundsson, A., 1990. Emplacement of dikes, sills and crustal magma chambers at divergent plate boundaries. Tectonophysics, 179: 257-275.

Harper, G.D., 1982. Evidence for large-scale rotations at spreading centers from the Josephine ophiolite. Tectonophysics, 82: 25-44.

Harris, R., 2004. Tectonic evolution of the Brooks Range Ophiolite, northern Alaska. Tectonophysics, 392: 143-163.

Hatherton, T., 1967. A geophysical study of Nelson-Cook Strait region, New Zealand. . New Zealand Journal of Geology and Geophysics, 10(1330-1347).

Hatherton, T., 1969. Geophysical anomalies over the eu- and miogeosynclinal systems of California and New Zealand. Geological society of America Bulletin, 80: 213-230.

Hatherton, T. and Sibson, R.H., 1970. Junction Magnetic Anomaly north of Waikato River. New Zealand Journal of Geology and Geophysics, 13: 655-662.

Hawkins, J.W., 2003. Geology of supra-subduction zones-Implications for the origin of ophiolites. Ophiolite Concept and the Evolution of Geological Thought, 373. The Geological Society of America Special Paper, Boulder, Colorado, 227-268 pp.

Hebert, R., Huot, F., Wang, C. and Liu, Z., 2003. Yarlung Zangbo ophiolite (southern Tibet) revisited: geodynamic implications from mineral record. Ophiolites in Earth History, 218. The Geological Society of London, London, 165-190 pp.

Hoek, J.D., 1991. A classification of dyke-fracture geometry with examples from Precambrian dyke swarms in the Vestfold Hills, Antarctica. Geologische Rundschau, 80(2): 233-248.

Hopson, C.A., 2007. Subvolcanic sheeted sills and nonsheeted dikes in ophiolites: Occurrence, origin, and tectonic significance for oceanic crust generation. In: M. Cloos, W.D. Carlson, M.C. Gilbert, J.G. Liou and S.S. Sorensen (Editors), Convergent Margin Terranes and Associated Regions: A Tribute to W. G. Ernst. Geological Society of America Special Paper, pp. 225-254.

Hopson, C.A. and Fanco, C.J., 1977. Igneous history of the Point Sal ophiolite, southern California. Northern American ophiolites, 95. Oregon Department of Geology and Mineral Industries Bulletin, 161-185 pp.

Hunt, T., 1978. Stokes magnetic anomaly system. New Zealand Journal of Geology and Geophysics, 21(5): 595-606.

Hurst, S.D., Moores, M.E. and Varga, R.J., 1994. Structure and geophysical expression of the Solea graben Troodos Ophiolite, Cyprus. Tectonics, 13: 139-156.

Hyslop, K.J., 1978. The Geology of the Serpentine Saddle Area, University of Otago.

Johnston, M.R., 1996. Geology of the D'Urville Area, Geological Map 16. Institute of Geological and Nuclear Sciences.

Jugum, D., 2008.

Karson, J.A., 1998. Internal structure of oceanic lithosphere: A perspective from tectonic windows. Faulting and Magmatism at Mid-Ocean Ridges, Geophysical Monograph 106. American Geophysical Union Washington, D.C., 177-218 pp.

Karson, J.A. and Rona, P.A., 1990. Block-tilting, transfer faults, and structural control of magmatic and hydrothermal processes in the TAG area, Mid-Atlantic Ridge 26^{o}N. Geological society of America Bullitin, 102: 1635-1645.

Kear, D. and Mortimer, N., 2003. Waipa Supergroup, New Zealand: A proposal. Journal of the Royal Society of New Zealand, 33: 149-163.

Kelsey, P.I., 1981. Geology of part of the East Eglinton Valley., University of Otago, Dunedin.

Khodayar, M. and Einarsson, P., 2004. Reverse-slip structures at oceanic divergent plate boundaries and their kinematic origin: Data form Tertiary crust West and South Iceland. Journal of Structural Geology, 26(11): 1945-1960.

Kimbrough, D.L., Mattinson, J.M., Coombs, D.S., Landis, C.A. and Johnston, M.R., 1992. Uranium-lead ages from the Dun Mountain ophiolite belt and Brook Street Terrane, South Island, New Zealand. Geological Society of America Bulletin, 104(4): 429-443.

Kimbrough, D.L. et al., 1994. Uranium-lead zircon ages from the Median Tectonic Zone, New Zealand. New Zealand Journal of Geology and Geophysics, 37: 393-419.

Kimbrough, D.L., Tulloch, A.J., Geary, E., Coombs, D.S. and Landis, C.A., 1993. Isotopic ages from the Nelson region of South Island, New Zealand: crustal structure and definition of the Median Tectonic Zone. Tectonophysics, 225: 433-448.

Laird, M.G. and Bradshaw, J.D., 2004. The Break-up of a long-term relationship: the Cretaceous separation of New Zealand from Gondwana. Gondwana Research, 7(1): 273-286.

Lamarche, G. et al., 1997. The Oligocene-Miocene Pacific-Australia plate boundary, south of New Zealand: Evolution from ocean spreading to strike-slip faulting. Earth and Planetary Science Letters, 148: 129-139.

Landis, C.A. and Bishop, D.G., 1972. Plate tectonic s and regional stratigraphic-metamorphic relations in the southern part of the New Zealand Geosyncline. Geological society of America Bulletin, 83: 2267-2284.

Landis, C.A. et al., 1999. Permian-Jurassic strata at Productus Creek, Southland, New Zealand; implications for terrane dynamics of the eastern Gondwanaland margin. New Zealand Journal of Geology and Geophysics, 42(2): 255-278.

Macdonell, B.J., 1982. The geology of the Telescope Hill area, Gorge Plateau, South Westland., University of Otago.

Malpas, J., Zhou, M., Robinson, P.T. and Reynolds, P.H., 2003. Geochemical and geochronological constraints on the origin and emplacement of the Yarlung Zangbo ophiolites, Southern Tibet. Ophiolite in Earth History, 218. The Geological Society of London, London, 191-206 pp.

MapToaster, 2001. 2001-2003.MetaMedia Ltd. (Editor).

Meurer, W.P. and Gee, J., 2002. Evidence for protracted construction of slow spread oceanic crust by small magmatic injections. Earth and Planetary Science Letters, 201: 45-55.

Mortimer, N., 2004. New Zealand's Geological Foundations. Gondwana Research, 7(1): 261-272.

Mortimer, N. et al., 1999. Overview of the Median Batholith, New Zealand: A new interpretation of the geology of the Median Tectonic Zone and adjacent rocks. Journal of African Earth Science, 29: 257-268.

Motoki, A. and Sichel, S.E., 2008. Hydraulic fracturing as a possible mechanism of dyke-sill transitions and horizontal discordant intrusions in trachtic tabular bodies of Arraial do Cabo, State of Rio de Janeiro, Brazil. Geofisica International, 47(1): 13-25.

Nicolas, A., 1989. Structure of ophiolites and dynamics of oceanic lithosphere. Kluwer Academic Publishers, Dordecht, The Netherlands.

Nur, A., Ron, H. and Scotti, O., 1986. Fault mechanics and the kinematics of block rotation. Geology, 14: 746-749.

O'Brien, J.P. and Rodgers, K.A., 1973. Alpine-type Serpentinites from the Auckland Province -1. The Wairere Serpentinite. Journal of the Royal Society of New Zealand, 3: 169-190.

Pettinga, J.R., Yetton, M.D., Van Dissen, R.J. and Downes, G., 2001. Earthquake source identification and characterisation for the Canterbury Region, South Island, New Zealand. Bulletin of the New Zealand Society for Earthquake Engineering, 34(4): 282-317.

Pillai, D.D.L., 1989. Upukerora Formation, Maitai Group, in Western Otago and northern Southland, University of Otago, Dunedin, New Zealand.

Price, N.J. and Cosgrove, J.W., 1990. Analysis of geological structures. Cambridge University Press.

Rattenbury, M.S., Cooper, R.A. and Johnston, M.R., 1998. Geology of the Nelson area. Institute of Geological and Nuclear Sciences Limited Lower Hutt, New Zealand.

Rickwood, P.C., 1990. The anatomy of a dyke and the determination of propagation direction and magma flow. Mafic dykes and emplacement mechanisms. A.A. Balkema Publishers, Rotterdam, Netherlands

Sano, S. et al., 1997. Geochemistry of dike rocks in Dun Mountain Ophiolite, Nelson, New Zealand. New Zealand Journal of Geology and Geophysics, 40(2): 127-136.

Schroetter, J.-M., Page, P., Bedard, H.J., Tremblay, A. and Becu, V., 2003. Fore-arc extension and sea-floor spreading in the Thetford Mines Ophiolite Complex. In: Y. Dilek and P.T. Robinson (Editors), Ophiolites in Earth History. Geological Society Special Publications, London.

Schwartz, J.J. et al., 2005. Dating growth of oceanic crust at a slow-spreading ridge. Science, 310: 654-657.

Sinton, J.M., 1975. Structure, petrology and Metamorphism of the Red Mountain ophiolite Complex New Zealand, University of Otago, Dunedin.

Sinton, J.M., 1980. Petrology and evolution of the Red Mountain ophiolite complex, New Zealand. American Journal of Science, Vol. 280-A, Part 1: 296-328.

Sivell, W.J., 1988. Geochemical constrains on the origin of Croisilles and Patuki ophiolites: Implications for Late Paleozoic-Mesozoic tectonics in New Zealand. Tectonics, 7: 1015-1032.

Sivell, W.J., 2002. Geochemistry and Nd-isotope systematics of chemical and terrigenous sediments from the Dun Mountain Ophiolite, New Zealand. New Zealand Journal of Geology and Geophysics, 45(4): 427-451.

Sivell, W.J. and McCulloch, M.T., 2000. Reassessment of the origin of the Dun Mountain Ophiolite, New Zealand; Nd-isotopic and geochemical evolution of magma suites. New Zealand Journal of Geology and Geophysics, 43(2): 133-146.

Sivell, W.J. and Rankin, P.C., 1982. Discrimination between ophiolitic metabasalts, north D'Urville Island, New Zealand. New Zealand Journal of Geology and Geophysics, 25: 275-293.

Stratford, J.M.C. et al., 2004. Stratigraphy of the Lower Maitai Group at West Dome Southland, New Zealand. Journal of the Royal Society of New Zealand, 34: 267-293.

Sutherland, R., 1995. The Australia-Pacific boundary and Cenzoic plate motions in the SW Pacific: Some constraints from Geoset data. Tectonics, 14(4): 819-831.

Sutherland, R., 1999. Basement geology and tectonic development of the greater New Zealand region: an interpretation from regional magnetic data. Tectonophysics, 308: 341-362.

Thy, P. and Dilek, Y., 2003. Development of ophiolitic perspective on models of oceanic magma chambers beneath active spreading centers. Ophiolite concept and the evolution of geological thought:, 373. Geological Society of America Special Paper, Boulder, Colorado, 187-226 pp.

Turnbull, I.M., 2000. Geology of the Wakatipu Area. 1:250000 map 18. Institute of Geological and Nuclear Science, Lower Hutt, New Zealand.

Varga, R.J., Gee, J.S., Bettison-Varga, J., Anderson, R.S. and Johnson, C.L., 1999. Early establishment of seafloor hydrothermal systems during structural extension: paleomagnetic evidence form the Troodos Ophiolite, Cyprus. Earth and Planetary Science Letters, 171(221-235).

Varga, R.J. and Moores, M.E., 1985. Spreading structure of the Troodos ophiolite, Cyprus. geology, 13: 846-850.

Verosub, K.L. and Moores, M.E., 1981. Tectonic Rotations in Extensional Regimes and Their Paleomagnetic Consequences for Oceanic Basalts. Journal of the Geophysical Research, 86(B7): 6335-6349.

Walcott, R.I., 1969. Geology of the Red Hill Complex, Nelson, New Zealand. Transactions of the Royal Society of New Zealand, Earth Sciences, 7: 57-88.

Wandres, A.M. and Bradshaw, J.D., 2005. New Zealand tectonostratigraphy and implications from conglomeratic rocks for the configuration of the SW Pacific margin of Gondwana. Geological Society Special Publications, 246: 179-216.

Weaver, S.D., Bradshaw, J.D. and Adams, C.J., 1991. Granitoids of the Ford Ranges, Marie Byrd Land, Antarctica. Geological evolution of Antarctica. Cambridge University Press, New York, 345-351 pp.

Wood, B.L., 1956. The Geology of the Gore Subdivision. New Zealand Geological Survey, 53.

Woodward, D.J. and Hatherton, T., 1975. Magnetic anomalies over southern New Zealand. New Zealand Journal of Geology and Geophysics, 18: 65-82.

Ziv, A., Rubin, A.M. and Agnon, A., 2000. Stability of dike intrusion along preexisting fractures. Journal of Geophysical Research: Solid Earth, 105(B3): 5947-5961.